Journal of Geotechnical and Geoenvironmental Engineering

Modelling Lifetime Performance of Monopile Foundations for Offshore Wind Applications

--Manuscript Draft--

Manuscript Number:	GTENG-9833R2
Full Title:	Modelling Lifetime Performance of Monopile Foundations for Offshore Wind Applications
Manuscript Region of Origin:	UNITED KINGDOM
Article Type:	Technical Paper
Manuscript Classifications:	Constitutive relations; Cyclic loads; Deep foundations; Models and modeling; Piles and pile driving
Funding Information:	
Abstract:	This paper explores the application of a numerical method for modelling pseudo-random cyclic loading, at very large cycle numbers, to the design of offshore wind turbine foundations. The work expands the development of a novel constitutive modelling framework, HARM, described by Houlsby et al. (2017), with a calibration method outlined in Abadie et al. (2019). HARM captures both the non-linear hysteretic behavior during cycling and the accumulation of permanent deformation (ratcheting) with large cycle numbers in a rigorous, yet computationally efficient manner, enabling the computation of foundation response over a lifetime of loading. This paper demonstrates how the approach can be applied to the cyclic pile field testing from the PISA project (Byrne et al. 2020a). Following calibration, the model is used to assess pile response to three load signals representative of operational and extreme loads throughout the lifetime of a full scale wind turbine foundation: (i) a short storm, (ii) a 35h storm and (iii) a lifetime loading. The paper discusses how computational efficiency can be achieved whilst maintaining a high level of calculation accuracy.
Corresponding Author:	Christelle Nadine Abadie, D.Phil University of Cambridge Cambridge, UNITED KINGDOM
Corresponding Author E-Mail:	cna24@cam.ac.uk
Order of Authors:	Christelle Nadine Abadie, D.Phil
	William J. A. P. Beuckelaers, D.Phil
	Byron Walter Byrne, BE(Hons) BCom MA DPhil
	Guy T Houlsby, MA DSc FREng FICE
	Harvey J Burd, MA DPhil CEng MICE
	Ross A McAdam, DPhil (Oxon) MEng
Additional Information:	
Question	**Response**
Authors are required to attain permission to re-use content, figures, tables, charts, maps, and photographs for which the authors do not hold copyright. Figures created by the authors but previously published under copyright elsewhere may require permission. For more information see http://ascelibrary.org/doi/abs/10.1061/9780784479018.ch03. All permissions must	No

be uploaded as a permission file in PDF format. Are there any required permissions that have not yet been secured? If yes, please explain in the comment box.	
ASCE does not review manuscripts that are being considered elsewhere to include other ASCE Journals and all conference proceedings (see next question for expanded conference proceeding requirements). Is the article or parts of it being considered for any other publication? If your answer is yes, please explain in the comments box below.	No
Each submission to ASCE must stand on its own and represent significant new information, which may include disproving the work of others. While it is acceptable to build upon one's own work or replicate other's work, it is not appropriate to fragment the research to maximize the number of manuscripts or to submit papers that represent very small incremental changes. ASCE may use tools such as CrossCheck, Duplicate Submission Checks, and Google Scholar to verify that submissions are novel. Does the manuscript constitute incremental work (i.e. restating raw data, models, or conclusions from a previously published study)?	No
Authors are expected to present their papers within the page limitations described in <u>Publishing in ASCE Journals: A Guide for Authors</u>. Technical papers and Case Studies must not exceed 30 double-spaced manuscript pages, including all figures and tables. Technical notes must not exceed 7 double-spaced manuscript pages. Papers that exceed the limits must be justified. Grossly over-length papers may be returned without review. Does this paper exceed the ASCE length limitations? If yes, please provide justification in the comments box below.	Yes
If yes, please provide justification in the comments box below. as follow-up to "Authors are expected to present their papers within the page limitations described in <u><a href="http://dx.doi.org/10.1061/978078447	The Figures shown in this paper require page wide space and therefore extend the length of the paper submitted, and sometimes result in leaving half a page blank in the submission.

9018" target="_blank">Publishing in ASCE Journals: A Guide for Authors</u></i>. Technical papers and Case Studies must not exceed 30 double-spaced manuscript pages, including all figures and tables. Technical notes must not exceed 7 double-spaced manuscript pages. Papers that exceed the limits must be justified. Grossly over-length papers may be returned without review. Does this paper exceed the ASCE length limitations? If yes, please provide justification in the comments box below. "	
All authors listed on the manuscript must have contributed to the study and must approve the current version of the manuscript. Are there any authors on the paper that do not meet these criteria? If the answer is yes, please explain in the comments.	No
Was this paper previously declined or withdrawn from this or another ASCE journal? If so, please provide the previous manuscript number and explain what you have changed in this current version in the comments box below. You may upload a separate response to reviewers if your comments are extensive.	No
Companion manuscripts are discouraged as all papers published must be able to stand on their own. Justification must be provided to the editor if an author feels as though the work must be presented in two parts and published simultaneously. There is no guarantee that companions will be reviewed by the same reviewers, which complicates the review process, increases the risk for rejection and potentially lengthens the review time. If this is a companion paper, please indicate the part number and provide the title, authors and manuscript number (if available) for the companion papers along with your detailed justification for the editor in the comments box below. If there is no justification provided, or if there is insufficient justification, the papers will be returned without review.	
If this manuscript is intended as part of a Special Issue or Collection, please provide the Special Collection title and name of the guest editor in the comments	

box below.	
Recognizing that science and engineering are best served when data aremade available during the review and discussion of manuscripts andjournal articles, and to allow others to replicate and build on workpublished in ASCE journals, all reasonable requests by reviewers formaterials, data, and associated protocols must be fulfilled. If you are restricted from sharing your data and materials, please explain below.	Some of the loading data used for input to the analysis have been provided by a third party through a collaboration agreement, and is presented in the paper anonymised as requested by the data provider (i.e. they wish to remain anonymous). Selected sequences of the time-history data, in anonymised form, for verification purposes could be made available upon reasonable request.
Papers published in ASCE Journals must make a contribution to the core body of knowledge and to the advancement of the field. Authors must consider how their new knowledge and/or innovations add value to the state of the art and/or state of the practice. Please outline the specific contributions of this research in the comments box.	This paper contributes to the numerical modelling of the response of monopile foundations to cyclic loading for very large cycle number by: (1) proposing a numerical method that comines the PISA 1D model and the HARM model for cyclic applications of pile design. (2) validating the model. This is achieved by using the numerical model and calibration procedure to capture field test data published as part of the PISA project; (3) demonstrating industrial feasibility and relevance. This is achieved by using the model to predict the foundation response to a lifetime worth of load, as well as random storm loading; (4) exploring methods for computational efficiency whilst maintaining a high level of calculation accuracy.
When submitting a new and revised manuscript, authors are asked to include a Data Availability Statement containing one or more of the following statements, with specific items listed as appropriate. Please select one or more of the statements below that apply to your manuscript. Also, please include the selected statements in a separate "Data Availability Statement" section in your manuscript, directly before the acknowledgments or references. The statement(s) listed in your manuscript should match those you select in your response to this question.	a. Some or all data, models, or code that support the findings of this study are available from the corresponding author upon reasonable request.; d. Some or all data, models, or code generated or used during the study are proprietary or confidential in nature and may only be provided with restrictions.
Please describe which data are proprietary or confidential and what restrictions apply. as follow-up to "When submitting a new and revised manuscript, authors are asked to include a Data Availability Statement containing one or more of the following statements, with specific items listed as appropriate. Please select one or more of the statements below that apply to your manuscript. Also, please include the selected statements in a separate	Elements of the work are either proprietary or confidential (e.g. the computational implementation of the PISA and HARM approaches), though much of the background has been published and is referenced in the paper (e.g. the PISA field tests, the PISA design model, the HARM approach). Selected sequences of the time-history data, in anonymised form, for verification purposes could be made available upon reasonable request. Some of the loading data used for input to the analysis have been provided by a third party through a collaboration agreement, and is presented in the paper anonymised as requested by the data provider (i.e. they wish to remain anonymous).

"Data Availability Statement" section in your manuscript, directly before the acknowledgments or references. The statement(s) listed in your manuscript should match those you select in your response to this question."	
The flat fee for including color figures in print is $800, regardless of the number of color figures. There is no fee for online only color figures. If you decide to not print figures in color, please ensure that the color figures will also make sense when printed in black-and-white, and remove any reference to color in the text. Only one file is accepted for each figure. Do you intend to pay to include color figures in print? If yes, please indicate which figures in the comments box.	No
Is this article or parts of it already published in print or online in any language? ASCE does not review content already published (see next questions for conference papers and posted theses/dissertations). If your answer is yes, please explain in the comments box below.	No
Has this paper or parts of it been published as a conference proceeding? A conference proceeding may be reviewed for publication only if it has been significantly revised and contains 50% new content. Any content overlap should be reworded and/or properly referenced. If your answer is yes, please explain in the comments box below and be prepared to provide the conference paper.	No
ASCE allows submissions of papers that are based on theses and dissertations so long as the paper has been modified to fit the journal page limits, format, and tailored for the audience. ASCE will consider such papers even if the thesis or dissertation has been posted online provided that the degree-granting institution requires that the thesis or dissertation be posted. <p>Is this paper a derivative of a thesis or dissertation posted or about to be posted on the Internet? If yes, please provide the URL or DOI permalink in the comment box below.	No
If there is anything else you wish to	

communicate to the editor of the journal, please do so in this box.	
ASCE offers authors the option to publish their work under an open access license for a fee of $2000. You can read more about ASCE's open access option here. If your manuscript is accepted, do you plan to publish it under an open access license? Note that your decision has no bearing on whether your paper will be accepted. Payment for open access is not collected until proof stage, and you will have the chance to change your mind before payment is due.	No
When submitting a manuscript, authors must include a section heading titled “Data Availability Statement” before the “Acknowledgments” section or after the “Conclusion." Within the section, authors will include one or more of the following statements, as well as all citations to data, code, or models. You can read more about the Data Availability Statement policy here. Please select one or more of the statements below that apply to your manuscript. The statement(s) listed in your manuscript should match those you select in your response to this question. *Note that regardless of your response to this question, all reasonable requests for data from reviewers during the review process must be fulfilled.*	a. Some or all data, models, or code that support the findings of this study are available from the corresponding author upon reasonable request.; d. Some or all data, models, or code generated or used during the study are proprietary or confidential in nature and may only be provided with restrictions.
Please describe which data are proprietary or confidential and what restrictions apply. as follow-up to "When submitting a manuscript, authors must include a section heading titled “Data Availability Statement” before the “Acknowledgments” section or after the “Conclusion." Within the section, authors will include one or more of the following statements, as well as all citations to data, code, or models. You can read more about the Data	Elements of the work are either proprietary or confidential (e.g. the computational implementation of the PISA and HARM approaches), though much of the background has been published and is referenced in the paper (e.g. the PISA field tests, the PISA design model, the HARM approach). Selected sequences of the time-history data, in anonymised form, for verification purposes could be made available upon reasonable request. Some of the loading data used for input to the analysis have been provided by a third party through a collaboration agreement, and is presented in the paper anonymised as requested by the data provider (i.e. they wish to remain anonymous).

Availability Statement policy here. Please select one or more of the statements below that apply to your manuscript. The statement(s) listed in your manuscript should match those you select in your response to this question. *Note that regardless of your response to this question, all reasonable requests for data from reviewers during the review process must be fulfilled*."	
COPYRIGHT TRANSFER AGREEMENT **I. Authorship Responsibility** To protect the integrity of authorship, only people who have significantly contributed to the research or project and manuscript preparation shall be listed as coauthors. The corresponding author attests to the fact that anyone named as a coauthor has seen the final version of the manuscript and has agreed to its submission for publication. Deceased persons who meet the criteria for coauthorship shall be included, with a footnote reporting date of death. No fictitious name shall be given as an author or coauthor. An author who submits a manuscript for publication accepts responsibility for having properly included all, and only, qualified coauthors. **II. Originality of Content** ASCE respects the copyright ownership of other publishers. ASCE requires authors to obtain permission from the copyright holder to reproduce any material that (1) they did not create themselves and/or (2)	None of the exceptions listed above apply.

has been previously published, to include the authors' own work for which copyright was transferred to an entity other than ASCE. For any figures, tables, or text blocks exceeding 100 words from a journal article or 500 words from a book, written permission from the copyright holder must be obtained and supplied with the submission. Each author has a responsibility to identify materials that require permission by including a citation in the figure or table caption or in extracted text.

More information can be found in the guide "Publishing in ASCE Journals: Manuscript Submission and Revision Requirements" (http://ascelibrary.org/doi/pdf/10.1061/9780784479018.ch05). Regardless of acceptance, no manuscript or part of a manuscript will be published by ASCE without proper verification of all necessary permissions to re-use. ASCE accepts no responsibility for verifying permissions provided by the author. Any breach of copyright will result in retraction of the published manuscript.

III. Copyright Transfer

ASCE requires that authors or their agents assign copyright to ASCE for all original content published by ASCE. The author(s) warrant(s) that the above-cited manuscript is the original work of the author(s) and has never been published in its present form.

The undersigned, with the consent of all authors, hereby transfers, to the extent that there is copyright to be transferred, the exclusive copyright interest in the above-cited manuscript (subsequently

called the “work”) in this and all subsequent editions of the work (to include closures and errata), and in derivatives, translations, or ancillaries, in English and in foreign translations, in all formats and media of expression now known or later developed, including electronic, to the American Society of Civil Engineers subject to the following:

• The undersigned author and all coauthors retain the right to revise, adapt, prepare derivative works, present orally, or distribute the work, provided that all such use is for the personal noncommercial benefit of the author(s) and is consistent with any prior contractual agreement between the undersigned and/or coauthors and their employer(s).

• No proprietary right other than copyright is claimed by ASCE.

• This agreement will be rendered null and void if (1) the manuscript is not accepted for publication by ASCE, (2) is withdrawn by the author prior to publication (online or in print), (3) ASCE Open Access is purchased by the author.

• Authors may post a PDF of the ASCE-published version of their work on their employers’ ***Intranet*** with password protection. The following statement must appear with the work: “This material may be downloaded for personal use only. Any other use requires prior permission of the American Society of Civil Engineers.”

• Authors may deposit the ***final draft*** of their work in an institutional repository or in their funding body’s designated archive upon publication in an ASCE Journal, provided the draft contains a link to the published version at ascelibrary.org, and may request public access 12 months after publication. “Final draft” means the version submitted to ASCE after peer review and prior to copyediting or other

ASCE production activities; it does not include the copyedited version, the page proof, a PDF, or full-text HTML of the published version.

• Authors may post the ***final draft*** of their work on open, unrestricted Internet sites 12 months after publication in an ASCE Journal, provided the draft contains a link to the published version at ascelibrary.org.

Exceptions to the Copyright Transfer policy exist in the following circumstances. Select the appropriate option below to indicate whether you are claiming an exception:

• U.S. GOVERNMENT EMPLOYEES: Work prepared by U.S. Government employees in their official capacities is not subject to copyright in the United States. Such authors must place their work in the public domain, meaning that it can be freely copied, republished, or redistributed. In order for the work to be placed in the public domain, ALL AUTHORS must be official U.S. Government employees. If at least one author is not a U.S. Government employee, copyright must be transferred to ASCE by that author.

• CROWN GOVERNMENT COPYRIGHT: Whereby a work is prepared by officers of the Crown Government in their official capacities, the Crown Government reserves its own copyright under national law. If ALL AUTHORS on the manuscript are Crown Government employees, copyright cannot be transferred to ASCE; however, ASCE is given the following nonexclusive rights: (1) to use, print, and/or publish in any language and any format, print and electronic, the above-mentioned work or any part thereof, provided that the name of the author and the Crown Government affiliation is clearly

indicated; (2) to grant the same rights to others to print or publish the work; and (3) to collect royalty fees. ALL AUTHORS must be official Crown Government employees in order to claim this exemption in its entirety. If at least one author is not a Crown Government employee, copyright must be transferred to ASCE by that author. • **WORK-FOR-HIRE**: Privately employed authors who have prepared works in their official capacity as employees must also transfer copyright to ASCE; however, their employer retains the rights to revise, adapt, prepare derivative works, publish, reprint, reproduce, and distribute the work provided that such use is for the promotion of its business enterprise and does not imply the endorsement of ASCE. In this instance, an authorized agent from the authors' employer must sign the form below. • **U.S. GOVERNMENT CONTRACTORS**: Work prepared by authors under a contract for the U.S. Government (e.g., U.S. Government labs) may or may not be subject to copyright transfer. Authors must refer to their contractor agreement. For works that qualify as U.S. Government works by a contractor, ASCE acknowledges that the U.S. Government retains a nonexclusive, paid-up, irrevocable, worldwide license to publish or reproduce this work for U.S. Government purposes only. This policy DOES NOT apply to work created with U.S. Government grants.	
Please type your name below to complete the copyright transfer agreement. This will serve as your digital signature. *I, the corresponding author, confirm that the authors listed on the manuscript are aware of their authorship status and qualify to be authors on the manuscript according to the guidelines above.*	Christelle Abadie

I, the corresponding author, confirm that the content, figures, drawings, charts, photographs, and tables in the submitted work are either original work created by the authors listed on the manuscript or work for which permission to re- use has been obtained from the creator.

I, the corresponding author, acting with consent of all authors listed on the manuscript, hereby transfer copyright or claim exemption to transfer copyright of the work as indicated above to the American Society of Civil Engineers.

as follow-up to "**COPYRIGHT TRANSFER AGREEMENT**

I. Authorship Responsibility

To protect the integrity of authorship, only people who have significantly contributed to the research or project and manuscript preparation shall be listed as coauthors. The corresponding author attests to the fact that anyone named as a coauthor has seen the final version of the manuscript and has agreed to its submission for publication. Deceased persons who meet the criteria for coauthorship shall be included, with a footnote reporting date of death. No fictitious name shall be given as an author or coauthor. An author who submits a manuscript for publication accepts responsibility for having properly included all, and only, qualified coauthors.

II. Originality of Content

ASCE respects the copyright ownership of other publishers. ASCE requires authors to obtain permission from the copyright

holder to reproduce any material that (1) they did not create themselves and/or (2) has been previously published, to include the authors' own work for which copyright was transferred to an entity other than ASCE. For any figures, tables, or text blocks exceeding 100 words from a journal article or 500 words from a book, written permission from the copyright holder must be obtained and supplied with the submission. Each author has a responsibility to identify materials that require permission by including a citation in the figure or table caption or in extracted text.

More information can be found in the guide "Publishing in ASCE Journals: Manuscript Submission and Revision Requirements" (http://ascelibrary.org/doi/pdf/10.1061/9780784479018.ch05). Regardless of acceptance, no manuscript or part of a manuscript will be published by ASCE without proper verification of all necessary permissions to re-use. ASCE accepts no responsibility for verifying permissions provided by the author. Any breach of copyright will result in retraction of the published manuscript.

III. Copyright Transfer

ASCE requires that authors or their agents assign copyright to ASCE for all original content published by ASCE. The author(s) warrant(s) that the above-cited manuscript is the original work of the author(s) and has never been published in its present form.

The undersigned, with the consent of all authors, hereby transfers, to the extent that there is copyright to be transferred,

the exclusive copyright interest in the above-cited manuscript (subsequently called the “work”) in this and all subsequent editions of the work (to include closures and errata), and in derivatives, translations, or ancillaries, in English and in foreign translations, in all formats and media of expression now known or later developed, including electronic, to the American Society of Civil Engineers subject to the following:

• The undersigned author and all coauthors retain the right to revise, adapt, prepare derivative works, present orally, or distribute the work, provided that all such use is for the personal noncommercial benefit of the author(s) and is consistent with any prior contractual agreement between the undersigned and/or coauthors and their employer(s).

• No proprietary right other than copyright is claimed by ASCE.

• This agreement will be rendered null and void if (1) the manuscript is not accepted for publication by ASCE, (2) is withdrawn by the author prior to publication (online or in print), (3) ASCE Open Access is purchased by the author.

• Authors may post a PDF of the ASCE-published version of their work on their employers’ ***Intranet*** with password protection. The following statement must appear with the work: “This material may be downloaded for personal use only. Any other use requires prior permission of the American Society of Civil Engineers.”

• Authors may deposit the ***final draft*** of their work in an institutional repository or in their funding body’s designated archive upon publication in an ASCE Journal, provided the draft contains a link to the published version at ascelibrary.org, and may request public access 12 months after publication. “Final draft” means the

version submitted to ASCE after peer review and prior to copyediting or other ASCE production activities; it does not include the copyedited version, the page proof, a PDF, or full-text HTML of the published version.

• Authors may post the ***final draft*** of their work on open, unrestricted Internet sites 12 months after publication in an ASCE Journal, provided the draft contains a link to the published version at ascelibrary.org.

Exceptions to the Copyright Transfer policy exist in the following circumstances. Select the appropriate option below to indicate whether you are claiming an exception:

• U.S. GOVERNMENT EMPLOYEES: Work prepared by U.S. Government employees in their official capacities is not subject to copyright in the United States. Such authors must place their work in the public domain, meaning that it can be freely copied, republished, or redistributed. In order for the work to be placed in the public domain, ALL AUTHORS must be official U.S. Government employees. If at least one author is not a U.S. Government employee, copyright must be transferred to ASCE by that author.

• CROWN GOVERNMENT COPYRIGHT: Whereby a work is prepared by officers of the Crown Government in their official capacities, the Crown Government reserves its own copyright under national law. If ALL AUTHORS on the manuscript are Crown Government employees, copyright cannot be transferred to ASCE; however, ASCE is given the following nonexclusive rights: (1) to use, print, and/or publish in any language and any format, print and electronic, the above-mentioned work or any part thereof,

provided that the name of the author and the Crown Government affiliation is clearly indicated; (2) to grant the same rights to others to print or publish the work; and (3) to collect royalty fees. ALL AUTHORS must be official Crown Government employees in order to claim this exemption in its entirety. If at least one author is not a Crown Government employee, copyright must be transferred to ASCE by that author. • WORK-FOR-HIRE: Privately employed authors who have prepared works in their official capacity as employees must also transfer copyright to ASCE; however, their employer retains the rights to revise, adapt, prepare derivative works, publish, reprint, reproduce, and distribute the work provided that such use is for the promotion of its business enterprise and does not imply the endorsement of ASCE. In this instance, an authorized agent from the authors' employer must sign the form below. • U.S. GOVERNMENT CONTRACTORS: Work prepared by authors under a contract for the U.S. Government (e.g., U.S. Government labs) may or may not be subject to copyright transfer. Authors must refer to their contractor agreement. For works that qualify as U.S. Government works by a contractor, ASCE acknowledges that the U.S. Government retains a nonexclusive, paid-up, irrevocable, worldwide license to publish or reproduce this work for U.S. Government purposes only. This policy DOES NOT apply to work created with U.S. Government grants."	

Modelling Lifetime Performance of Monopile Foundations for Offshore Wind Applications

Abadie, C.N.
Department of Engineering, University of Cambridge, previously Department of Engineering Science, University of Oxford
ORCID: 0000-0002-5586-6560

Beuckelaers, W.J.A.P.
OffshoreWind.io bv, Diepestraat 201 C, 3080 Tervuren, Belgium, previously Department of Engineering Science, University of Oxford

Byrne, B.W.
Department of Engineering Science, University of Oxford
ORCID: 0000-0002-9704-0767

Houlsby, G.T.
Department of Engineering Science, University of Oxford
ORCID: 0000-0001-5807-8781

Burd, H.J.
Department of Engineering Science, University of Oxford
ORCID: 0000-0002-8328-0786

McAdam, R.A.
Ørsted Power (UK), previously Department of Engineering Science, University of Oxford
ORCID: 0000-0003-0292-3549

Contact details of corresponding author:
Email: cna24@cam.ac.uk
Phone no: +44 1223 3 30278
Address: Civil Engineering Building, National Research Facility for Infrastructure Sensing; 7a JJ Thomson Avenue, Cambridge, CB3 0FA

Dates text written and revised:
Paper first submitted on: 29/01/2021
This version: 24/08/2022

Abstract

This paper explores the application of a numerical method for modelling pseudo-random cyclic loading, at very large cycle numbers, to the design of offshore wind turbine foundations. The work expands the development of a novel constitutive modelling framework, HARM, described by Houlsby et al. (2017), with a calibration method outlined in Abadie et al. (2019). HARM captures both the non-linear hysteretic behavior during cycling and the accumulation of permanent deformation (ratcheting) with large cycle numbers in a rigorous, yet computationally efficient manner, enabling the computation of foundation response over a lifetime of loading. This paper demonstrates how the approach can be applied to the cyclic pile field testing from the PISA project (Byrne et al. 2020a). Following calibration, the model is used to assess pile response to three load signals representative of operational and extreme loads throughout the lifetime of a full scale wind turbine foundation: (i) a short storm, (ii) a 35h storm and (iii) a lifetime loading. The paper discusses how computational efficiency can be achieved whilst maintaining a high level of calculation accuracy.

Keywords

Lifetime performance, Cyclic loading, Monopile, Offshore wind, Constitutive modelling

Introduction

Offshore wind plays an important role in the transition to a green economy, with rapid development over the past decade, in particular in Europe, and more recently in East-Asia and North America. Offshore wind turbines are substantial structures, for which optimized and robust design is central to capital cost reduction, allowing a more rapid build-out of wind farms offshore, including in deeper water and with larger turbines. Offshore wind turbines are commonly supported by short rigid monopiles, typically of embedded length-to-diameter ratio 3 to 6 (see Figure 1).

The wind turbine structure is subjected to large lateral repetitive loads arising from the action of the winds, waves and currents, as well as inertial loads, leading to a combined moment and horizontal force at the top of the embedded pile. Due to the nature of the environmental loads, the design load scenarios include extreme lateral loads (Ultimate Limit State, ULS), cyclic load packets of variable amplitudes and magnitudes (Serviceability Limit State, SLS), and small amplitude loading but with very large cycle number (Fatigue Limit State, FLS), typically involving about 10^8 cycles. The design objective is to ensure sufficient capacity and limited deformation over 25 years of service life. For example, a maximum tilt rotation of the support structure is usually specified by the turbine manufacturer to guarantee good operation of the turbine (DNV 2014; Golightly 2014, Section 10.3.2.6, p. 173). Typically, the maximum tolerance for the foundation tilt over its lifetime (including installation tolerance) is 0.5 degrees (Achmus et al. 2009; DNV 2014; Lombardi et al. 2013; Malhotra 2011), with a maximum requirement of 0.25 degrees rotation induced by SLS (DNV 2014).

Recent research has led to improved design guidelines for ULS conditions (e.g. Byrne et al. 2017, 2019; Jeanjean et al. 2017; Puech 2017), that should lead to optimization of the next generation of monopiles. As foundation design for the ULS condition is further optimized, cyclic loading considerations may become the design limiting condition. However, tracking the effects of cyclic load history is an extremely complex problem, due to the non-linear behavior of soil, and can lead to prohibitive computational costs. As a result, cyclic design is typically assessed using empirical

methods (e.g. Achmus et al. 2009; LeBlanc et al. 2010a;b; Little and Briaud 1988; Poulos 1982) and/or by the application of safety factors on the ULS condition (e.g. API 2010; DNV 2014; O'Neill and Murchison 1983; Reese et al. 1974). However, these methods are approximate, do not account for load-sets of varying magnitude and cycle number, and therefore require conservative safety factors. In consequence, significant research on the simulation of high-cyclic monopile tilt has been undertaken in recent years. This includes conventional finite element-based approaches, but with improved cyclic constitutive models, such as by Liu et al. (2021, 2022), and whilst these might track the detailed cycling behavior well, they tend to be very computationally intensive for large cycle numbers. Alternative methods, focusing specifically on large cycle numbers, involve hybrid methods where detailed finite-element cycle-by-cycle modelling is used to calibrate a faster "high cycle accumulation" model, as illustrated by Staubach and Wichtmann (2020), building on earlier work by Wichtmann et al. (2010), and also described in the work of Page et al. (2020). These methods work well when there are uniform cycles applied but may not be so well adapted to non-uniform or pseudo-random cycling. A different approach is to adapt, typically by degrading, the conventional p-y model for the effects of cyclic loading through cyclic strain contour diagrams, calibrated by cyclic soil element testing, such as described by Zhang et al. (2020). These models do not capture the cycle-by-cycle behavior but might capture the overall response following a large number of cycles. A more sophisticated approach was taken by Kementzetzidis *et al*. (2022), who implemented a p-y model expressed in terms of the bounding surface approach, emhanced specifically to account for high numbers of cycles.

This paper presents a new modelling approach that can be used to predict cyclic loading effects on monopile response. The work is based on HARM (Hyperplastic Accelerated Ratcheting Model; Houlsby et al. 2017), a theoretical model that accurately captures both the hysteretic behavior commonly observed during cycling, as well as the accumulation of deformation with cycle number. For a constant amplitude load packet, with a high number of cycles, this model allows computation of the ratcheting effects to be "accelerated" rigorously (see below); thus faciltating, for example, the computation of foundation response over the wind turbine's lifetime (Abadie et al. 2020b). The objective of this paper is to demonstrate the advantages of HARM, first, through modelling of the PISA field pile test results (Byrne et al. 2020a), and then through calculations for three realistic

cyclic loading sequences for a full scale turbine. The selected load sequences are representative of an extreme storm event, a 35hr storm and a lifetime of loading for an offshore wind turbine foundation. The loading considered is uni-directional, but the approach can be extended to address multi-directional loading.

Modelling technique

Key Modelling Features

HARM is a constitutive modelling framework for cycling, derived within the hyperplasticity approach (Houlsby and Puzrin 2006), and developed for capturing ratcheting while conforming approximately to the well-established Masing behavior (Masing 1926). The modelling framework is summarized in Appendix A, and a detailed description can be found in Houlsby et al. (2017). The calibration method is outlined in Abadie et al. (2019), based on the experimental results of Abadie et al. (2017), with the key steps of the method summarized in Appendix B.

The model is based on a kinematic hardening multi-surface plasticity modelling framework, supplemented with an additional "ratcheting" element as shown in Figure 2 (see also Appendix A). The ratcheting element results in the accumulation of deformation with cycling, while the Masing behavior arises from the underlying multi-surface kinematic hardening model. The rate at which permanent deformation is accumulated during cycling is governed by the ratcheting rate, R_n. The shape of the hysteresis loop is defined by the backbone curve (see Appendix B), itself determined by the parameters H_0, H_n, k_n. One of the strengths of the model is that the amount of ratcheting strain, accumulated during *N* repetitions of any group of cycles, can be "accelerated" by simulating just one such group, whilst multiplying the ratcheting rate R_n by the factor *N*. This feature allows computationally efficient simulation of very long loading histories.

The model tracks each load increment, regardless of the load history, so that, in the case of multi-amplitude load packets, the model follows the response step-by-step without the need to introduce additional assumptions such as rainflow counting of cycles or the use of Miner's rule (e.g. LeBlanc et al. 2010a; Miner 1945). Modifications are needed to apply the acceleration technique when the load magnitude and/or amplitude change. In particular, each load-set of a

given magnitude, amplitude and cycle number $N_{cycle,packet}$ must be accelerated independently. A standard incremental calculation of the first cycle is needed, prior to acceleration of the remaining cycles in the load-set, to ensure that the Masing behavior is computed correctly. A long-term cyclic load history that contains a total of $N_{packets}$ of load-sets, requires the computation of at least $2N_{packets}$ of individual cycles as a basis for the acceleration technique. It is good practice to compute a total of $3N_{packets}$ cycles, with the first and last cycle of each packet computed incrementally in order to extract the cyclic response properties at the end of each load packet (e.g. stiffness, residual deformation, permanent ratcheting strain, etc.) excluding the effects of the acceleration process. Using this procedure, the ratcheting rate is accelerated by $R_{fac} = N_{cycle,packet} - 2$.

The model can be expressed as either a series (s-HARM, Figure 2(a)) or parallel (p-HARM, Figure 2(b)) configuration (Houlsby et al. 2017). For unidirectional response, Abadie et al. (2019) and Beuckelaers et al. (2018) demonstrate that the two models produce indistinguishable stress-strain responses when k_n, H_n and α_r are chosen appropriately. This is demonstrated in Figure 2(c-f), with parameters and ratcheting rate definition chosen following Abadie et al. (2019), (see Equation (21) and Table (2) of that paper). The series model is well adapted for load-controlled problems, while the parallel version is better suited for strain-control (e.g. for use within finite element codes). This offers possibilities of using the different forms for computational advantage, with confidence that the results obtained are indistinguishable for unidirectional loading, and very similar for more complex loadings.

Modelling method

This paper focuses on prediction of the global moment-rotation response of a monopile (Figure 1). Common approaches for lateral pile design are listed in Table 1. The HARM framework can be used to specify the constitutive response at any level of detail (macro-response of the pile, a Winkler model or local soil response) and could in principle be integrated within many of the current modelling approaches used for the design of monopiles. Because the model takes the monotonic pile response as the input backbone curve, it is naturally compatible with recent approaches for monotonic loading predictions, such as the PISA approach (Byrne et al. 2019,

2020b) or that described by Jeanjean et al. (2017). Either the 0-D or 1-D design approach can be developed, as illustrated in Figure 3.

The simplest, and fastest, approach would be the 0-D model: in this case the foundation reaction is captured using a macro-scale moment-rotation response (Figure 3) only. 0-D models provide an efficient link to structural analysis as they allow a very fast representation of the soil-structure interaction, but yield no information about the detailed load distribution in the pile. It is recognized that the lateral load-displacement "H-v_G" component can be added, as well as the induced cross-coupling terms between moment and horizontal force, but that aspect is not further developed here. The additional computational cost is likely to be marginal, but the gain in accuracy is also relatively small as the overall response is dominated by the moment-rotation behavior. For the calculations presented in this paper, the moment load is specified as input, with pile rotation computed; HARM is used in load-control mode, so that the series form, s-HARM, is adopted for the 0-D model.

The framework of the PISA approach (Byrne et al. 2017, 2019, 2020b) has been used to demonstrate the 1D implementation of the HARM approach. The soil reaction on the pile is captured by four soil reaction components: a distributed lateral load p, a distributed moment m, a base horizontal force H_e and a base moment M_e. The monotonic backbone curve (H_0, H_n, k_n) for each soil reaction component is derived from the conic function used in the PISA approach (as in Byrne et al. (2020a), but with the depth variation functions and parameters given in Table 8), with HARM adopted locally for the cyclic response for each of these components. The formulation of the 1D model demonstrates the use of the p-HARM approach.

As indicated in Table 1, HARM could in principle also be applied at an element level and implemented within a 3D FE calculation. Such an approach offers the possibility of formulating a link between parameter values established from element testing and those required for macroscopic pile modelling. Work is in progress in this area, but this approach has not yet been developed to a stage that firm conclusions can be drawn. Work is also in progress for

consideration regarding the applicability of this modelling approach to cases including more pronounced dynamics and/or pore pressure effects.

Calibration

Field test data

The HARM approach, at 0-D and 1-D, is applied to the PISA field pile tests at Cowden (Byrne et al. 2020c) to demonstrate that it produces realistic results by comparison with the tests. For the two different models, it is necessary to calibrate the following features at either macro level (0-D) or local soil reaction level (1-D) (see Figure 3):

1. The backbone curve, *i.e.* the values of H_0, H_n, k_n
2. The ratcheting behavior, *i.e*. the values of R_n

Three tests are used for this process: a monotonic test CM9, and two cyclic tests CM5 and CM6 (Byrne et al. (2020b). The properties of the test piles are given in Table 2, while the load sequences for CM6 and CM5 are shown in Table 3 and Table 4 respectively.

Zdravković et al. (2020) present a three dimensional finite element analysis for CM9, so that these calculations underpin calibration of the backbone curves for the HARM calculations. The ultimate capacity of the pile is calculated as the minimum moment at either a ground-level displacement of $v_{G,R} = 10\% \times D$ or a ground-level rotation of $\psi_{G,R} = 2°$. For the CM9 pile test data this gives:

$$H_R = 116.18\ kN,\ M_R = 1161.8\ kNm,\ v_{G,R} = 0.0762m = 0.1 \times D,\ \psi_{G,R} = 1.82° \quad \textbf{Equation 1}$$

When this criterion is applied to the CM9 3D FE computation this leads to:

$$H_R = 96.58kN,\ M_R = 965.8\ kNm,\ v_{G,R} = 0.0762m = 0.1 \times D,\ \psi_{G,R} = 1.73° \quad \textbf{Equation 2}$$

CM6 involves a short series of cycles of three load-sets at increasing load magnitudes, while CM5 involves a more extensive series of load-sets, of larger numbers of cycles. Calibration follows the steps outlined by Abadie et al. (2019), in which the model is expressed in terms of a normalized "stress" and normalized "strain". For the 0-D model:

$$\sigma = \frac{M}{M_R} \quad \textbf{Equation 3}$$

$$\varepsilon = \frac{\psi_G}{\psi_{G,R}}$$ **Equation 4**

with the values of M_R and $\psi_{G,R}$ from Equation 2. When $M = M_{max}$, $\sigma_{max} = \zeta_b$ with ζ_b defined by Leblanc et al. (2010b).

Calibration method: Backbone curve

Test CM9 underpins the backbone curve calibration. For both 1-D and 0-D models, the stiffness H_n and strength k_n parameters for the model are calculated using the methodology set out by Houlsby et al. (2017) and Abadie et al. (2019), and summarized in Appendix B.

- 1-D model: a set of parameterized soil-reaction components was defined using the PISA approach. For this purpose the 'representative offshore site' parameters presented in Byrne et al. (2020b) cannot be used directly, as the relationship between the (reduced scale) pile dimensions and the soil stratigraphy at the Cowden test site differ significantly from the conditions employed in the Byrne et al. (2020b) calibration. A separate calibration procedure was therefore conducted for the Cowden site, employing data from the 3D finite element analyses in Zdravkovic et al. (2020). The PISA design model employs a (smooth) conic function for the soil reaction curves. These soil reaction curves were used to calibrate HARM models for the distributed lateral load and moment components applied to the pile, together with the base horizontal force and moment components. The backbone curve is computed using the PISA method described in Byrne et al. (2020a), but with the depth variation functions and parameters given in Table 8).
- 0-D model: to match with the 1-D calculation the 3D FE data for CM9 are used directly as the reference, with the moment-rotation curve at ground-level determining the values of k_n and H_n.

The calculations from the 0-D and 1-D models are compared to the test data and the 3D FE data in Figure 4. A comparison (Figure 4(a)) is also made with the experimental framework from Abadie et al. (2018) and Abadie (2015), with the power-law fit having the exponent $1/m_h$, and a value $m_h = 3$, consistent with the previous work gathered and published in Abadie et al. (2019). Either

curve can be used as an input to calibrate the backbone curve, following the method outlined in Appendix B.

Without ratcheting, the 1-D and 0-D models result in a similar macro-response backbone curve, consistent with the PISA approach (Figure 4(b,c); 1-D / 0-D kinematic hardening, no HARM). Also note that the 0-D model does not use the pile geometry (*L* or *D*) as an explicit input, although this information is implicit in the parameters defining the backbone curve and the ultimate capacity. In the following, a single calibration is applied to the model and then used to predict the three different pile responses. No allowance is made for the minor variations in ground conditions at the different pile locations, even though these resulted in minor variations in the pile test results.

Calibration method: Ratcheting strain

The small fraction of strain accumulated at each load increment is controlled by the ratcheting rate, R_n, which is the only parameter that needs to be calibrated to specify the ratcheting behavior. The introduction of ratcheting strain is the main novelty in the HARM framework, and its calibration is summarized in Appendix B, which describes a simplified version of the procedure in Abadie (2015), Abadie et al. (2017b) and Beuckelaers et al. (2017). It also corresponds to that used in Abadie et al. (2017a) and Abadie et al. (2020b). The method adopts the assumption that ratcheting effects observed at a macro-level are reflected in the soil reaction curves below ground. Therefore, the values of the dimensionless 0-D HARM parameters are applied to all four components of the soil reaction curves for 1-D HARM. The calibration uses field test data from CM5 and CM6, with the extracted parameters checked against model test results from Abadie (2015). The methodology follows the steps described by Abadie et al. (2019). The form of the ratcheting rate R_n is chosen to capture (i) a decreases with load history, and (ii) an increase with the load level, using:

$$R_n = R_o \left(\frac{k_n}{k_U}\right)\left(\frac{\beta}{\beta_o}\right)^{-m_r}\left(\frac{|\sigma|}{\sigma_0}\right)^{m_s} \qquad \textbf{Equation 5}$$

Where β is the accumulated ratcheting strain, which acts as a memory of the cyclic history; β_0 is an arbitrarily small value used for normalization purposes; σ_0 is the ultimate stress level. Details

of the calibration procedure are given in Appendix B, and the resulting values for each of the parameters in Equation 5 are provided in Table 5.

Correction of the backbone curve

The addition of ratcheting to the kinematic hardening model leads to a stretch in the x-direction of the backbone curve,. This is caused by the accumulated deformation that occurs during the initial loading (shown in Figure 4(b,c)). To adjust for this effect, a correction has to be made to balance the additional ratcheting strain, in order to recover the original backbone curve. In this instance the adjustment is achieved using a standard optimization solver, such as *fminsearch* (MATLAB), to revise the values of H_n that define the backbone curve. For the 1-D model this is performed for each reaction curve at each Gauss point down the pile. There are minor differences between the original backbone calculation and the backbone calculation after correction (with ratcheting) due to the tolerances adopted in the optimization. The following calculations adopt the 0-D and 1-D monotonic response after correction, to provide a common baseline for comparison (see HARM 0-D / 1-D, with optimization in Figure 4(b,c)).

Further improvement of the calculations could be achieved through optimization of the ratcheting parameters (Abadie et al. 2019), but this is not pursued further here, as it would make no material difference to the conclusions drawn from the study.

Modelling of field test results: PISA

The 0-D and 1-D models described above are first used to simulate the PISA field tests. To retain accuracy and efficiency, each cycle is divided into 500 increments for the 0-D model and 20 increments for the 1-D model.

Short-term cyclic loading: CM6

The load sequence of CM6 (Table 3) is sufficiently short that a full incremental modelling approach can be undertaken using the 1-D and 0-D models. The results shown in Figure 5 demonstrate that the analyses capture the cyclic behavior well, with the deviation explained by:

1. Variations in ground properties between the pile sites, leading to minor differences in the backbone curves between tests CM9 and CM6
2. The predictions from HARM 1-D and HARM 0-D only account for kinematic hardening and ratcheting, but do not explicitly account for other relevant phenomena, such as gapping and rate dependency, which might be required to capture the test results more accurately. These developments are not pursued in this paper.
3. The adopted ratcheting calibration focuses on the response to large numbers of cycles, rather than short-term cyclic loading.

For completeness, the results in Figure 5 show the evolution of the residual rotation (i.e. rotation after unloading to zero load, which, for 1-way loading corresponds to the minimum load) with cycle number, and the evolution of the accumulated rotation for each load packet with cycle number. Figure 5 also shows the amount of ratcheting strain generated by the load history within the 0-D model, demonstrating that the contribution of ratcheting to the overall response is significant in this case.

The results obtained from the 1-D and 0-D models match reasonably well, for instance Figure 5(d) shows that the calculated accumulated rotation at minimum and maximum load are the same from both analyses for a given load packet. These results demonstrate that:

1. Using a 0-D model for calculations, which is more time efficient, might be sufficient for some design scenarios, such as for conceptual design. In this instance the simulation with the 0-D model was computed in 0.089 s using 500 increments per cycle on a PC with an Intel® core i7-8565U and 16GB RAM. The same loading sequence with the 1-D model with 20 increments per cycle required about 15 minutes, using a similar computer.
2. The results give confidence that some of the ratcheting parameters, and probably m_r and m_s, might be invariant with respect to the level of detail used in the analysis.

While the 0-D model provides very fast results, there are advantages in running simulations using the 1-D model. Principally the 1-D model provides information on the soil reactions down the length of the pile, which might indicate the soil “utilization” at a given depth due to the loading

history, as illustrated in Figure 6. In that figure note that (a) at the highest elevation the displacements are of course largest, (b) further down the pile the displacements are smaller, but the reactions are larger because of the higher soil stiffness and strength, (c) towards the toe of the pile the displacements are in the reverse direction.

Long-term cyclic loading: CM5

Unlike CM6, the load-sets for CM5 (Table 4) involve large numbers of cycles, and so an appropriate acceleration programme is used to make the calculation more efficient, especially for the 1-D model case. In both the approaches described below, for the 0-D model 500 increments are used per load cycle, and 40 surfaces are employed in the multisurface model. These choices allow each cycle to be defined to a high precision, as confirmed by sensitivity studies. For each load increment an iteration is carried out in which the plastic strain, ratcheting rate and "generalized stress" is recomputed, and convergence is accepted when the yield surface is within a tolerance of 0.0001. Two approaches are adopted:

(i) The first approach – which tracks the loading path precisely – consists of modelling each individual packet, but accelerating the load-sets involving large cycle numbers. An example of this is given with acceleration Programme 1 in Table 6. In this table, the computational time provided for the 0-D model corresponds to the time needed to compute the constitutive equations to resolve the HARM model for all the cycle number of the accelerated programme. This reduces the required number of cycles for computation by a factor of 50. While the reduction using this method is significant, this still may not be enough for an efficient calculation using the 1-D model.

(ii) To reduce the calculation time further, a second approach involves a selection of relevant load cases for computation, using the acceleration method. It is assumed (based on experience from past analyses) that the majority of plastic and ratcheting deformation is caused when loading exceeds the maximum past load, together with the cyclic load packet of similar amplitude. For CM5 this makes load packets 1, 2, 3 and 11 most critical, while load-sets 4, 5, 6, 7, 8, 9 and 10 (which all involve load magnitudes lower than the maximum historic load) could be ignored. An example of

this approach is shown in accelerated Programme 2 in Table 6, which reduces the number of cycles by a further factor of 4.6 compared to Programme 1.

It is emphasized that the timings presented in Table 6 would be highly dependent on the hardware and software used, as well as choices of increment sizes, tolerances and the detailed implementation of the computational algorithm. They should be regarded as indicative only of the relative computation times required for the different strategies adopted. Clearly both the "acceleration" technique (reducing timings by a factor of about 50) and the elimination of smaller load packets (reducing timings by a further factor of 4.6) are useful in this regard, whilst maintaining comparable levels of accuracy, although small differences are observed as detailed below.

The computed results using the two programmes are displayed in Figure 7, showing that Programme 2 compares well to the incremental and Programme 1 calculations. The two methods identify how computational efficiency can be achieved without compromising calculation accuracy. Both 100 and 500 increments per cycles were tested, showing similar results, but with the 100 increment calculation deviating by up to 5% above the original backbone curve. Further development of this approach might lead to an optimal selection and acceleration procedure for relevant load packets given the loading history to be modelled.

Finally, the results from the 0-D and 1-D modelling compare favorably in Figure 7, adopting the accelerated Programme 2 for input. Note that, for the bottom left figure, the accumulated deformation induced by load packet 1 has not been plotted. This is because the maximum load is very low, and hence, close to the elastic limit, inducing very little accumulated deflection (none in the case of the 0-D modelling).

Assessment of lifetime performance

The calibrated 0-D modelling framework is now used to explore pile response to three loading regimes relevant to design: (i) a short storm event, (ii) a 35 hour storm and (iii) a lifetime loading. Table 7 summarizes the relevant values for each of the three load signals considered. The 1-D modelling framework could also be used, but would not be as computationally efficient.

The values of moment and rotation at ultimate capacity are required for defining σ_0 and ε_U (Equation 3 and Equation 4), and for normalization of the ratcheting behavior. Rotation at ultimate capacity is defined as ε_U=2 degrees. σ_0 is calculated based on the maximum load event that occurs during the short storm (the largest load event of the three load regimes), multiplied by a factor of safety of 1.35 (*i.e.* $\sigma_0 = M_{ULS}$ = FoS × (max load), giving M_{ULS} = 532 MNm.

The backbone curve adopted for the analysis is that defined for the PISA field test calibration, but scaled to represent the response of a full scale monopile subjected to realistic storm loading. This involves scaling by $(\psi_{ULS,Design}/\psi_{ULS,PISA})$ for the ε axis and $(M_{ULS,Design}/M_{ULS,PISA})$ for the σ axis. The H_n and k_n values are also scaled by $(\psi_{ULS,Design}/\psi_{ULS,PISA})/(M_{ULS,Design}/M_{ULS,PISA})$ and $(M_{ULS,Design}/M_{ULS,PISA})$ respectively. The ratcheting parameters, being dimensionless, do not require further scaling. The 0-D model does not require further information on pile geometry (*L* or *D*) for input, as that is captured fully by the backbone curve. Bespoke calibration for specific field cases would be required but is not covered here – it could be calibrated by using the PISA 1-D model design approach. The purpose of the following calculations is to demonstrate how the HARM approach can be used to explore pile response under different loading regimes. With sufficient computational resource the calculations could also be achieved with the 1-D model.

Short storm

The short storm can be modelled entirely incrementally, with no need for acceleration. The signal (Figure 8(a)) consists of a small to medium pseudo-random signal dominated by a peak load. The results of the simulation, given in Figure 8(b,c), display the evolution of the deformation with load and cycle number, as well as the residual rotation after the final unloading to zero. These demonstrate that the effect of ratcheting to the overall response is limited, with the response dominated by deformations induced by the largest load event.

35h storm

The 35 hour storm load signal as initially provided consisted of multi-amplitude load packets, arranged in an artificial and unrealistic sequence (Figure 9(a)) suited for rainflow counting, which might bias the results. To obtain more realistic results, the load sequence was re-arranged to a random order (Figure 9(b)). Different sequences were adopted, demonstrating that the order of

the random series has little influence on the overall outcome for the 35 hour storm. The response was computed using both accelerated and incremental forms, giving identical results.

The results of the incremental calculation are shown in Figure 9(b) and (c), where the response appears to be dominated by the largest events, with ratcheting effects again being of second order. This aligns with results from the short storm, suggesting that accurate prediction of the backbone curve is crucial for the modelling of storm load regimes.

Lifetime load series

The lifetime load series (Table 7) was modelled using the acceleration technique described earlier. As for the 35 hour storm, the original loading sequence consisted of a series of multi-amplitude load packets, arranged in an artificial and unrealistic sequence (Figure 10(a)). This was re-ordered into a random sequence (Figure 10(b)).

The resulting response is shown in Figure 10(c) and (d). Here, the effect of ratcheting on the response is much more significant, becoming the main contributor to the final deformation. It is noteworthy that both the short storm and 35 hour storm involve a number of one-way loading events, while the lifetime loading involves both one-way and two-way loading events. This allows some investigation of the influence of 2-way loading on the response, addressing whether, as a result of the change in loading direction, the accumulated ratcheting strain decreases or is cancelled.

Discussion

Load history effect

By combining the short storm and lifetime load signals, the effect of a storm event at different stages within the lifetime loading can be investigated. The results are shown in Figure 11, where three cases are studied, involving: (1) a storm immediately following installation, followed by the lifetime, (2) a storm during the middle of the lifetime and (3) a storm following the lifetime event. The results show that the time at which the storm occurs has a noticeable effect on the overall final response.

When the storm occurs prior to the lifetime loading the final rotation is largest, principally as the pile has not experienced any hardening behavior prior to the storm, so that the effects of the large storm load on both the plastic and ratcheting deformation are maximum. Ratcheting generated by the subsequent lifetime loading is similar to the “no storm” case, because the initial storm event is too short to have had any significant impact on decreasing the ratcheting rate.

Conversely, the scenario that generates the least deformation appears to be when the storm occurs during the lifetime loading. Hardening occurs during the first half of the lifetime enabling a stiffer response to the large storm load event, limiting the amount of plastic and ratcheting deformations. Following the large load event, the ratcheting rate appears to drop significantly, with the remaining half lifetime of loading leading to reduced accumulated ratcheting strain.

Finally, the case with the storm at the end is only slightly less severe than if it occurs at the beginning, in terms of maximum total deformation, and much less severe when the ratcheting strain and residual rotation are considered. Here, the cyclic load history has a beneficial effect on the large load event by (i) reducing the ratcheting rate by a significant proportion before the large load is applied, so that the dependence on stress level and the rate is counter-balanced, and, (ii) the response is hardened, resulting in a stiffer response to the large load. As a result, the large load has little impact on the accumulated ratcheting strain.

Although only a small number of simulations are shown, they demonstrate how HARM can be used to improve understanding of cyclic loading effects. Minor variations in the choice of calibration parameters are unlikely to change the main conclusions that are drawn. However, the importance of calibrating the model against robust data is emphasized.

Minimum load threshold

The possible existence of a threshold value $\tau > 0$ (cutting threshold) below which any cyclic load contained between $[-\tau, \tau]$ can be ignored (Figure 12(a)), is an important concept that could affect cyclic pile design calculation time. It has been observed from the calculations that small cycles

usually have a limited effect on the final response, and so could potentially be disregarded to improve modelling efficiency.

An initial study had already been performed using the signal Figure 6 (Table 6) by omitting certain load-sets that were not perceived as important. The results of the analyses (Figure 5(b,d)) show that the evolution of the peak and final deflection is not affected by this simplification, while enabling significant computational time savings (Table 6). A more systematic approach is to progressively remove load-sets using the procedure illustrated in Figure 12(a). The evolution of the peak and residual deflection, as a fraction of the corresponding deflection obtained with the entire signal is shown in Figure 12(b), demonstrating that, for this load sequence, any load cycle below 50% of the maximum load did not affect the final response significantly. Cutting these load cycles from the simulated load signal reduced the number of load packets by about 58%. To illustrate the computational gains, the number of load cases and computational time have also been plotted. Above the 50% threshold, further simplification of the load signal leads to an error in estimation that depends entirely on when the large load events occur.

Further development

For the model to be routinely applied in design, some areas require further development:

(1) Further understanding of the calibration process is needed, for example to relate the values obtained from the macro-behavior to that of the local soil reaction. The comparison of the 1-D and 0-D models provides confidence that similar ratcheting parameters can be used in each of these approaches. The importance of stress level and scale needs to be further explored, see for instance Richards et al. (2020).

(2) Experimental results from model scale tests (e.g. LeBlanc et al., 2010, Klinkvort, 2012, Abadie, 2015, Kirkwood, 2015) demonstrate a change in secant stiffness with load history. This was not observed in the PISA field test results, and hence, was not included in the modelling subsequently adopted.

(3) The modelling explores loads in a single direction. However, full-scale monopile loading is likely to be multi-directional. It is anticipated that multi-directionality may have a

beneficial effect on the accumulated rotation and any subsequent change of foundation properties (*e.g.* damping, stiffness). See Richards et al. (2020).

(4) The PISA tests identified that rate effects are important for both the Cowden clay and the Dunkirk sand site (Byrne et al., 2020c; McAdam et al., 2020). Such effects can be readily incorporated into the modelling framework that has been described here, see Beuckelaers (2017).

(5) The numerical modelling for the PISA project, and observations of the PISA field testing, identified that gapping around the pile, particularly for clay soils, may be important. Such effects could potentially be incorporated for the 1-D model, but would introduce a significant degree of complexity to the work. The PISA design method, which is calibrated against the numerical modelling, already explicitly accounts for gapping around the pile for the Cowden clay (as the numerical analyses allowed the gap to form). Therefore, if the cyclic modelling adopts the backbone curve from PISA then the integrated effect of gapping will be captured.

Conclusion

This paper demonstrates the capabilities of the HARM approach for modelling the cyclic loading response of offshore wind turbine foundations to realistic load scenarios. The model was first calibrated and validated against the PISA cyclic tests, expanding application of the calibration procedure described by Abadie et al. (2019) to large-scale field test data. The calibrated model was then applied to three realistic loading cases, including to two extreme cyclic loading events as well as a lifetime load signal of 3×10^8 cycles. The results demonstrate that, for the adopted set of parameters, which were intended to represent a full scale pile with an appropriate safety factor on loads, the residual pile deflection remains below the design limit of 0.5 degrees for all three cases, but is close to this limit for the case where an extreme storm would occur immediately following installation and then followed by a lifetime of loading. The model shows promising capabilities for application to design of monopile foundations to very large cycle number in a computationally efficient manner, with avenues for further optimization to reduce computational time if needed.

Data Availability Statement

Some or all data, models, or code that support the findings of this study are available from the corresponding author upon reasonable request. Some or all data, models, or code generated or used during the study are proprietary or confidential in nature and may only be provided with restrictions.

Acknowledgements

The authors acknowledge the contributions by Ørsted in providing support and funding for the development of this work. Byrne is supported by the Royal Academy of Engineering under the Research Chairs and Senior Research Fellowships scheme.

References

Abadie, C. N. (2015). “Cyclic Lateral Loading of Monopile Foundations in Cohesionless Soils.” DPhil Thesis, University of Oxford.

Abadie, C. N., Byrne, B. W., and Houlsby, G. T. (2017). “Modelling of Monopile Response to Cyclic Lateral Loading in Sand.” Offshore Site Investigation Geotechnics 8th International Conference Proceedings, 1046–1053.

Abadie, C. N., Byrne, B. W., and Houlsby, G. T. (2018). “Rigid pile response to cyclic lateral loading: laboratory tests.” Géotechnique, 69(10), 863–876. doi: 10.1680/jgeot.16.P.325

Abadie, C. N., Byrne, B. W., Houlsby, G. T., Burd, H. J., McAdam, R. A., and Beuckelaers, W. J. A. P. (2020b). “Modelling of offshore wind monopile lifetime performance.” 4th International Symposium on Frontiers in Offshore Geotechnics (ISFOG), Austin, Texas.

Abadie, C. N., Houlsby, G. T., and Byrne, B.W. (2019). “A method for calibration of the Hyperplastic Accelerated Ratcheting Model (HARM).” Computers and Geotechnics, 112, 370–385. doi: 10.1016/j.compgeo.2019.04.017

Achmus, M., Kuo, Y.-S., and Abdel-Rahman, K. (2009). “Behavior of monopile foundations under cyclic lateral load.” Computers and Geotechnics, 36(5), 725–735. doi: 10.1016/j.compgeo.2008.12.003

API. (2010). Recommended Practice for Planning, Designing and Constructing Fixed Offshore Platforms, RP2A-WSD, Washington. American Petroleum Institute.

Beuckelaers, W. J. A. P. (2017). “Numerical Modelling of Laterally Loaded Piles for Offshore Wind Turbines.” DPhil Thesis, University of Oxford.

Beuckelaers, W. J. A. P., Houlsby, G. T., and Burd, H. J. (2018). “A comparison of the series and parallel Masing-Iwan model in 2D.” Numerical Methods in Geotechnical Engineering IX, Porto, Portugal, 173–178.

Byrne, B. W., Burd, H. J., Zdravkovic, L., Abadie, C. N., Houlsby, G. T., Jardine, R. J., Martin, C. M., McAdam, R. A., Pacheco Andrade, M., Pedro, A. M. G., Potts, D. M., and Taborda, D. M. G. (2019). “PISA Design Methods for Offshore Wind Turbine Monopiles.” Offshore Technology Conference, Offshore Technology Conference, Houston, Texas.

Byrne, B. W., Houlsby, G. T., Burd, H. J., Gavin, K. G., Igoe, D. J. P., Jardine, R. J., Martin, C. M., McAdam, R. A., Potts, D. M., Taborda, D. M. G., and Zdravković, L. (2020a). “PISA design model for monopiles for offshore wind turbines: application to a stiff glacial clay till (PISA#7).” Géotechnique, 70(11), 1030–1047. doi: 10.1680/jgeot.18.P.255.

Byrne, B. W., McAdam, R. A., Burd, H. J., Beuckelaers, W. J. A. P., Gavin, K. G., Houlsby, G. T., Igoe, D. J. P., Jardine, R. J., Martin, C. M., Muir Wood, A., Potts, D. M., Skov Gretlund, J., Taborda, D. M. G., and Zdravković, L. (2020b). “Monotonic laterally loaded pile testing in a stiff glacial clay till at Cowden (PISA#3).” Géotechnique 70(11), 970-985. doi: 10.1680/jgeot.18.PISA.003

Byrne, B. W., McAdam, R. A., Burd, H. J., Houlsby, G. T., Martin, C. M., Beuckelaers, W. J. A. P., Zdravkovic, L., Taborda, D. M. G., Potts, D. M., Jardine, R. J., Ushev, E., Liu, T., Abadias, D., Gavin, K., Igoe, D., Doherty, P., Gretlund, J. S., Andrade, M. P., Wood, A. M., Schroeder, F., Turner, S., and Plummer, M. (2017). “PISA: New Design Methods for Offshore Wind Turbine Monopiles.” Offshore Site Investigation Geotechnics 8th International Conference Proceedings, 142–161.

DNV. (2014). Offshore Standard DNV-OS-J101, Design of offshore wind turbine structures.

Golightly, C. (2014). “Tilting of monopiles - Long, heavy and stiff; pushed beyond their limits.” Technical Note, Ground Engineering, (January) 20-23.

Houlsby, G.T., Abadie, C.N., Beuckelaers, W.J.A.P., and Byrne, B.W. (2017). “A model for nonlinear hysteretic and ratcheting behaviour.” International Journal of Solids and Structures, 120, 67-80. doi: 10.1016/j.ijsolstr.2017.04.031

Houlsby, G. T., and Puzrin, A. M. (2006). Principles of Hyperplasticity. Springer Verlag

Jeanjean, P., Zhang, Y., Zakeri, A., Andersen, K., Gilbert, R., and Senanayake, A. (2017). “A Framework for Monotonic P-Y Curves in Clays.” Offshore Site Investigation Geotechnics 8th International Conference Proceedings.

Kementzetzidis, E., Pisano, F. and Metrikine, A.V. (2022) A memory-enhanced p-y model for piles in sand accounting for cyclic ratcheting and gapping effects, Computers and Geotechnics, Vol. 148, Article 104810, DOI: 10.1016/j.compgeo.2022.104810

603 Kirkwood, P. B. (2015). “Cyclic lateral loading of monopile foundations in sand.” PhD Thesis,
604 University of Cambridge.
605 Klinkvort, R. T. (2012). “Centrifuge modelling of drained lateral pile-soil response.” PhD Thesis,
606 DTU.
607 LeBlanc, C., Byrne, B. W., and Houlsby, G. T. (2010a). “Response of stiff piles to random two-
608 way lateral loading.” Géotechnique, 60(9), 715–721. doi: 10.1680/geot.09.T.011
609 LeBlanc, C., Houlsby, G. T., and Byrne, B. W. (2010b). “Response of stiff piles in sand to long-
610 term cyclic lateral loading.” Géotechnique, 60(2), 79–90. doi: 10.1680/geot.7.00196
611 Little, R., and Briaud, J.-L. (1988). Cyclic horizontal load tests on six piles in sands at Houston
612 Ship Channel. Research report 5640 to USAE Waterways Experiment Station. Texas
613 A&M University, USA..
614 Liu, H., Kementzetzidis, E., Abell, J.A. and Pisano, F. (2021). From cyclic sand ratcheting to tilt
615 accumulation of offshore monopiles: 3DFE modelling using SANISAND-MS.
616 Géotechnique, Ahead of print. doi:10.1680/jgeot.20.P.029.
617 Liu, H., Pisano, F., Jostad, H.P. and Sivasithamparam, N. (2022). Impact of cyclic strain
618 accumulation on the tilting behaviour of monopiles in sand: An assessment of the Miner’s
619 rule based on SANDISAND-MS 3D FE modelling. Ocean Engineering 250 110579.
620 Lombardi, D., Bhattacharya, S., and Muir Wood, D. (2013). “Dynamic soil-structure interaction of
621 monopile supported wind turbines in cohesive soil.” Soil Dynamics and Earthquake
622 Engineering, 49, 165–180. doi: 10.1016/j.soildyn.2013.01.015
623 Malhotra, S. (2011). Chapter 10 - Selection, Design and construction of Offshore Wind Turbine
624 Foundations (online). INTECH Open Access Publisher. (accessed 03 May 2022)
625 Masing, G. (1926). “Eiganspannungen und Verfestigung beim Messing.” Proceedings for the 2nd
626 International Congress of Applied Mechanics.
627 Miner, M. A. (1945). “Cumulative damage in fatigue.” Journal of applied mechanics 12(3), 159-
628 165. doi: 10.1115/1.4009458
629 O’Neill, M. W., and Murchison, J. M. (1983). An evaluation of p-y relationships in cohesionless
630 soils. Research report 82-41-1 to the American Petroleum Institute and GT-DF02-83 to
631 the University of Houston, Department of Civil Engineering.
632 Page, A.M., Klinkvort, R.T., Bayton, S., Zhang, Y. and Jostad, H.P. (2020). A procedure for
633 predicting the permanent rotation of monopiles in sand supporting offshore wind turbines.
634 Marine Structures 75 102813
635 Poulos, H. G. (1982). “Single pile response to cyclic lateral load” Journal of the Geotechnical
636 Engineering Division, 108(GT3), 355–375. doi: 10.1061/AJGEB6.0001255
637 Puech, A. (2017). Recommandations pour le dimensionnement des pieux sous chargements
638 cycliques projet national SOLCYP.
639 Reese, L. C., Cox, W. R., and Koop, F. D. (1974). “Analysis of laterrally loaded piles in sand.”
640 Proceedings of the 6th Offshore Technology Conference, Houston 2.
641 Richards, I.A., Byrne, B.W., and Houlsby, G.T. (2020). “Monopile rotation under complex cyclic
642 lateral loading in sand.” Géotechnique 70(10), 916-930. doi: 10.1680/jgeot.18.P.302
643 Staubach, P. and Wichtmann, T. (2020). Long-term deformations of monopile foundations for
644 offshore wind turbines studied with a high-cycle accumulation model. Computers and
645 Geotechnics 124, 103553.
646 Wichtmann, T., Niemunis, A., and Triantafyllidis, T. (2010). “Strain accumulation in sand due to
647 drained cyclic loading: On the effect of monotonic and cyclic preloading (Miner’s rule).”
648 Soil Dynamics and Earthquake Engineering, 30(8), 736–745. doi:
649 10.1016/j.soildyn.2010.03.004
650 Zdravković, L., Taborda, D. M. G., Potts, D. M., Abadias, D., Burd, H. J., Byrne, B. W., Gavin, K.
651 G., Houlsby, G. T., Jardine, R. J., Martin, C. M., McAadam, R. A., and Ushev, E. (2019).
652 “Finite-element modelling of laterally loaded piles in a stiff glacial clay till at Cowden
653 (PISA#5).” Géotechnique 70(11), 999-1013. doi: 10.1680/jgeot.18.PISA.005
654 Zhang, Y., Andersen, K.H., Jeanjean, P., Karlsrud, K. and Haugen, T. (2020) Validation of
655 monotonic and cyclic p-y framework by lateral pile load tests in stiff, overconsolidated
656 clay at the Haga site. ASCE Journal of Geotechnical and Geoenvironmental Engineering
657 146 9 04020080
658

Appendix A: HARM modelling framework

The HARM framework used here is described in Houlsby et al. (2017). That paper proposes various options for the choice of some variables, and in particular for the definition of ratcheting and hardening strains and for the evolution of the ratcheting rate. It presents formulations for both parallel and series forms of the model, and for both rate dependent and rate-independent media. To apply the model to monopile design, choices described below and in the main body of the paper have to be made. For consistency, the notation used here follows Houlsby et al. (2017). Thus any load quantity ("*H*" or "*M*", but also soil lateral reaction "*p*" or moment "*m*") is referred to in terms of stress "σ" and any deformation quantity (displacement "*v*", rotation "ψ"), in terms of strain "ε".

The constitutive response observed in Figure 2 can be considered as the result of two phenomena: one producing the hysteresis loop and one achieving ratcheting (Figure 13). The hysteretic behavior, as shown on the left of Figure 13, is commonly achieved using a multi-surface kinematic hardening model, as shown schematically in Figure 2(a) or (b), without the ratcheting element in red. On loading the system, the springs (H_n) of each individual unit contribute to the global response when the corresponding slider reaches the threshold value (k_n). The strain of each unit contributes to the global response, resulting in a **backbone curve** as depicted in Figure 14.

The novelty of the HARM model lies in the introduction of a new feature, the ratchet shown in red in Figure 2(a, b), that results in an additional ratcheting strain. The plastic deformation of the kinematic hardening model is supplemented by a small quantity –ratcheting strain α_r – which is a small fraction of the plastic strain. This results in the total strain response 'slipping' from one cycle to the next, producing a hysteresis loop that does not close at the end of each cycle (right hand of Figure 13), in contrast to the underlying kinematic hardening model (left hand, Figure 13) which never exhibits ratcheting. The small fraction of accumulated strain is controlled by the ratcheting rate, *R*, which is the only parameter that needs calibration for the ratcheting behavior.

688 The key equations that define the s-HARM framework, used for the 0-D model, are provided
689 below. The “free energy” (in either Helmholtz or Gibbs form) is defined by:

$$f = \sum_{n=1}^{N_S} \frac{H_n}{2}(\varepsilon - \alpha_n - \alpha_r)^2 + \frac{H_{N_S+1}}{2}(\varepsilon - \alpha_r)^2 \qquad \textbf{Equation 6}$$

$$g = -\frac{1}{2E_0}\left(\sigma + \sum_{n=1}^{N_s} H_n \alpha_n\right)^2 - \sigma\alpha_r + \sum_{n=1}^{N_s} \frac{H_n}{2}\alpha_n^2 \qquad \textbf{Equation 7}$$

690

691 The dissipated power is given by:

$$d = \sum_{n=1}^{N} (k_n|\dot{\alpha}_n|) + \sigma\dot{\alpha}_r \qquad \textbf{Equation 8}$$

692

693 To maintain options for development of both the series and parallel models, the definition of
694 ratcheting strain is chosen to ensure the same results for unidirectional loading with either model.
695 This requires the ratcheting strain to be a function of the dissipated energy within any unload-
696 reload cycle. This is achieved through the constraint Equation 9:

$$c_r = \dot{\alpha}_r - S(\sigma)R\sum_{n=1}^{N_S}\left(\frac{k_n}{\sigma_0}\right)|\dot{\alpha}_n| = 0 \qquad \textbf{Equation 9}$$

697 The parameter β is then defined by a further constraint as the accumulated ratcheting strain,
698 which acts as a memory of the cyclic history by summing the ratcheting strain from each
699 increment.

$$c_\beta = \dot{\beta} - |\dot{\alpha}_r| = 0 \qquad \textbf{Equation 10}$$

700

701 Following the method outlined in Houlsby et al. (2017)), the constraints can be incorporated into
702 the dissipation function using the method of Lagrangean multipliers:

$$d^* = \sum_{n=1}^{N} (k_n|\dot{\alpha}_n|) + \sigma\dot{\alpha}_r + \Lambda_r c_r + \Lambda_\beta c_\beta \qquad \textbf{Equation 11}$$

From these basic definitions it is possible to define the yield surface, which may be expressed in terms of stresses as:

$$\forall n \in [1, N_S] \quad y_n = |\sigma - H_n \alpha_n| - k_n \leq 0 \qquad \textbf{Equation 12}$$

If the "accelerated" method for ratcheting strain is used, then Equation 9 becomes modified to:

$$c_r = \dot{\alpha}_r - R_{fac} S(\sigma) R \sum_{n=1}^{N_S} \left(\frac{k_n}{\sigma_0}\right) |\dot{\alpha}_n| = 0 \qquad \textbf{Equation 13}$$

Appendix B: Calibration

Calibration of the backbone curve (no correction)

The model relies on accurate fitting of the backbone curve, here produced using the 3D FE data from the PISA project (Zdravkovic et al., 2020). This backbone curve is used as an input for calibration of parameters H_0, H_n and k_n, and corrected to account for ratcheting following the methodology described by Abadie et al. (2019).

In the case of the 1-D model, the k_n and H_n are calculated for the reaction curve of each Gauss point, based on the parameterized curves using the PISA method described in Byrne et al. (2020a), but with the depth variation functions and parameters given in Table 8. For the 0-D model, the fitting is applied the backbone curve for the moment-rotation response of the pile. The methodology used in both cases is briefly described below.

The monotonic relationship of the desired stress-strain curve is discretized by a number of break points corresponding to the number of yield surfaces of the kinematic hardening model (each spring-slider unit in Figure 2). The break points and the tangent moduli (see Figure 14) are defined by:

$$\sigma_n = \sum_{i=1}^{n} k_i + \sum_{i=n+1}^{N_S+1} H_i \varepsilon_n = \sum_{i=1}^{n} k_i + \frac{k_n}{H_n} \sum_{i=n+1}^{N_S+1} H_i \ , \ n = 1...N_S \qquad \textbf{Equation 14}$$

$$\varepsilon_n = \frac{k_n}{H_n} \ , \ n = 1...N_S \qquad \textbf{Equation 15}$$

$$E_n = \sum_{i=n+1}^{N_S+1} H_i \ , \ n = 0...N_S \qquad \textbf{Equation 16}$$

726

727 Hence, the values of the k_n and H_n can be deduced from Equation 15 to Equation **16**. This
728 provides the monotonic response shown in Figure 4, which matches that obtained from the 1D
729 PISA design model.

730 *Calibration of the ratcheting element*

731 The small fraction of strain accumulated in each load increment is controlled by the ratcheting
732 rate, *R*, the only parameter specifying the ratcheting behavior. The calibration procedure below is
733 a simplified version of that in Abadie (2015), Abadie et al. (2017b) and Beuckelaers et al. (2017),
734 and also corresponds to that used in Abadie et al. (2017a) and Abadie et al. (2020b).

735

736 The form of ratcheting rate R is chosen to capture (i) a decrease with load history, and (ii) an
737 increase with the load level, using:

$$R = R_0 \left(\frac{\beta}{\beta_0} \right)^{-m_r} \left(\frac{|\sigma|}{\sigma_0} \right)^{m_s} \qquad \textbf{Equation 17}$$

738 Where β_0 is an arbitrarily small value and σ_0 is the ultimate stress level. In this equation, the term

739 $\left(\frac{\beta}{\beta_0} \right)^{-m_r}$, through the value of m_r, controls the evolution of the ratcheting rate with load history,

740 and the term $\left(\frac{|\sigma|}{\sigma_0} \right)^{m_s}$, through the value of m_s, controls the dependence on stress/load level.

741 Finally, R_0 defines the base rate at which these phenomena occur.

Load History Effect (m_r)

At large cycle number, various authors including LeBlanc et al. (2010), Abadie (2015) have found a decreasing rate of accumulated rotation with cycle number, which can be expressed as:

$$\Delta\theta \sim N^{\alpha} \qquad \textbf{Equation 18}$$

where the power α has been found to be approximately 0.31. The accumulation of ground level rotation throughout the load sets of CM5 and CM6 are compared to this power in Figure 15. For CM6, only a small number of load cycles were applied and therefore the accumulation of rotation does not yet tend towards the slope for high cycle numbers. In test CM5, where larger cycle numbers were applied, the data tends towards the lower slope of 0.31. Although the limited data is not necessarily conclusive for the slope at high cycle numbers, the value proposed by LeBlanc et al. (2010) seems to give a reasonable fit and will be used in further analysis.

At large cycle number, where the hysteresis loops are almost closed, the stress component and the dissipation component do not vary with cycle number. The hardening parameter can be written as: $\beta = \int_0^N |\dot{\alpha}_r| dN + \beta_0$, where the constant can be neglected at high cycle number. The ratcheting strain can therefore be expressed as function of the cycle number by:

$$\Delta\theta \sim \int_0^N |\dot{\alpha}_r| dN \rightarrow \dot{\alpha}_r \sim N^{0.31-1} \qquad \textbf{Equation 19}$$

$$\dot{\alpha}_r \sim \beta^{-m_r} \rightarrow N^{0.31-1} \sim \left(N^{0.31}\right)^{-m_r} \rightarrow m_r = \frac{1-0.31}{0.31} = 2.2 \qquad \textbf{Equation 20}$$

These equations show that with a value of: $m_r = 2.2$, the ratcheting slope of 0.31 can be achieved at high cycle numbers.

The initial hardening parameter β_0 defines the location of the transition zone where the slope of the accumulated rotation decreases to a value of 0.31. The data in the PISA field tests do not provide enough information to accurately determine this parameter. An estimated value of $\beta_0 = 0.01\varepsilon_u$, where ε_u represents the ultimate displacement or rotation in the soil reaction curve, results in reasonable results for the ratcheting behavior and therefore this value has been used

in further analysis. For the case of the 1-D model, the values of β_0 are linked to the ultimate strain ε_{pu} of each independent soil-curve ($\bar{v}_{pu}$, $\bar{\psi}_{mu}$, $\bar{v}_{Hu}$, $\bar{\psi}_{Mu}$, first line of each soil reaction component in Table 8), and hence vary for each of the soil-reaction curves.

Load Magnitude Effect (m_s)

The effect of load magnitude on the ratcheting response can be calibrated using a similar methodology. The overall rotation of the foundation with load magnitude can generally be described by:

$$\Delta\theta \sim \tilde{\tilde{T}}_{bc}(\zeta_b) \qquad \textbf{Equation 21}$$

where $\zeta_b = M_{\max} / M_{ult}$ is the dimensionless cyclic load magnitude. In the experimental tests by Abadie (2015), $T_b(\zeta_b)$ has been found to fit well with a power exponent of 4 ($\Delta\theta \sim \sigma^{m_t}$ with: $m_t = 4$). The experimental results and the power law fit are compared in Figure 16 to Abadie (2015) and the values obtained from CM6. This figure shows that a value $m_t = 4$ is consistent with these tests.

The behavior of the ratcheting element with cycle amplitude is analysed for a single cycle:

$$\Delta\theta \sim \int_0^{\sigma_{\max}} \dot{\alpha}_r d\sigma + \int_{\sigma_{\max}}^0 \dot{\alpha}_r d\sigma \sim \int_0^{\sigma_{\max}} \left(\frac{\beta}{\beta_0}\right)^{-m_r} \left(\frac{|\sigma|}{\sigma_0}\right)^{m_s} \sum_{n=1}^{N_S} \left(\frac{k_n}{\sigma_0}\right) |\dot{\alpha}_n| d\sigma \qquad \textbf{Equation 22}$$

In the unload part of the cycle, the accumulated ratcheting is very low as the effect of the stress component and the dissipation component reach their maxima at opposite points during unloading. Therefore the analysis can be simplified by only considering the upward part of the load cycle. To analyze the effect of the stress magnitude on the ratcheting element, the evolution of each of the individual components need to be identified.

Since: $\beta \sim \int_0^N |\dot{\alpha}_r| dN$ at high cycle numbers, both terms increase with the same exponent with regards to cycle amplitude. Therefore, we can write: $\beta \sim \sigma^{m_t}$. The stress term simply increases with its exponent m_s . The evolution of the dissipation term with cycle amplitude can be evaluated by analysing the evolution of dissipated energy by the foundation within a load cycle. This has

been evaluated using the kinematic hardening model applied to the 1-D model for varying ζ_b, illustrated in Figure 17. The resulting dissipated energy can be approximated well using a power law fit as $E_{diss} \sim \zeta_m^{m_d}$ where: $m_d = 3$. Since it is expected that this dissipation is reflected in each of the soil reaction curves, we can write that:

$$\sigma^{m_d} \sim \int_0^{\sigma_{max}} \sum_{n=1}^{N_S} \left(\frac{k_n}{\sigma_0} \right) |\dot{\alpha}_n| d\sigma \rightarrow \sum_{n=1}^{N_S} \left(\frac{k_n}{\sigma_0} \right) |\dot{\alpha}_n| \sim \sigma^{m_d - 1} \qquad \textbf{Equation 23}$$

Combining the effects of all terms of the ratcheting element, we arrive at:

$$\sigma^{m_t} \sim \int_0^{\sigma_{max}} \beta^{-m_r} \sigma^{m_s} \sigma^{m_d - 1} d\sigma \sim \sigma_{max}^{m_s + m_d - m_r\, m_t} \qquad \textbf{Equation 24}$$

$$\rightarrow m_t = m_s + m_d - m_r\, m_t \rightarrow m_s = m_t(1 + m_r) - m_d \qquad \textbf{Equation 25}$$

which results in a value of $m_s = 9.9$, for values of $m_t = 4$, $m_r = 2.2$ and $m_d = 3$.

Rate of Ratcheting (R_0)

Finally, the rate of ratcheting is chosen heuristically to fit the data closely.

For the 1-D analyses the assumption is made that the ratcheting effect observed at a macro-level is reflected in the soil reaction curves below ground, so that the same calibration of the HARM model at macro-level applies to all four components of the soil reaction curves. Hence, the calibration procedure is achieved using the model test results from Abadie (2015) and the resulting values are used within all the ratcheting elements, for both the 1-D and 0-D model.

List of Figures

802 ## List of Tables

803

804 **Table 1. Identification of the role of HARM in lateral pile design approach**

3-D FE (3-D)	Winkler-type model (1-D)	Macro-model (0-D)
Model the entire soil continuum and capture complete pile-soil interaction	Model soil response by series of soil reaction curves down the pile length	Model entire pile-soil interaction by representative consitutive model at the soil surface
HARM to define the stress-strain constitutive behavior of each soil element	HARM to define each soil reaction curve	HARM to define the relationship of the macro-model
Computationally intensive (getting faster) and (probably) most accurate	Compromise between accuracy and time	Computationally fast but (probably) least accurate
Model detailed soil stratigraphy, and complex pile-soil interface response	Discretise soil layers, but no interaction between layers	Difficult to calibrate for piles in layered soil and in-homogeneous strength profiles
Any foundation geometry	Common pile design tool (the *p-y* model)	Well established for shallow foundations (*e.g.* spudcans) and pipelines

805
806
807 **Table 2. Geometry of Cowden field test pile geometry for CM9, CM5 and CM6 (T4)**

Pile property	*D* (m)	*h* (m)	*h*/*D*	*L* (m)	*L*/*D*	*t* (mm)	*D*/*t*
Values	0.76	10	13.2	4.0	5.25	11	58

808

809 **Table 3: Load sequence applied for CM6**

Load set	Max Load (kN)	$\zeta_b = \frac{\text{Max Load}}{\text{Ultimate Load}}$	$\zeta_c = \frac{\text{Min Load}}{\text{Max Load}}$	Cycles
1	43.5	0.37	0	9
2	70	0.60	0	9
3	90	0.77	0	37

810 **Table 4: Load sequence applied for CM5**

Load set	Max Load (kN)	$\zeta_b = \frac{\text{Max Load}}{\text{Ultimate Load}}$	$\zeta_c = \frac{\text{Min Load}}{\text{Max Load}}$	Cycles
1	10	0.09	0	7000
2	20	0.17	0	7000
3	60	0.52	0	2500
4	20	0.17	0	1100
5	30	0.26	0	3300
6	40	0.34	0	1400
7	20	0.17	0	500
8	40	0.34	0.5	1000
9	20-30-40	0.17-0.26-0.34	0	1500
10	20-30-40-60	0.17-0.26-0.34-0.52	0	1000
11	90	0.77	0	145

811

812

813 **Table 5. List of parameters for calibration of the HARM 0-D model to the PISA tests CM5**

	Definition	Equation	0-D Analytical	1-D
$\boldsymbol{\beta_0}$	Initial ratcheting strain	Arbitrarily small value	1×10^{-4}	$\varepsilon_{pu}/100$
$\boldsymbol{m_r}$	Exponent defining the decrease of ratcheting rate with cyclic history	$m_r = \frac{1}{m_\alpha} - 1$	2.2	2.2
$\boldsymbol{m_s}$	Exponent defining the increase of ratcheting rate with load intensity	$m_s = m_\sigma (m_r + 1) - m_h - 1$	8.9	8.9
$\boldsymbol{R_0}$	Initial ratcheting rate	$R_\beta = R_0 {\beta_0}^{m_r} = \frac{{T_0}^{m_r+1}}{\varepsilon_{pU} \kappa_{m0} \kappa_m}$	R_0=1e+09 R_β =1.7	R_0=1e+05 R_β varies

814

815

816 **Table 6. Acceleration Programme for test CM5**

Load set	Max Load (kN)	Min Load / Max Load	Incremental		Programme 1		Programme 2	
			Cycles	R_{fac}	**N**	R_{fac}	**N**	R_{fac}
1	10	0	7000	1	10 1 10	1 6980 1	10 9 9 6	1 10 100 1000
2	20	0	7000	1	10 1 10	1 6980 1	10 9 9 6	1 10 100 1000
3	60	0	2500	1	10 1 10	1 2480 1	10 9 9 3	1 10 100 500
4	20	0	1100	1	10 1 10	1 1080 1	0	-
5	30	0	3300	1	10 1 10	1 3280 1	0	-
6	40	0	1400	1	10 1 10	1 1380 1	0	-
7	20	0	500	1	10 1 10	1 480 1	0	-
8	40	0.5	1000	1	10 1 10	1 980 1	0	-
9	20-30-40	0	1500	1	30 30 30	1 48 1	0	-
10	20-30-40-60	0	1000	1	40 40 40	1 20.5 1	0	-
11	90	0	145	1	145	1	10 14	1 10
Computed number of cycles:			**26,445**		**523**		**113**	
Computed time 0-D (Intel® core i7-8565U, 16GB RAM) 100 increments/cycle 500 increments/cycle			 8.3 s 43.40 s		 0.16 s 0.92 s		 0.043 s 0.21 s	
Computed time 1-D (Intel® core i7-8565U, 16GB RAM)			-		-		30 min	

817

818

819 **Table 7. Load regime characteristics respective modelling information**

	Short Storm	**35 hr Storm**	**Lifetime**
Maximum Moment [MNm]	394	284	222
M_{max}/M_{ULS}	1/1.35=0.74	0.53	0.42
M_{min}/M_{max}	-0.37	-0.70	-0.97
No. of cycles	150	35,919	2.6503×10^8
No. of load events	150	530	65,534
Modelling	Incremental	Incremental / Accelerated	Accelerated
Computed Number of Cycles	150	35,919 / 1,359	187,459
Calculation time (0-D) (Intel® core i7-8565U, 16GB RAM)			
100 increments	0.066 s	11.8 s / 0.58 s	382 s
500 increments	0.42 s	78.7 s / 3.5 s	1803 s

820
821

822 **Table 8. Parameters for normalised soil reaction curves for Cowden field test (*z* positive**
823 **downwards)**

Soil reaction component	**Parameter**	**Expression**
Distributed lateral load, p	Ultimate strain, $\bar{v}_{pu}$	200
	Initial stiffness, k_p	$-0.41\frac{z}{D}+5.14$
	Curvature, n_p	$-0.009\frac{z}{D}+0.96$
	Ultimate reaction, $\bar{p}_u$	$8.50 - 5.24 \exp\left(-0.21\frac{z}{D}\right)$
Distributed moment, m	Ultimate rotation, $\bar{\psi}_{mu}$	n/a
	Initial stiffness, k_m	$-0.06\frac{z}{D}+0.57$
	Curvature, n_m	0
	Ultimate moment, $\bar{m}_u$	$-0.02\frac{z}{D}+0.29$
Base horizontal force, H_B	Ultimate strain, $\bar{v}_{Hu}$	300
	Initial stiffness, k_H	$-0.04\frac{L}{D}+0.98$
	Curvature, n_H	0.94
	Ultimate reaction, $\bar{H}_{Bu}$	$0.25\frac{L}{D}+1.29$
Base moment, M_B	Ultimate rotation, $\bar{\psi}_{Mu}$	200
	Initial stiffness, k_M	$-0.014\frac{L}{D}+0.10$
	Curvature, n_M	$-0.01\frac{L}{D}+0.89$
	Ultimate reaction, $\bar{M}_{Bu}$	0.84

824

Figure

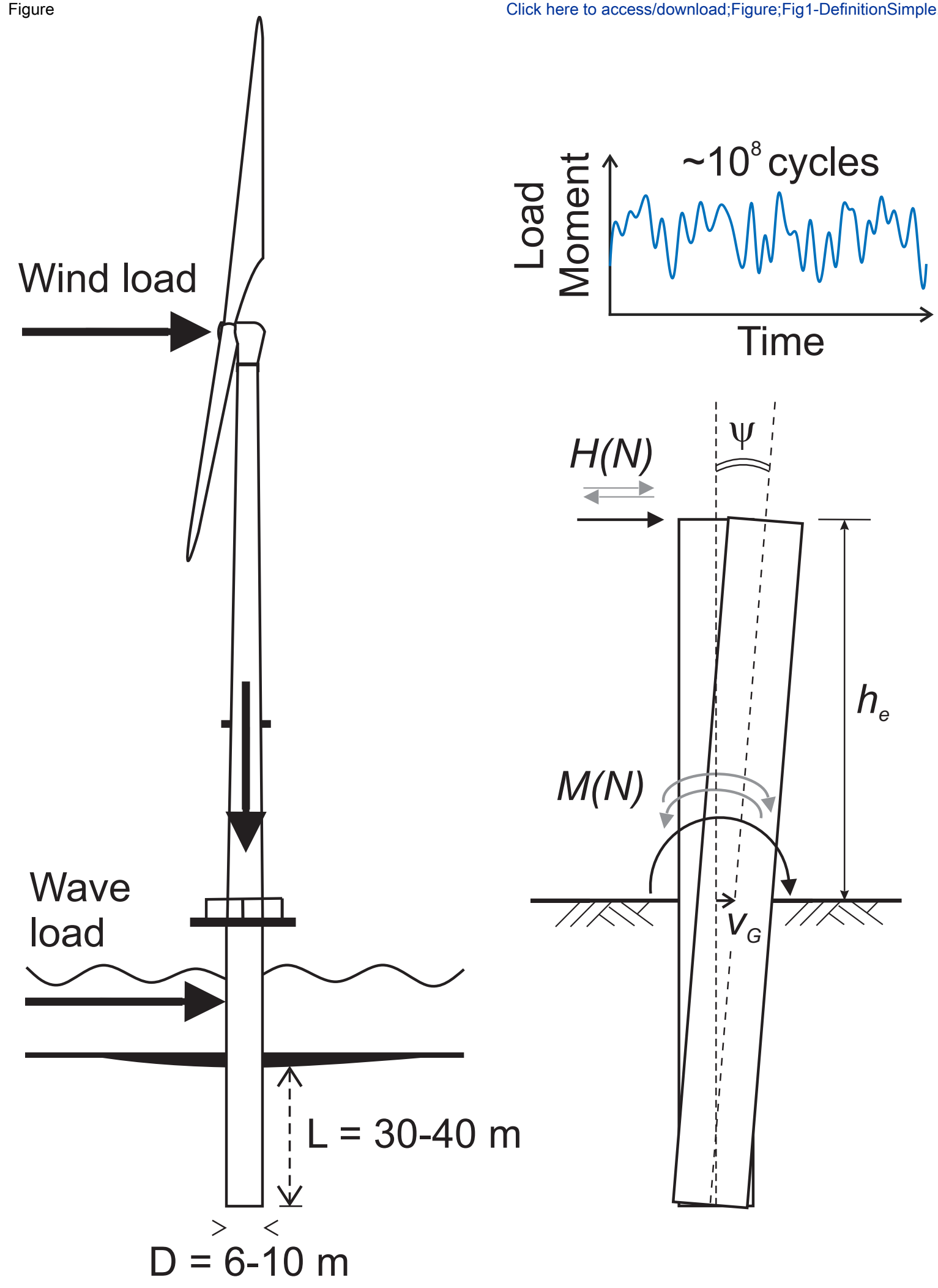

Figure

Click here to access/download;Figure;Fig2a-Series-Parallel.tif

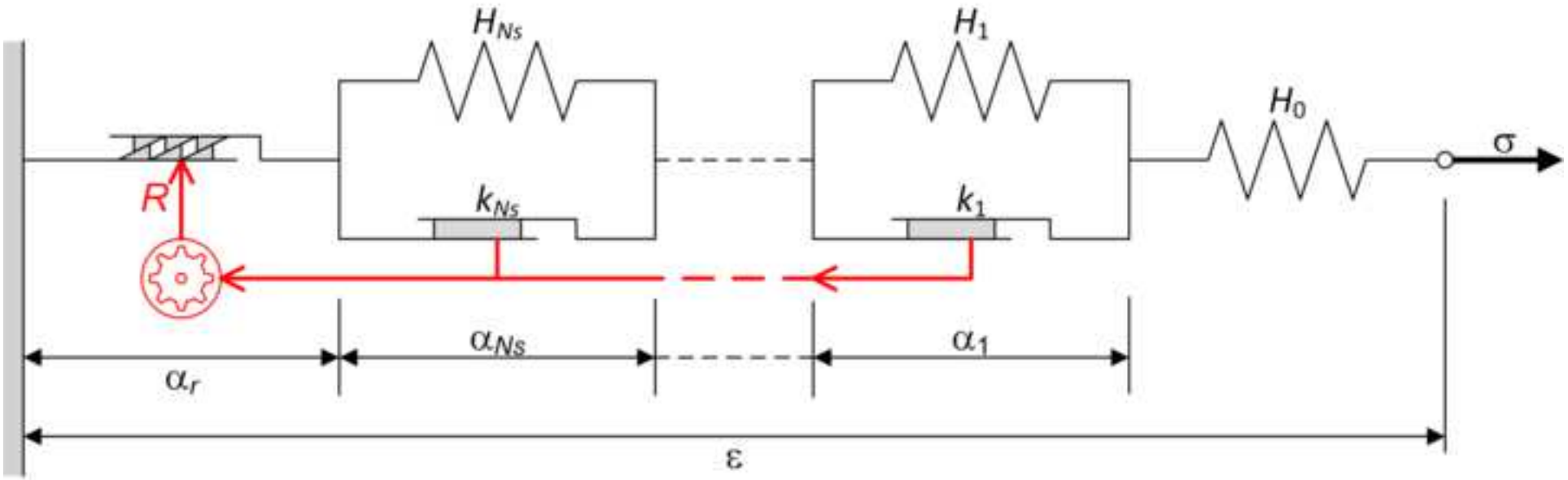

Figure

Click here to access/download;Figure;Fig2b-Series-Parallel.tif

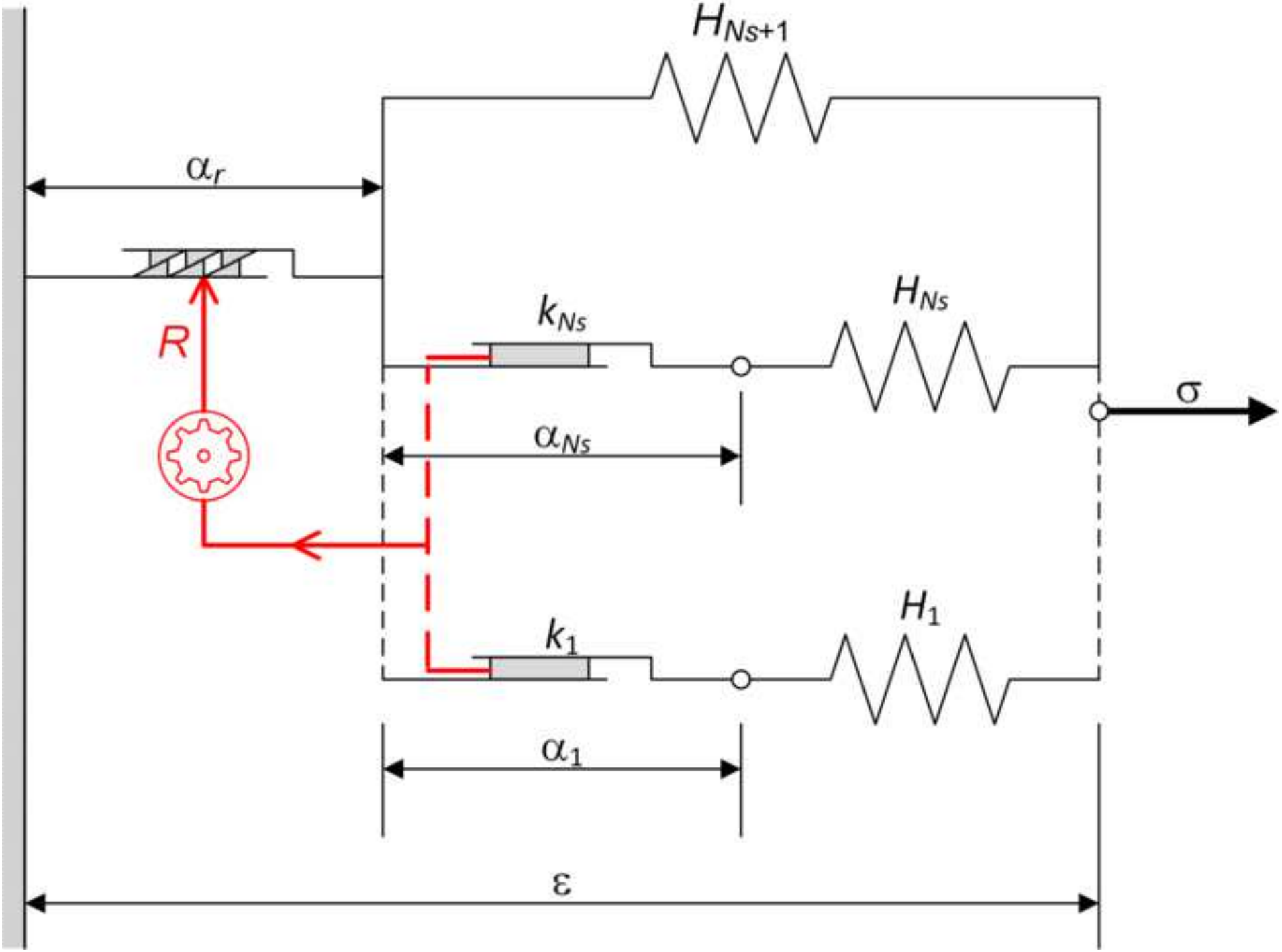

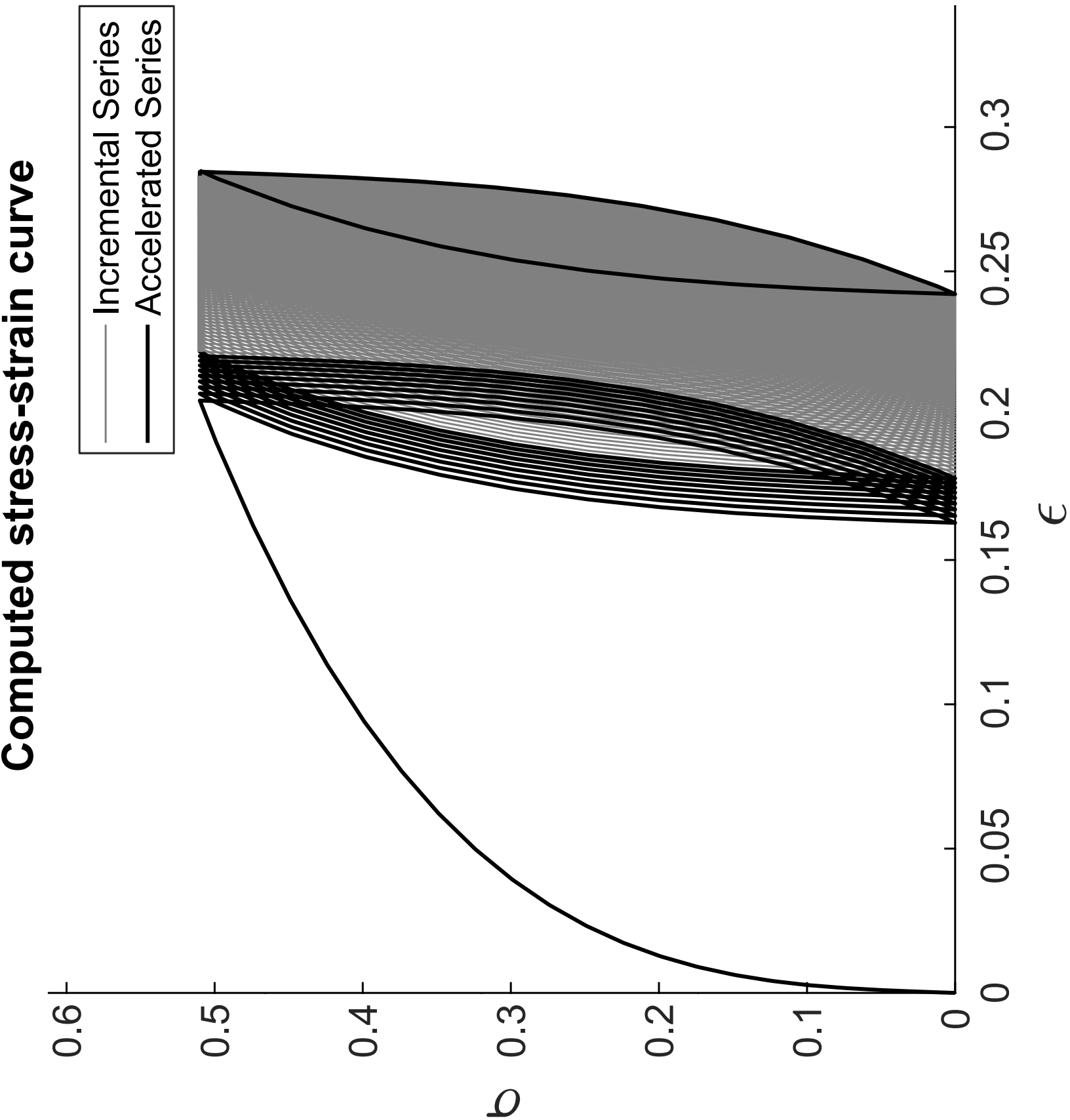

Figure

Click here to access/download;Figure;Fig2d-Series-Parallel.eps

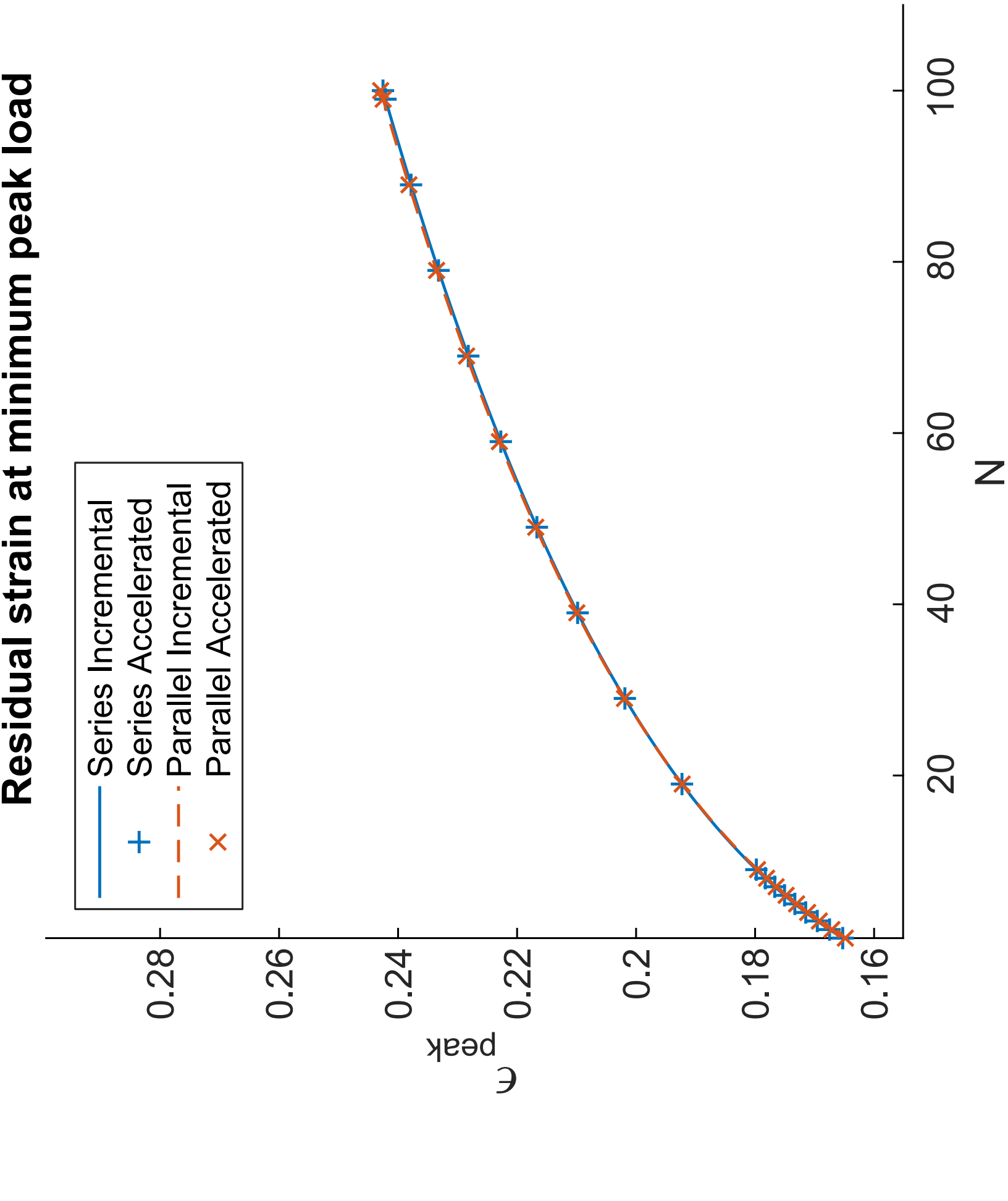

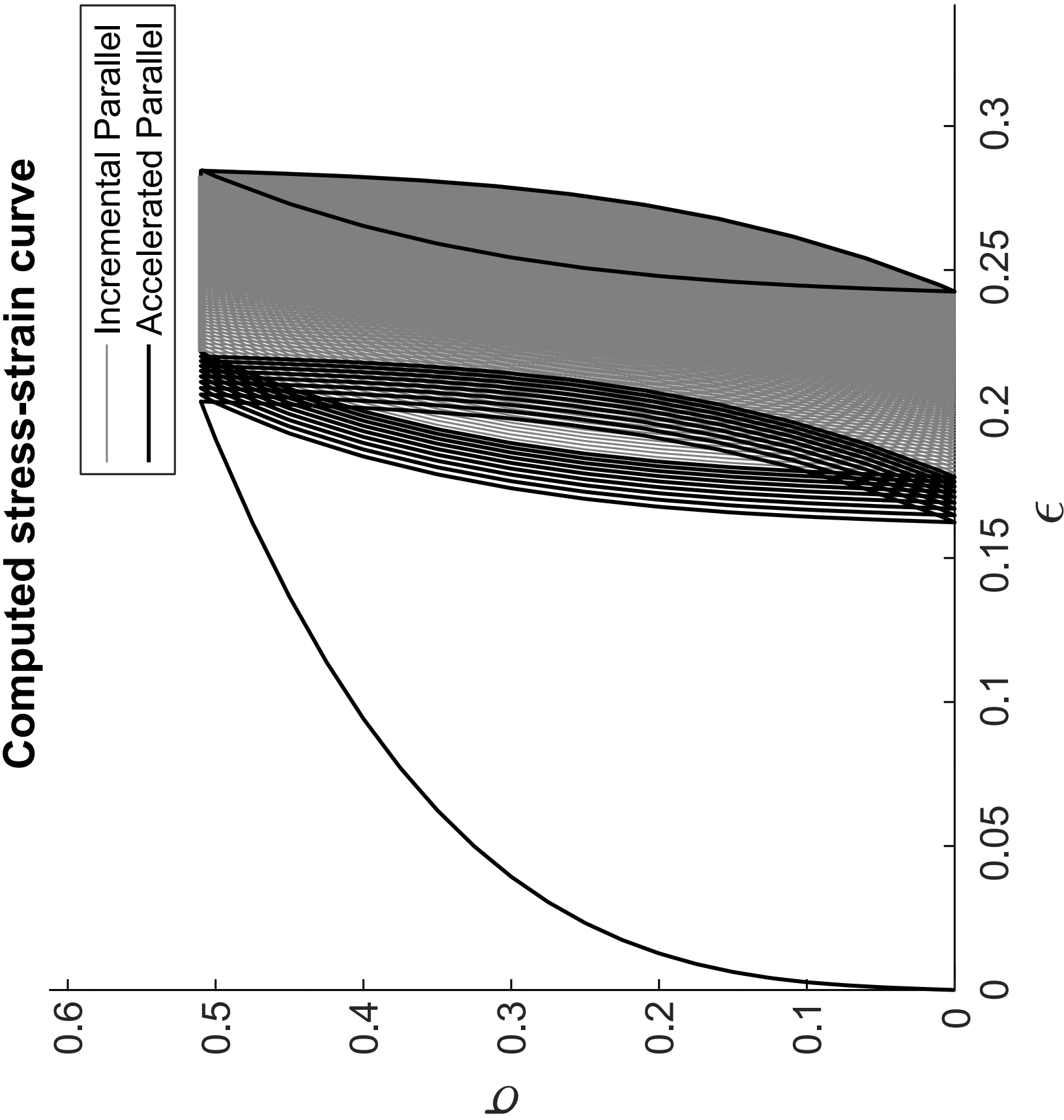

Figure

Click here to access/download;Figure;Fig2f-Series-Parallel.eps

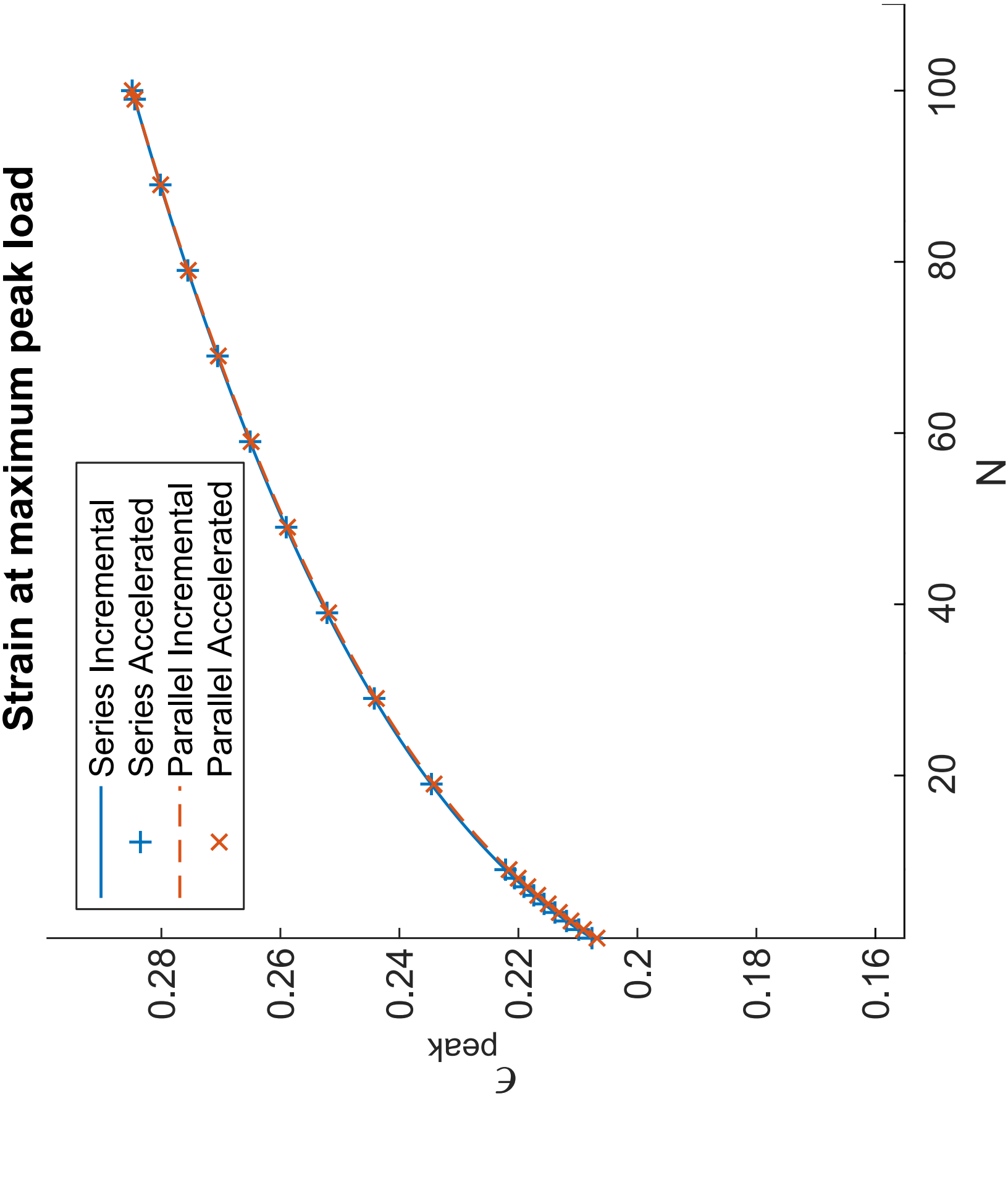

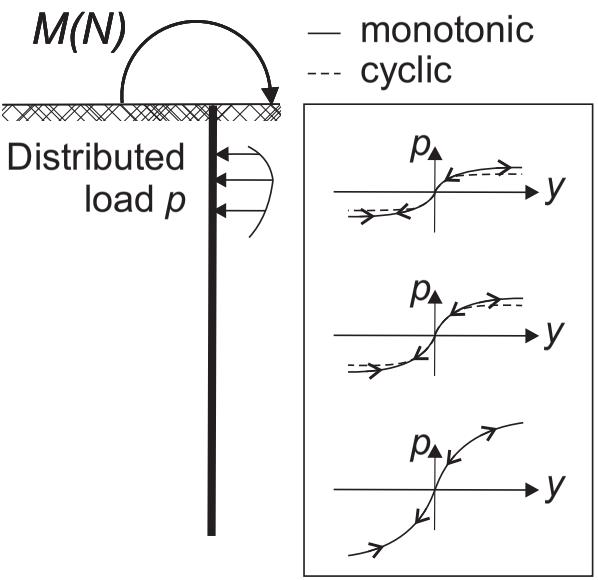

Current *cyclic p-y* curves

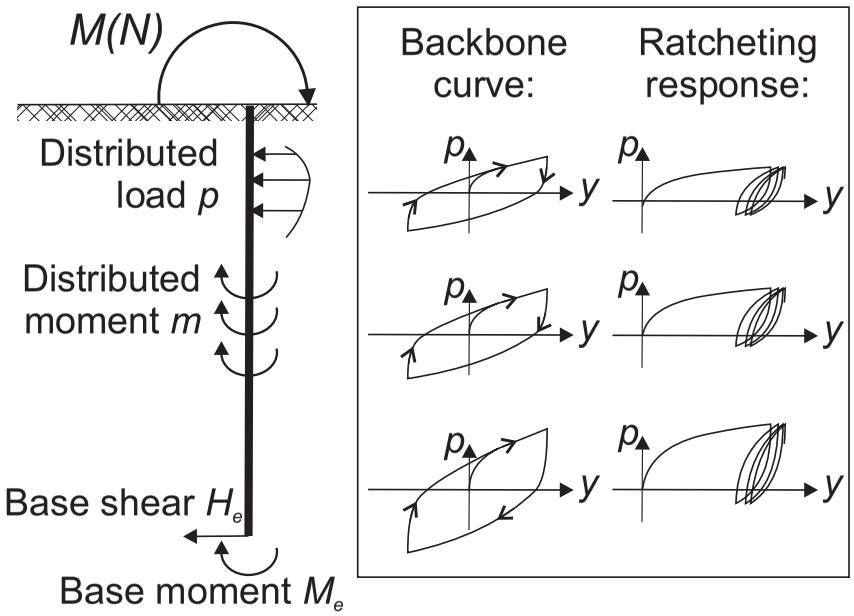

1-D model (based on PISA method)

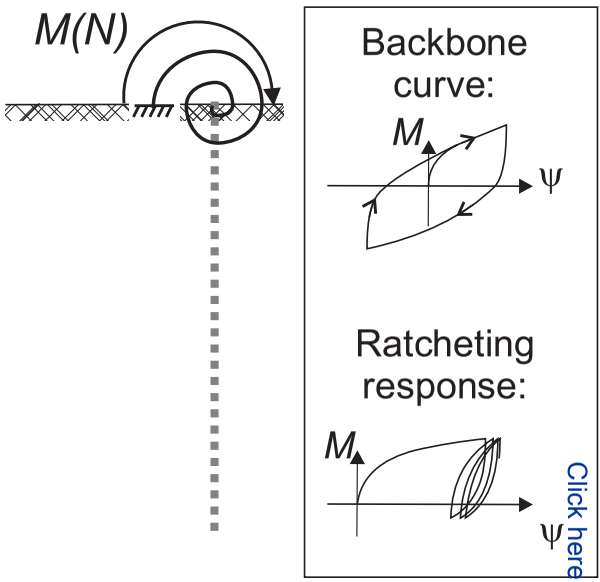

0-D model (macro-element)

Figure

Click here to access/download;Figure;Fig4a-Comparison.eps

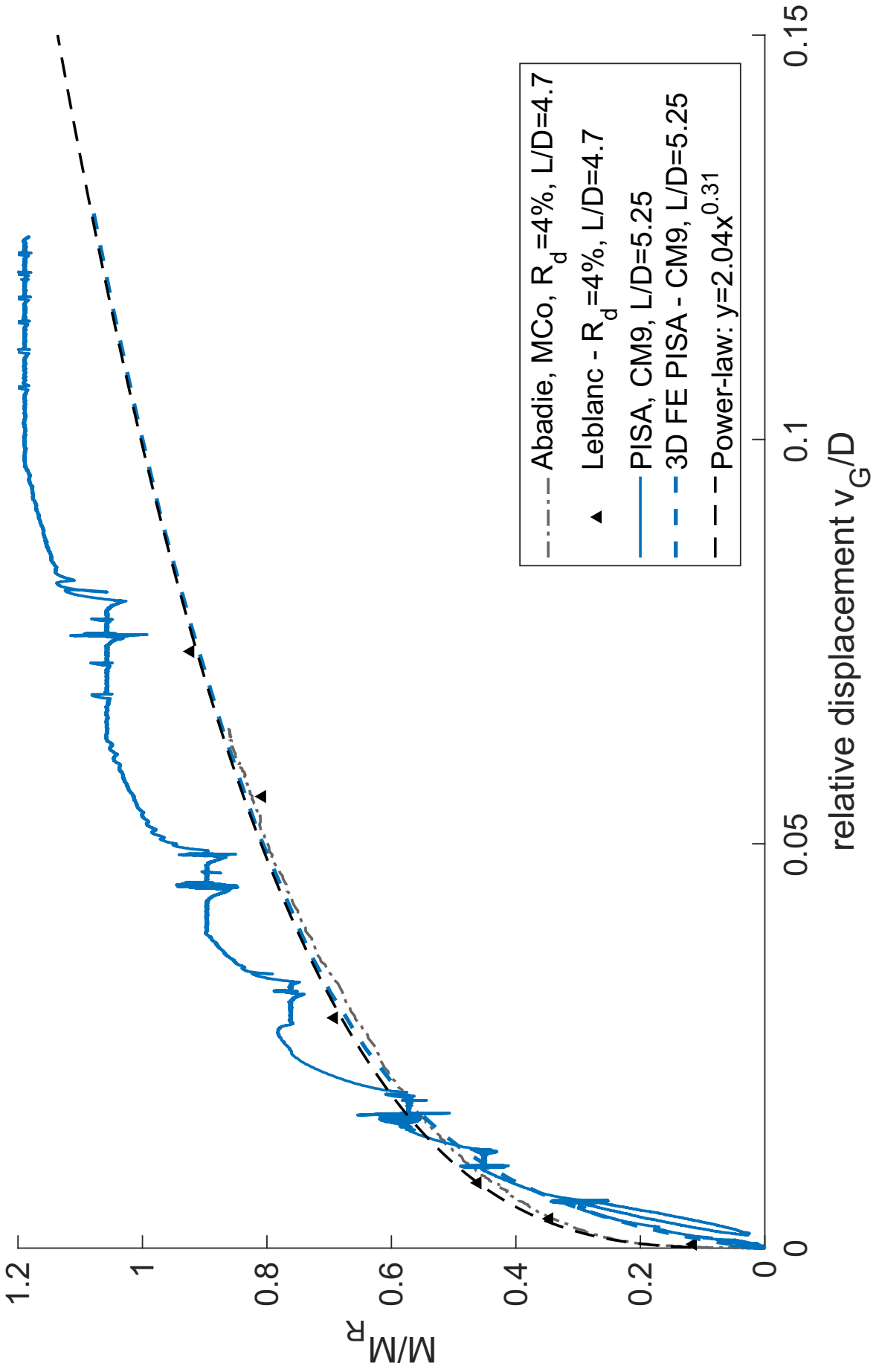

Figure

Click here to access/download;Figure;Fig4b-HARM1D-0D.eps

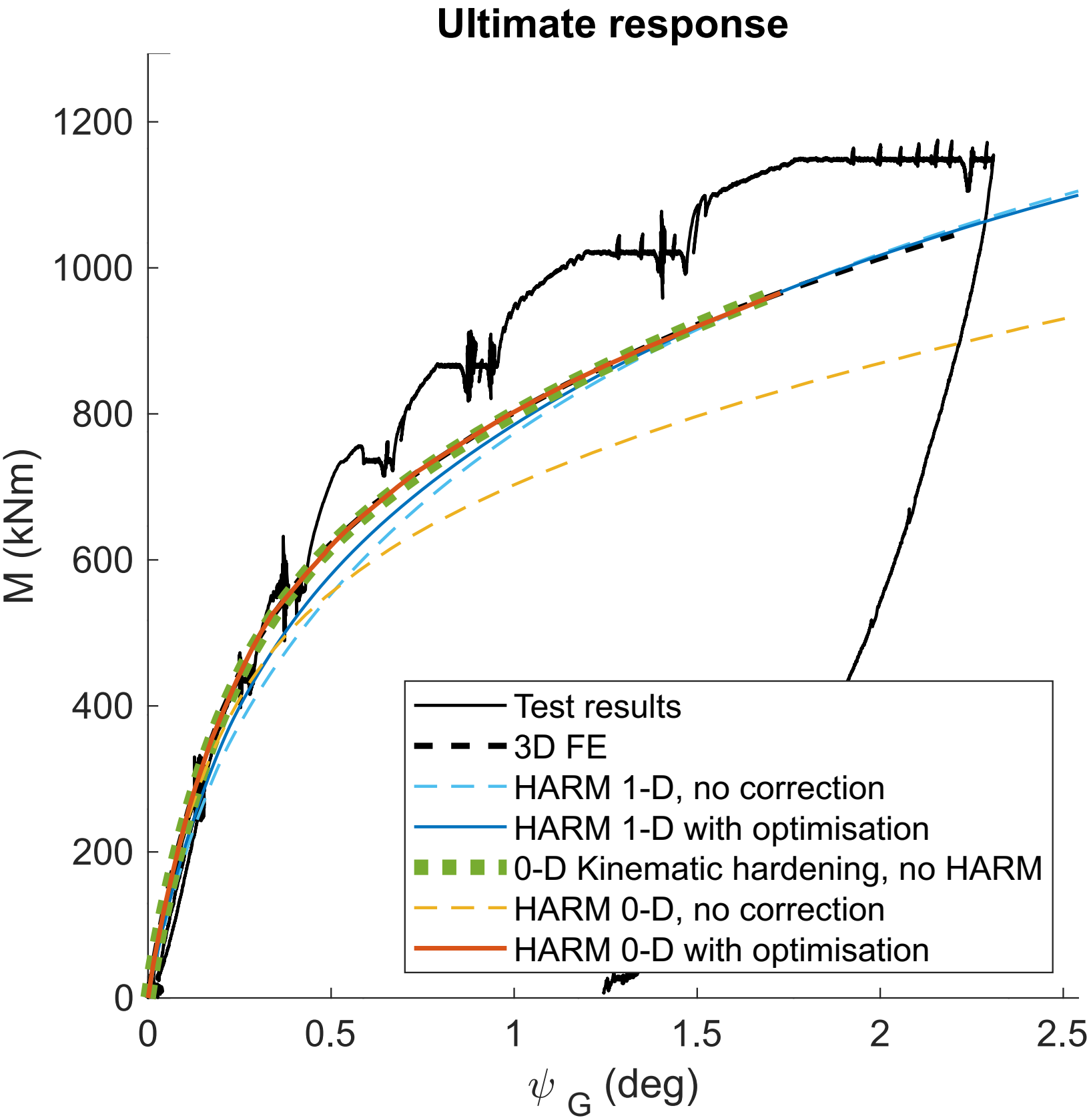

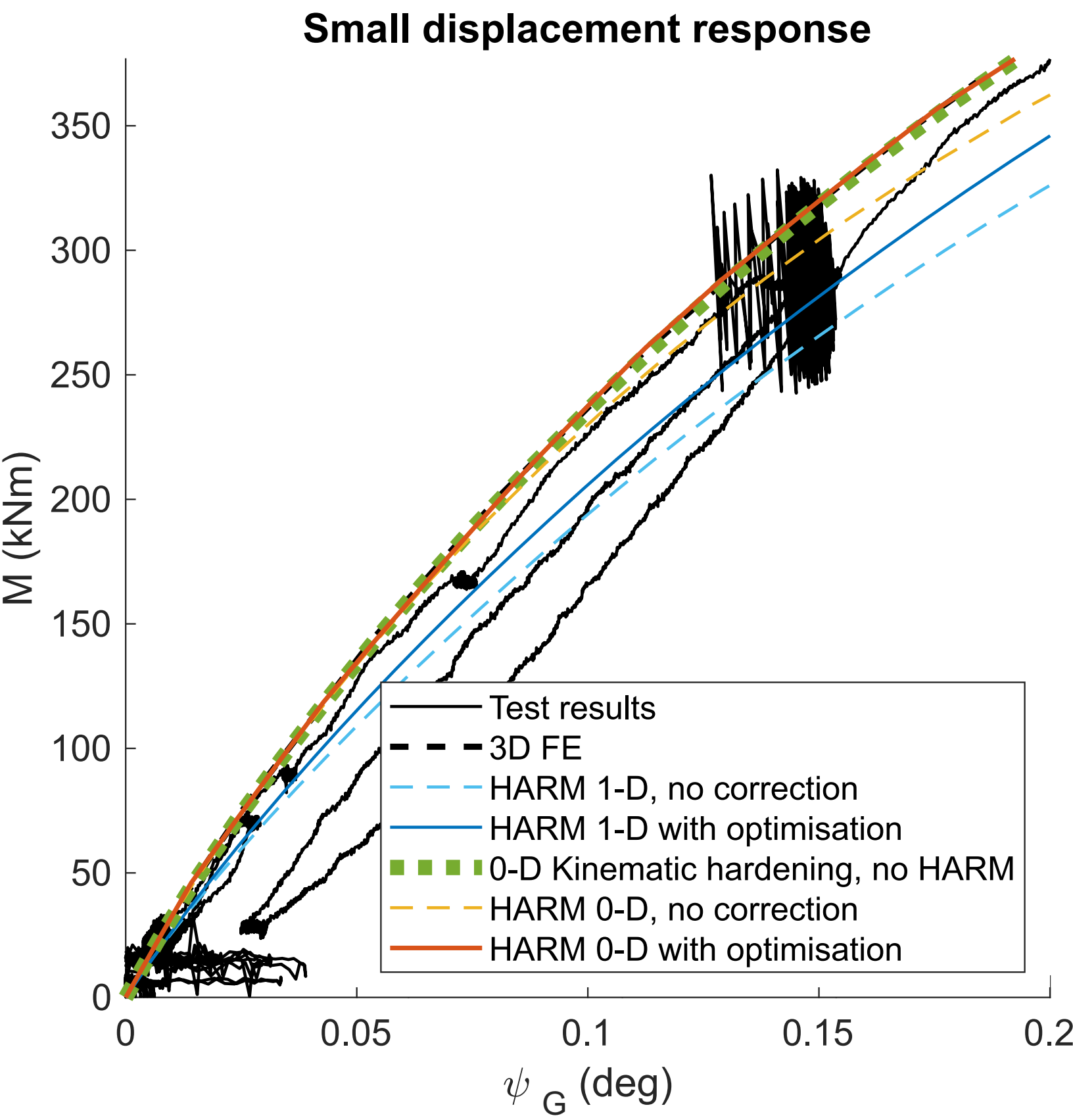

Figure

Click here to access/download;Figure;Fig5a-CM6.eps

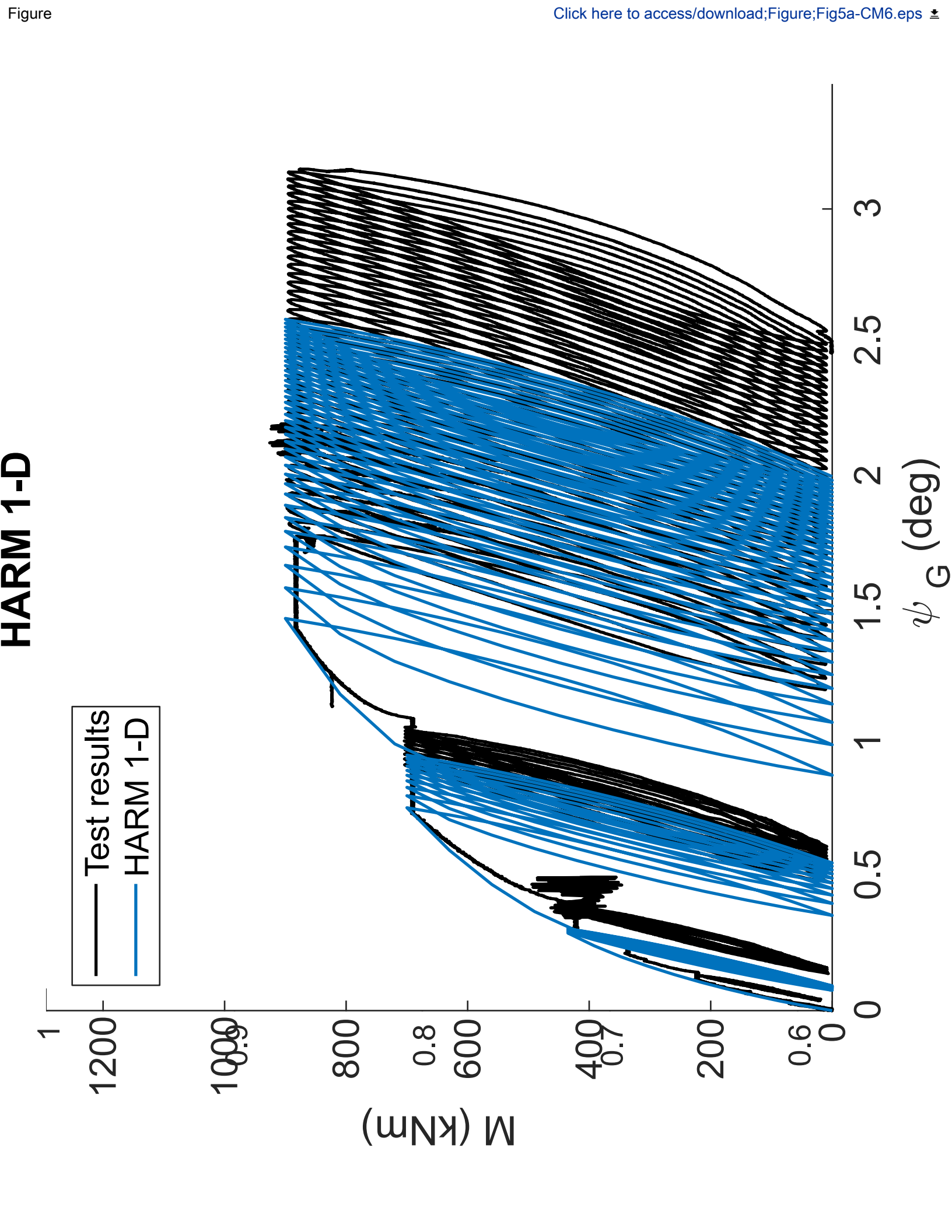

Figure

Click here to access/download;Figure;Fig5b-CM6.eps

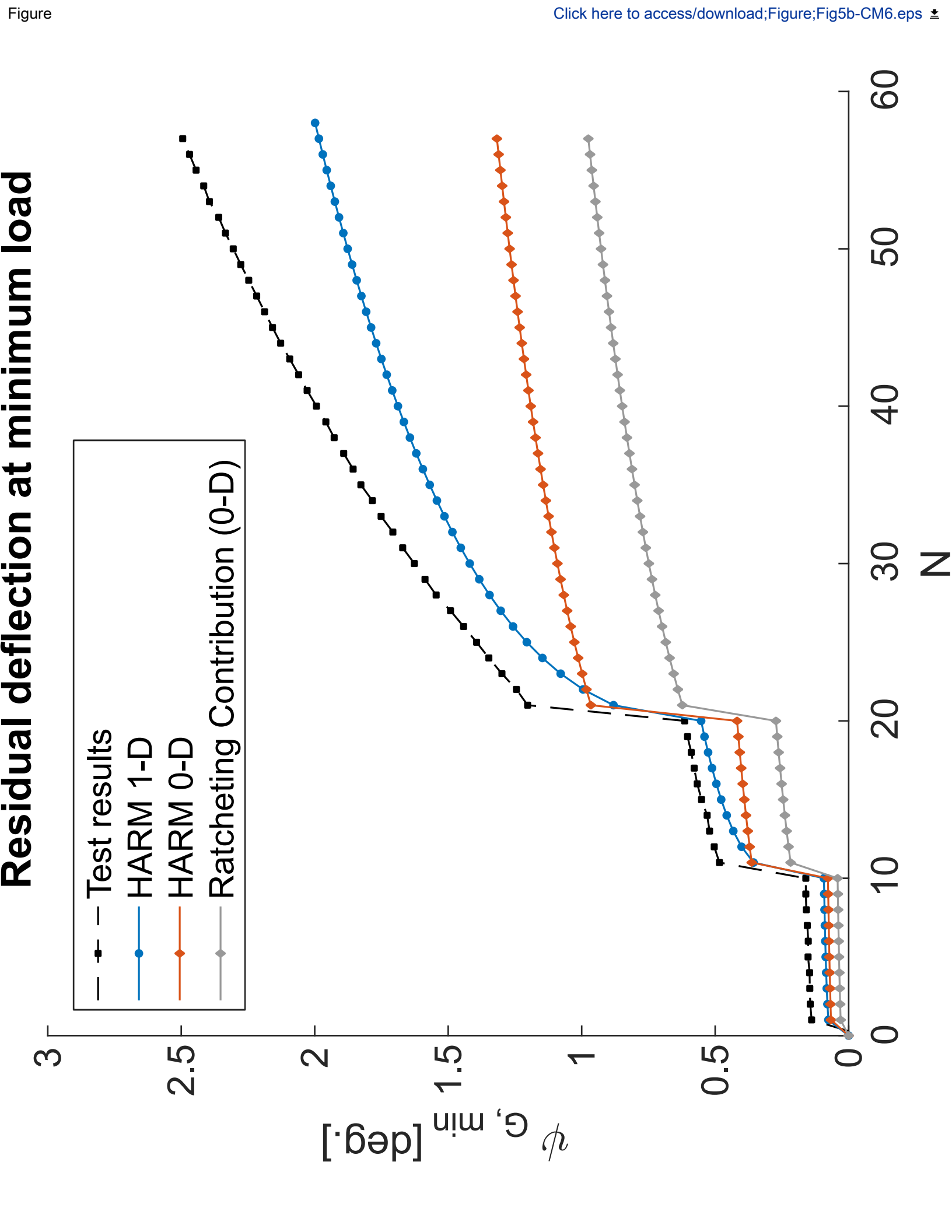

Figure

Click here to access/download;Figure;Fig5c-CM6.eps

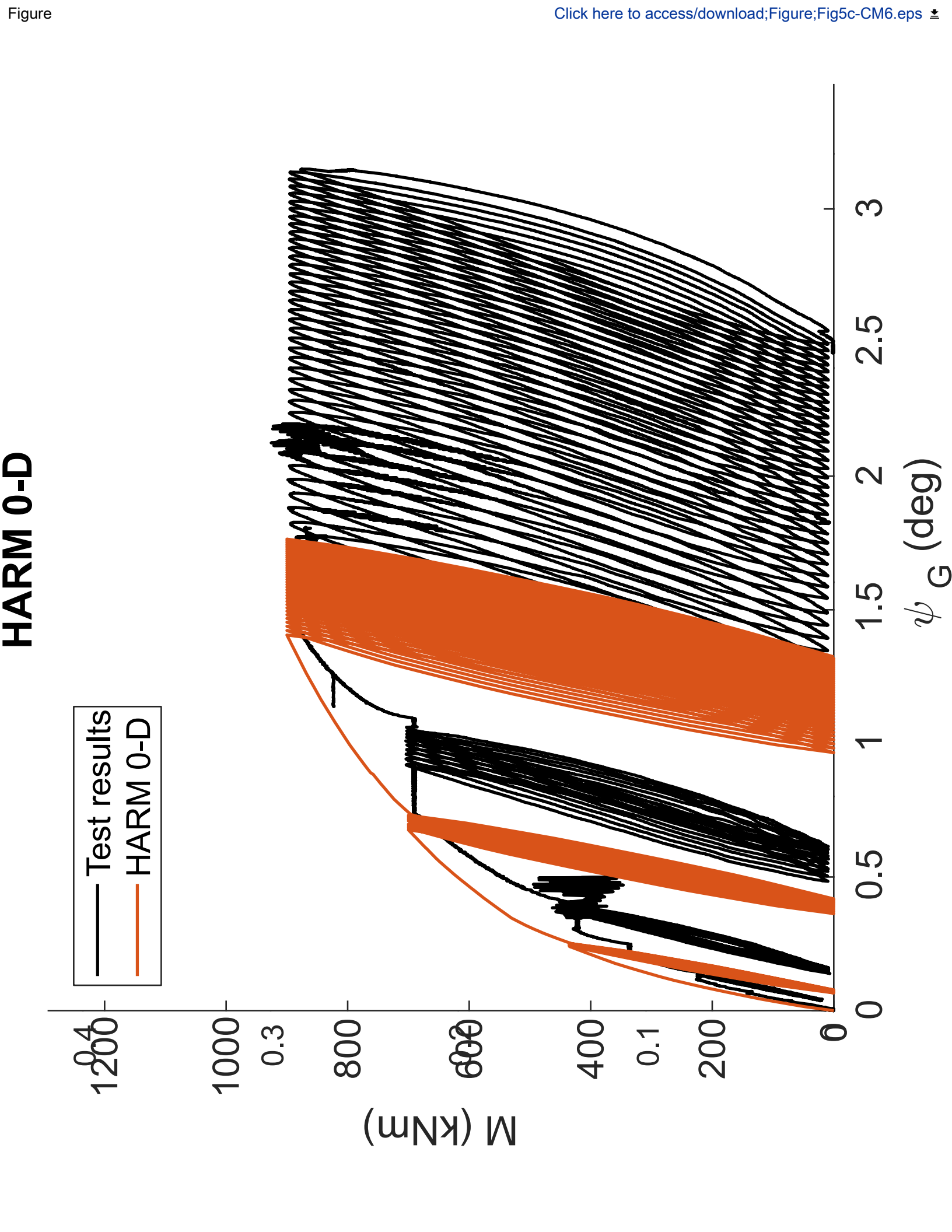

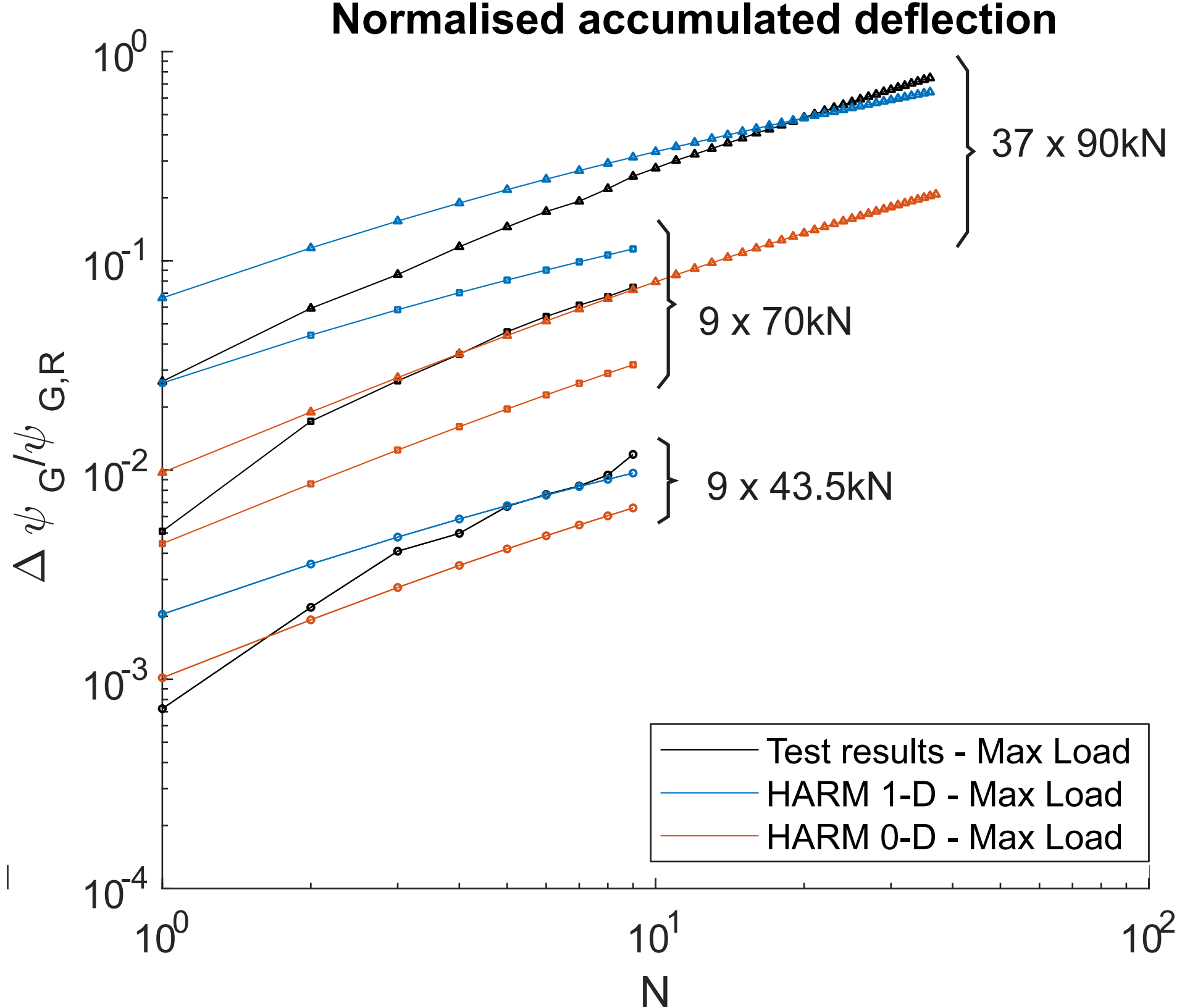

Figure

Click here to access/download;Figure;Fig6-pycyclic.eps

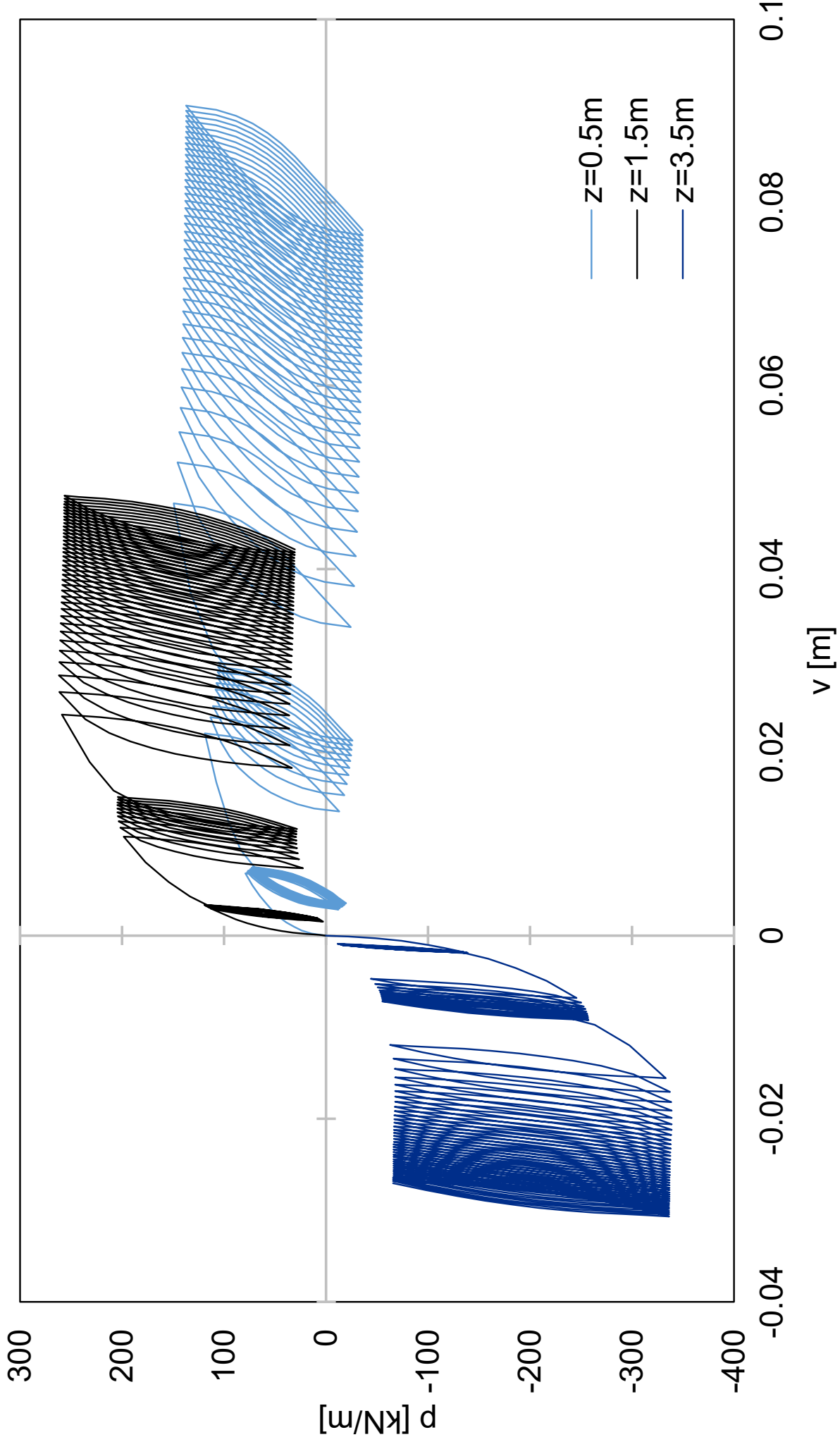

Figure

Click here to access/download;Figure;Fig7a-CM5.eps

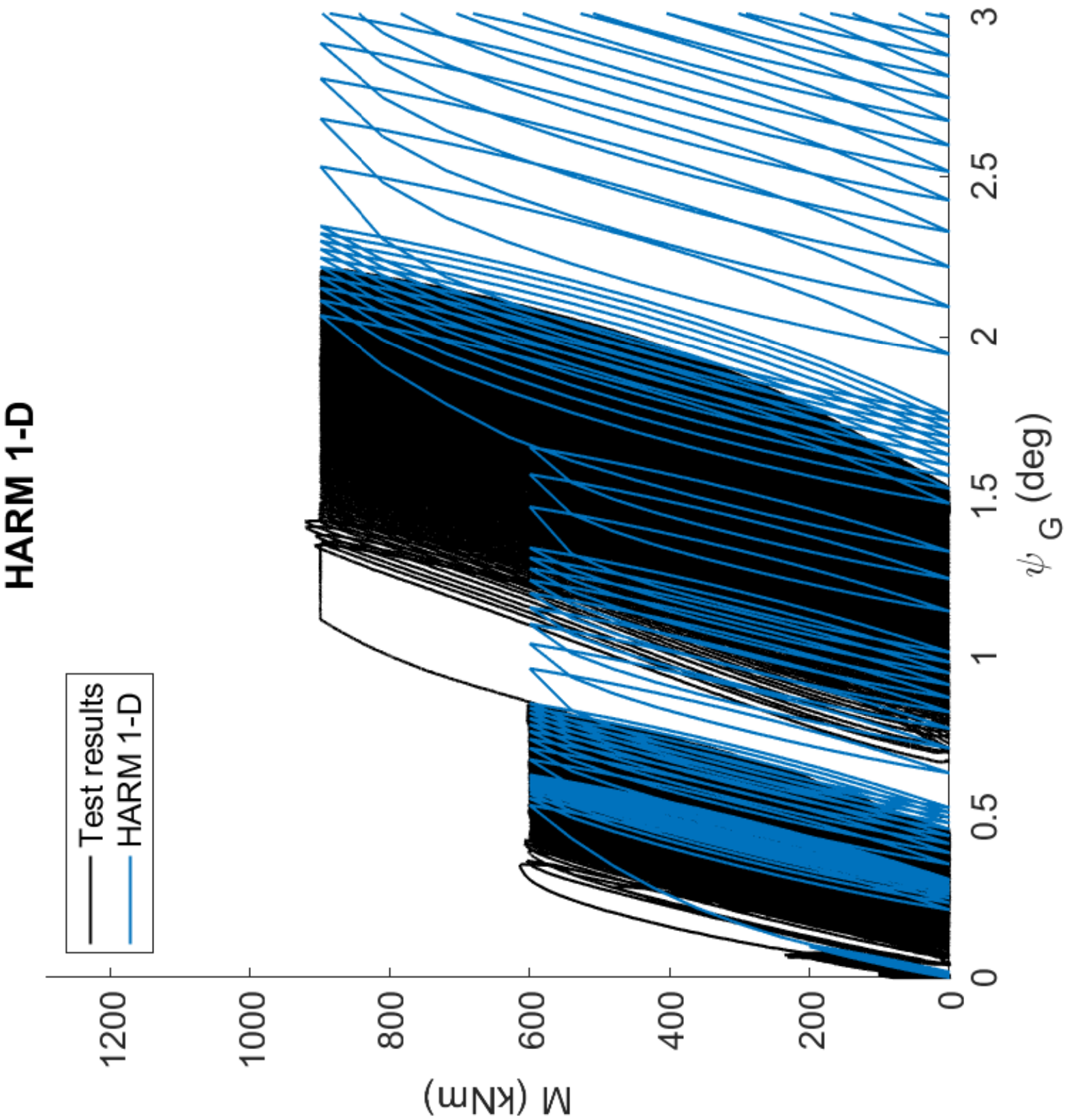

Figure

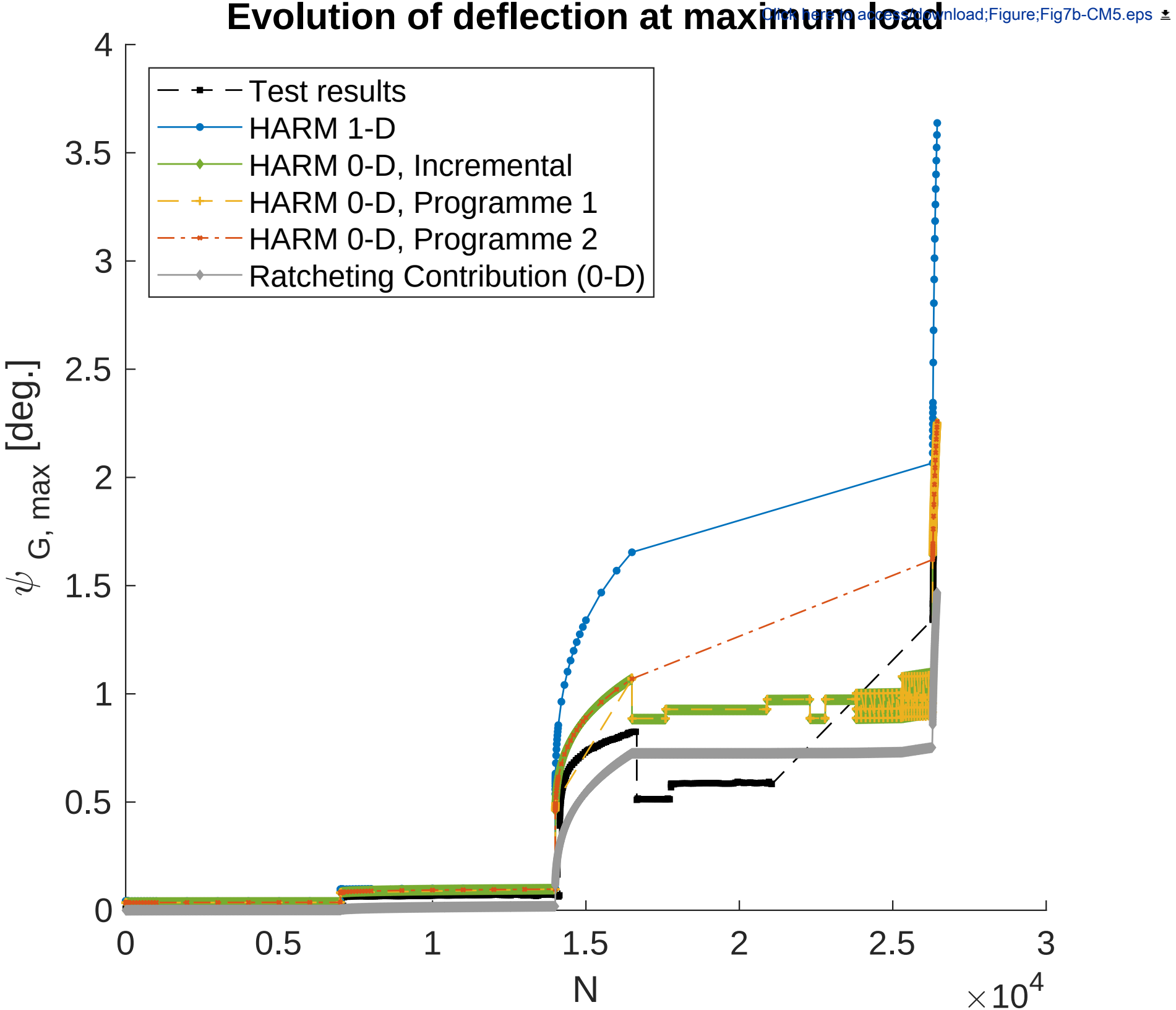

Figure

Click here to access/download;Figure;Fig7c-CM5.eps

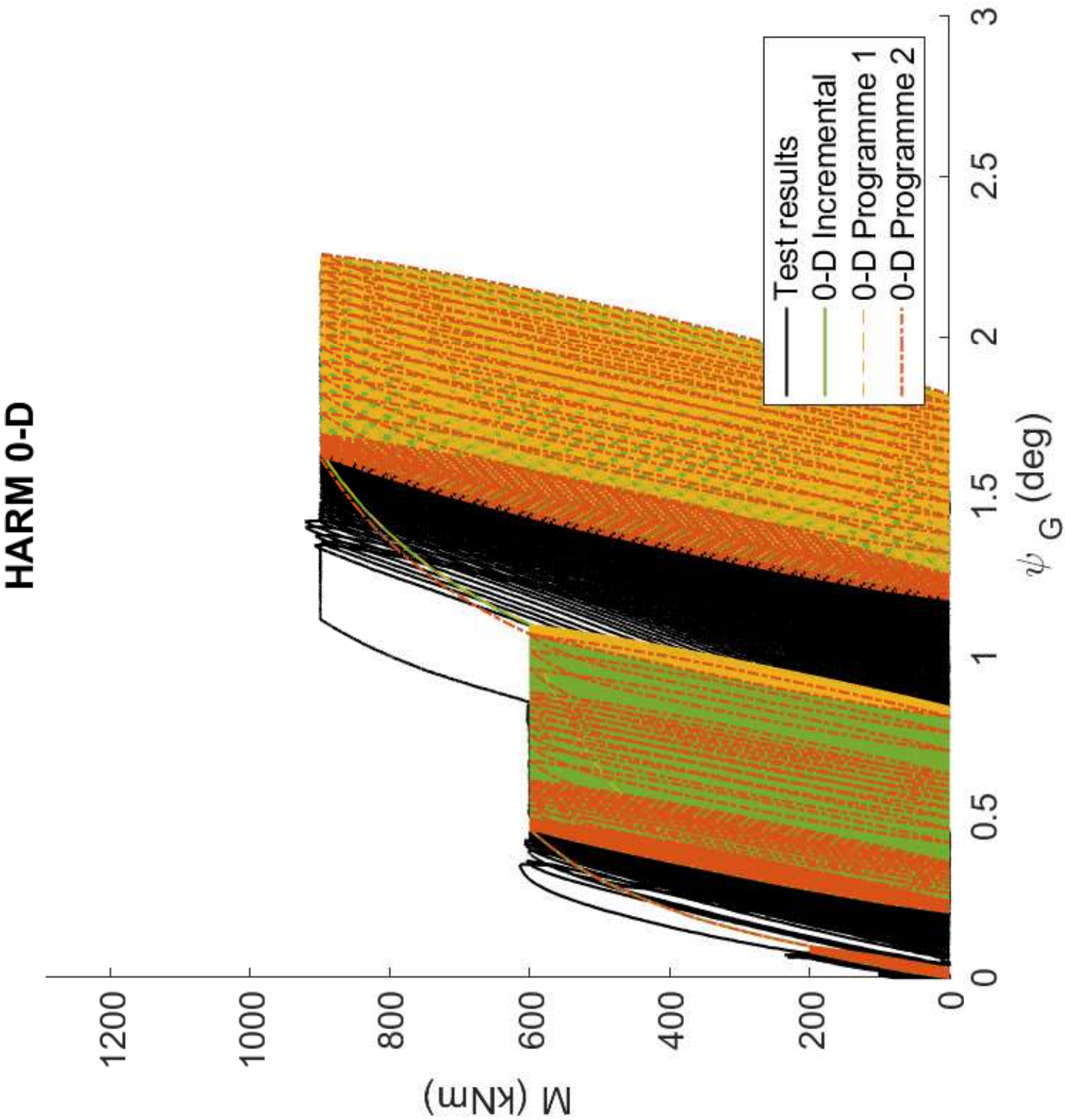

Figure

Evolution of deflection at maximum load: Zoom on last cycles

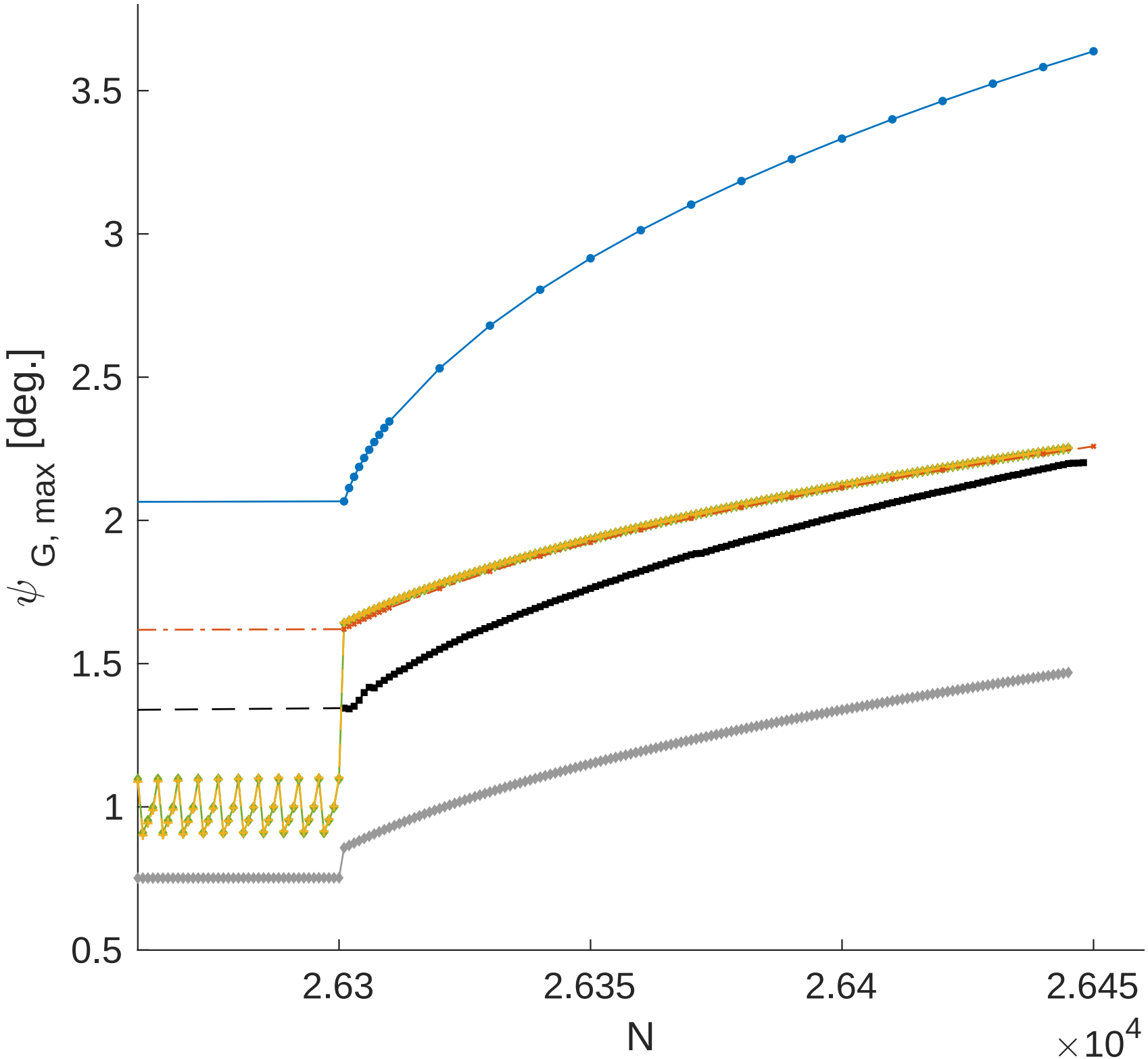

Figure

Click here to access/download;Figure;Fig7e-CM5acc.eps

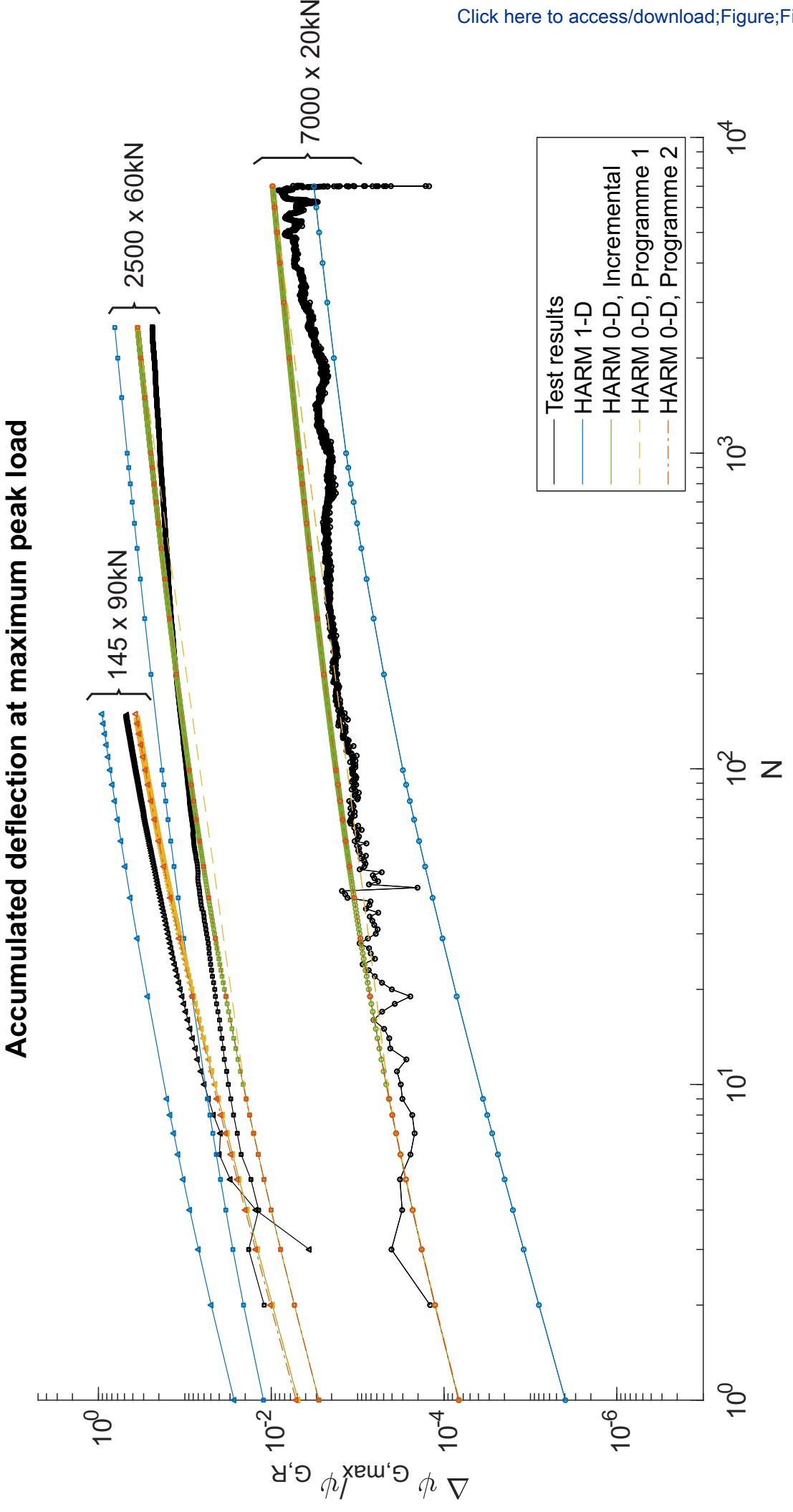

Figure

Click here to access/download;Figure;Fig8a-ShortStorm.eps

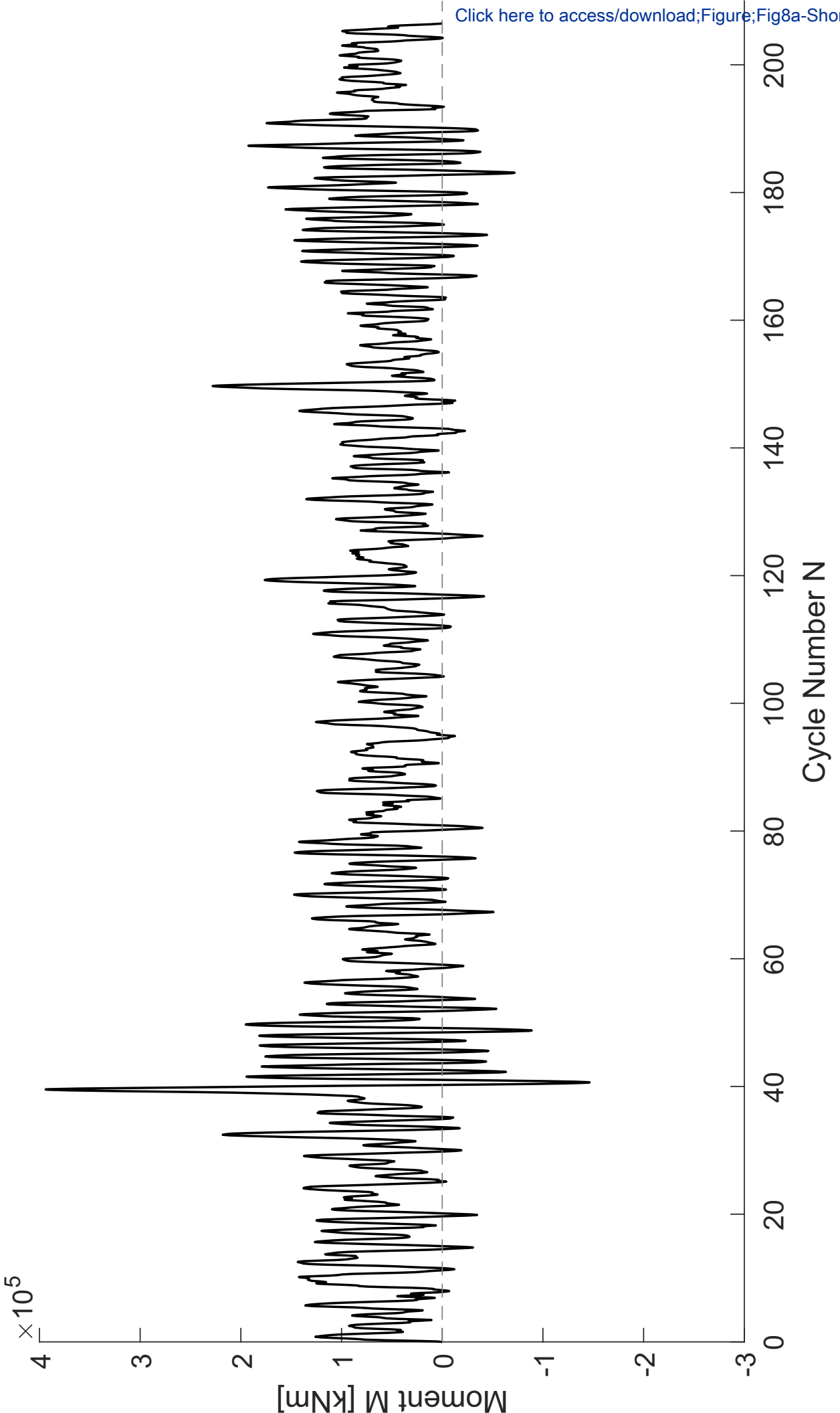

Figure

Click here to access/download;Figure;Fig8b-ShortStorm.eps

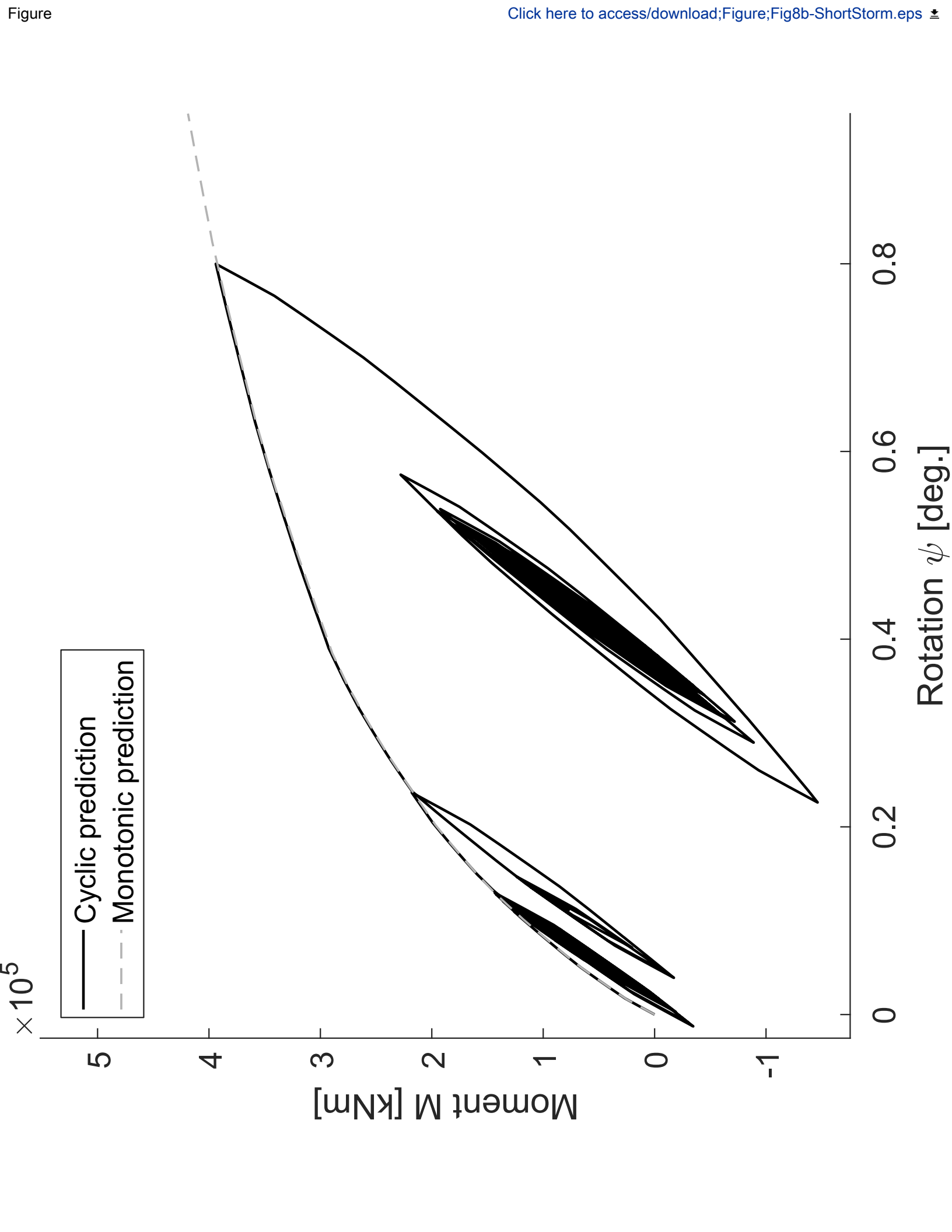

Figure

Click here to access/download;Figure;Fig8c-ShortStorm.eps

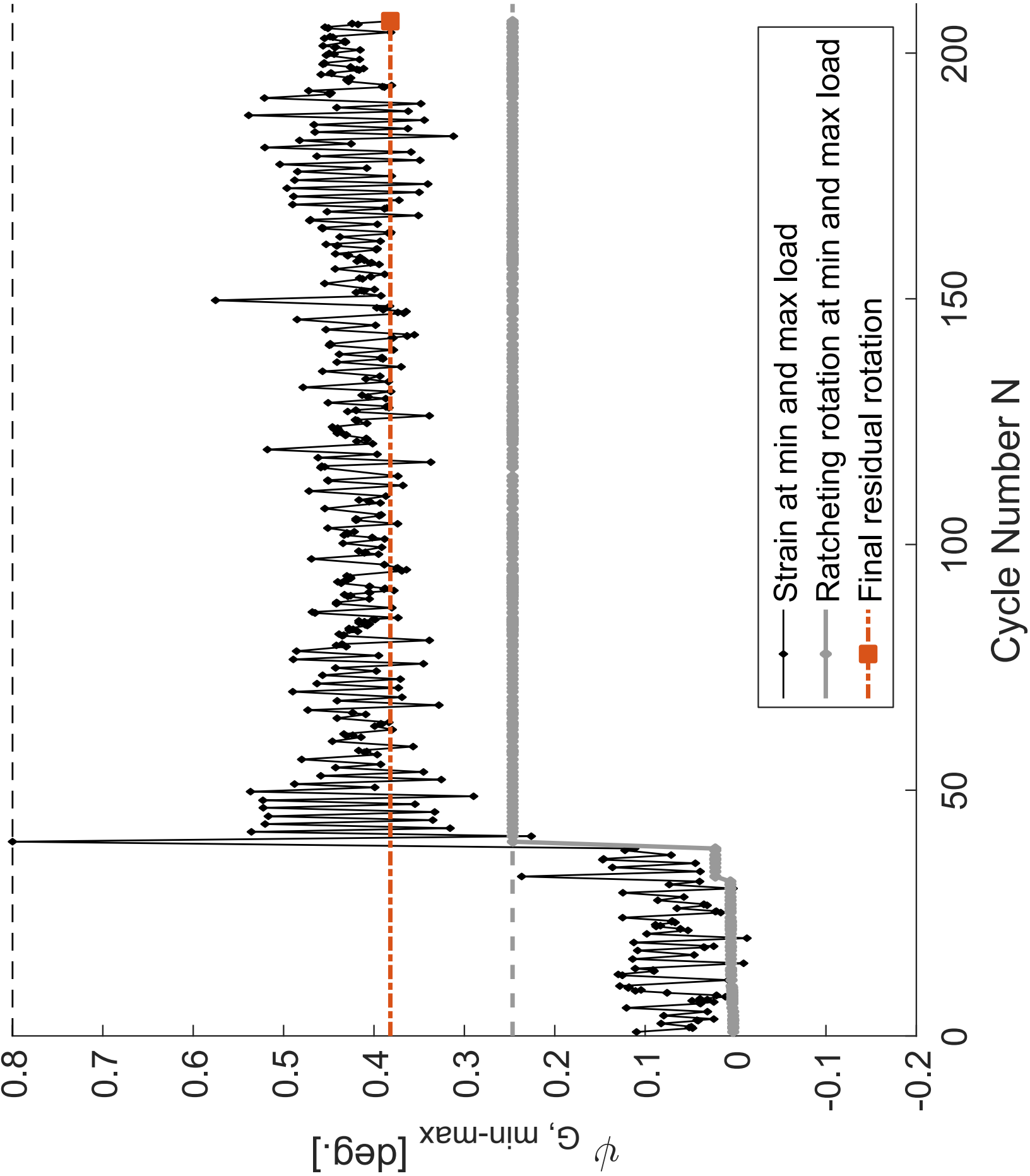

Figure

Click here to access/download;Figure;Fig9a-35hStorm.eps

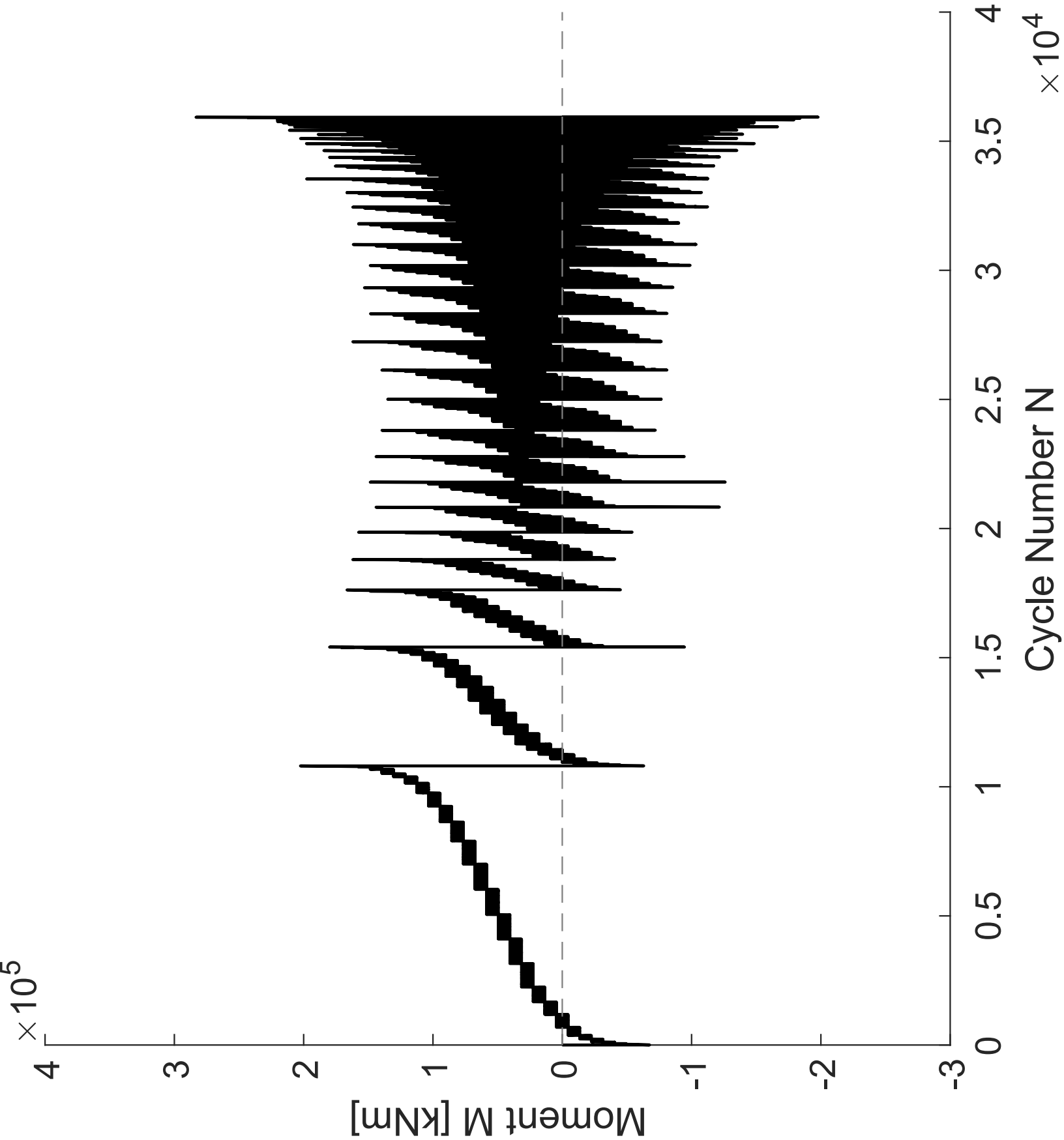

Figure

Click here to access/download;Figure;Fig9b-35hStorm.eps

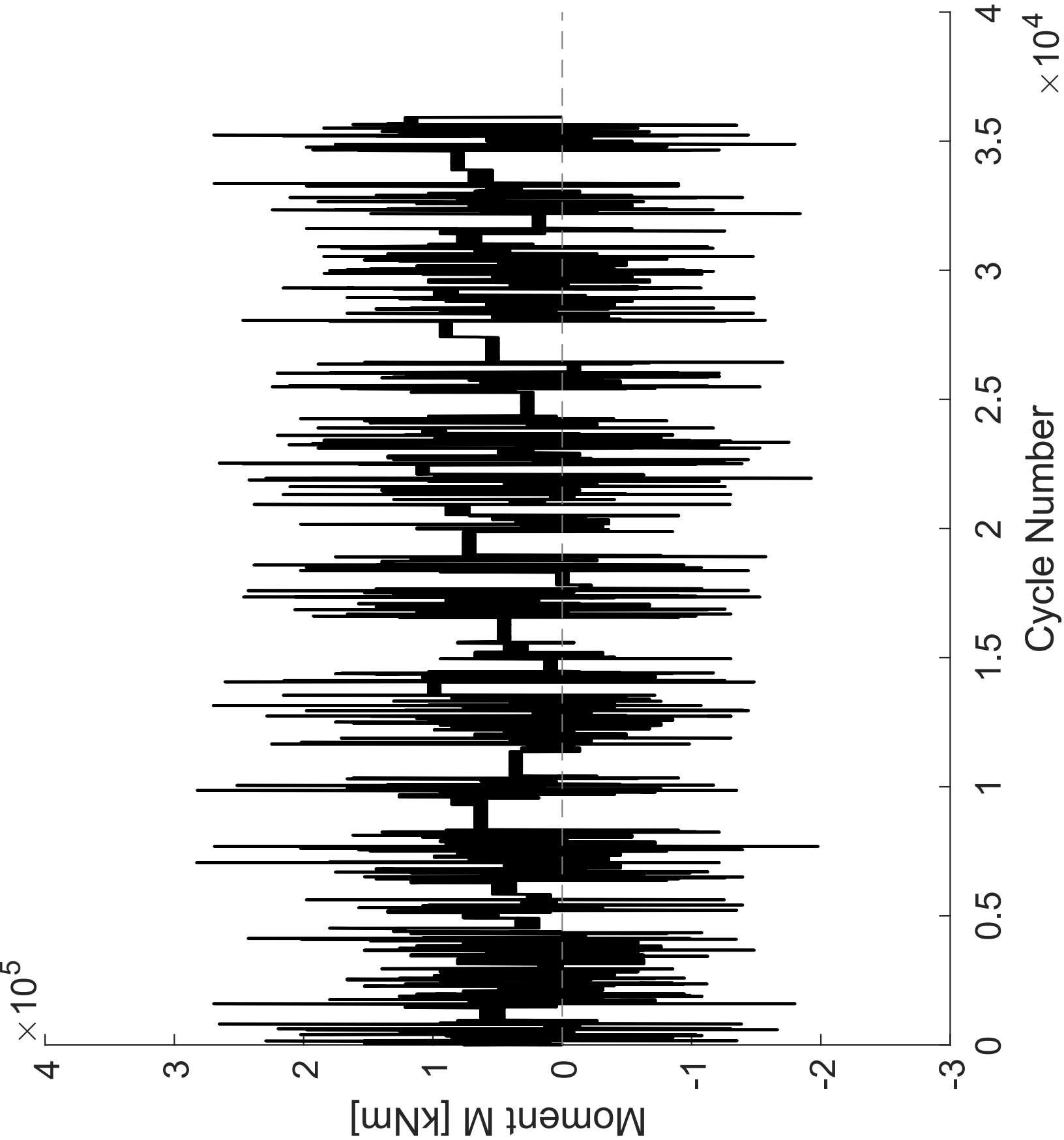

Figure

Click here to access/download;Figure;Fig9c-35hStorm.eps

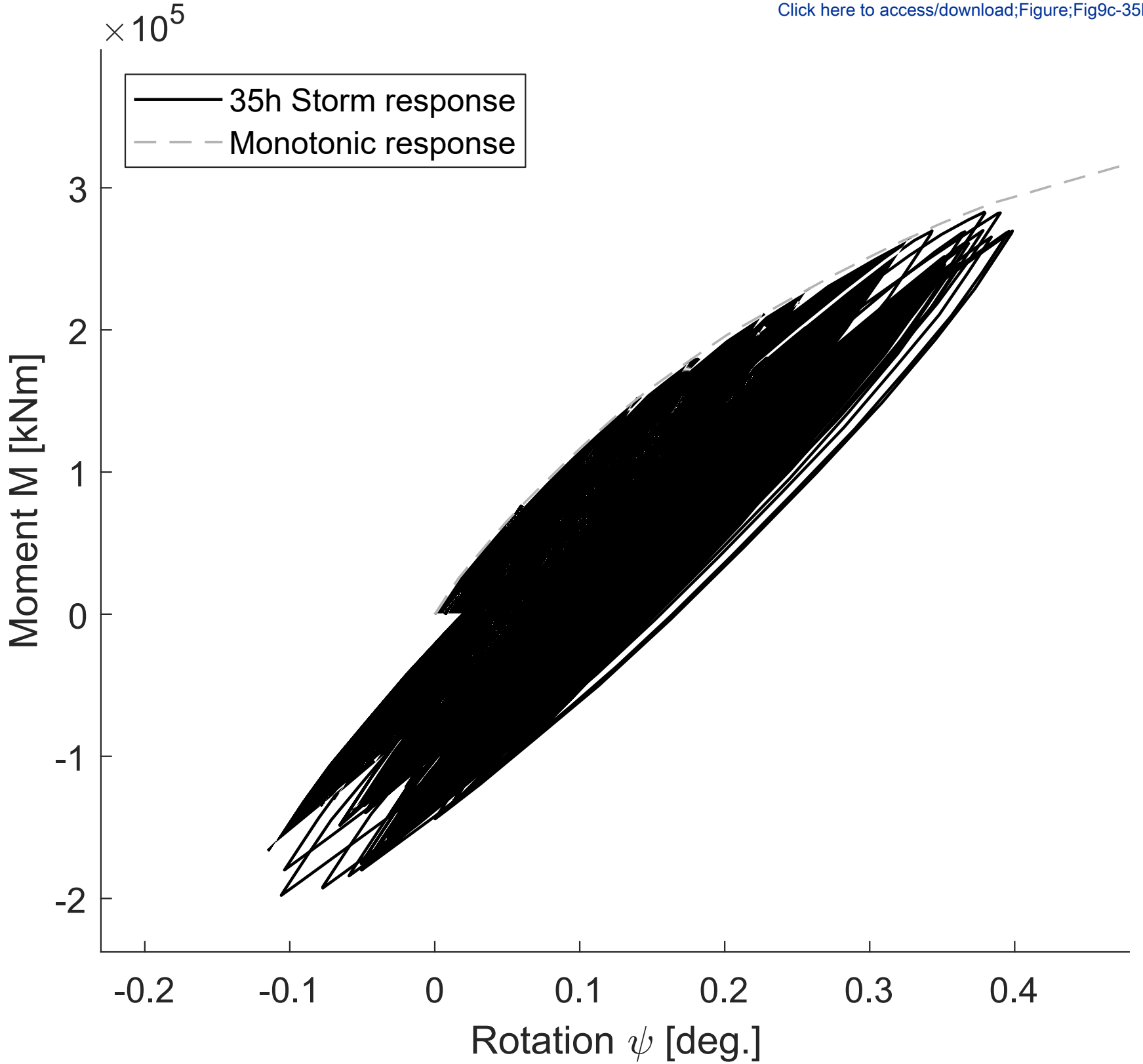

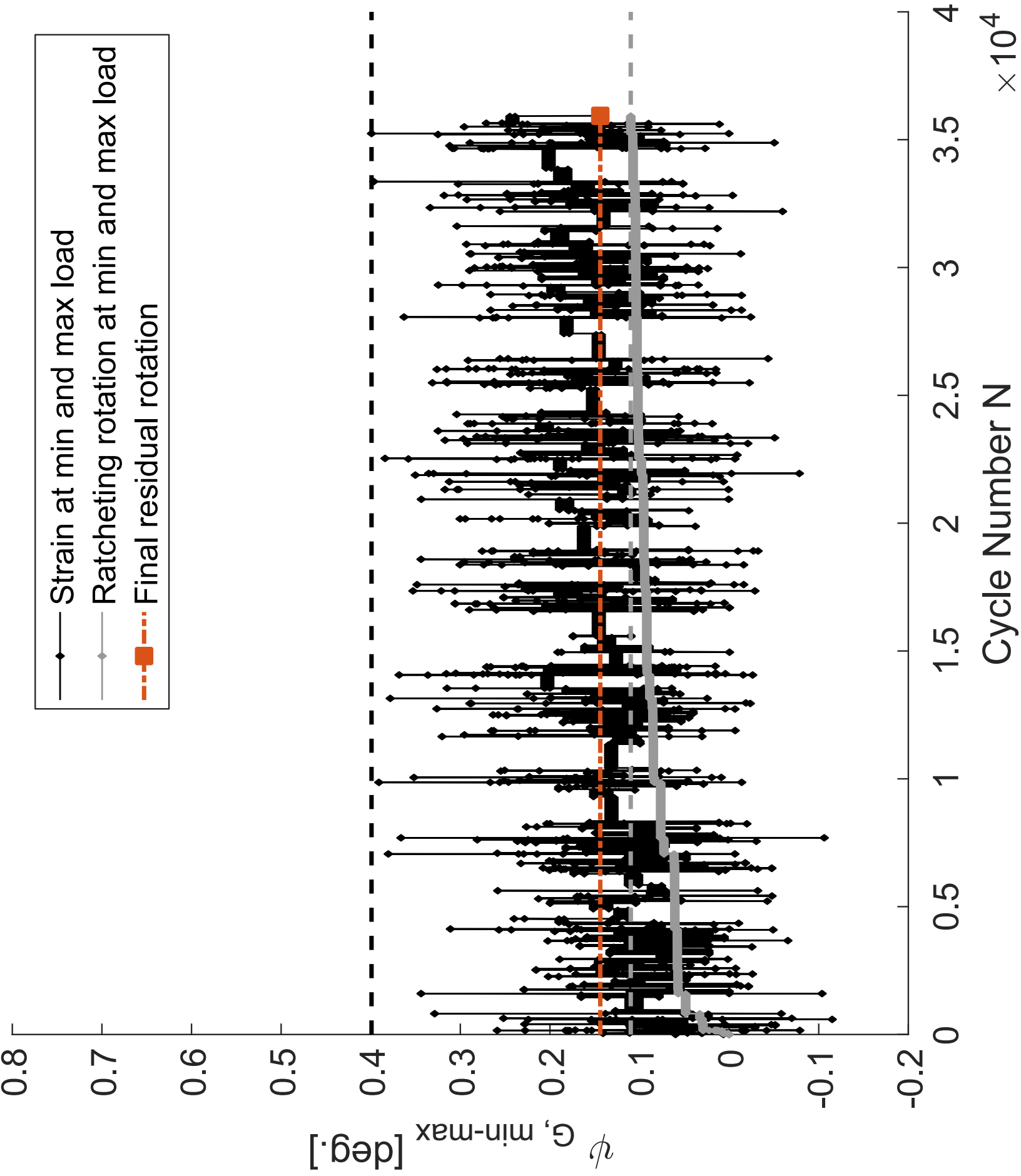

Figure

Click here to access/download;Figure;Fig10a-LifetimeLoad.eps

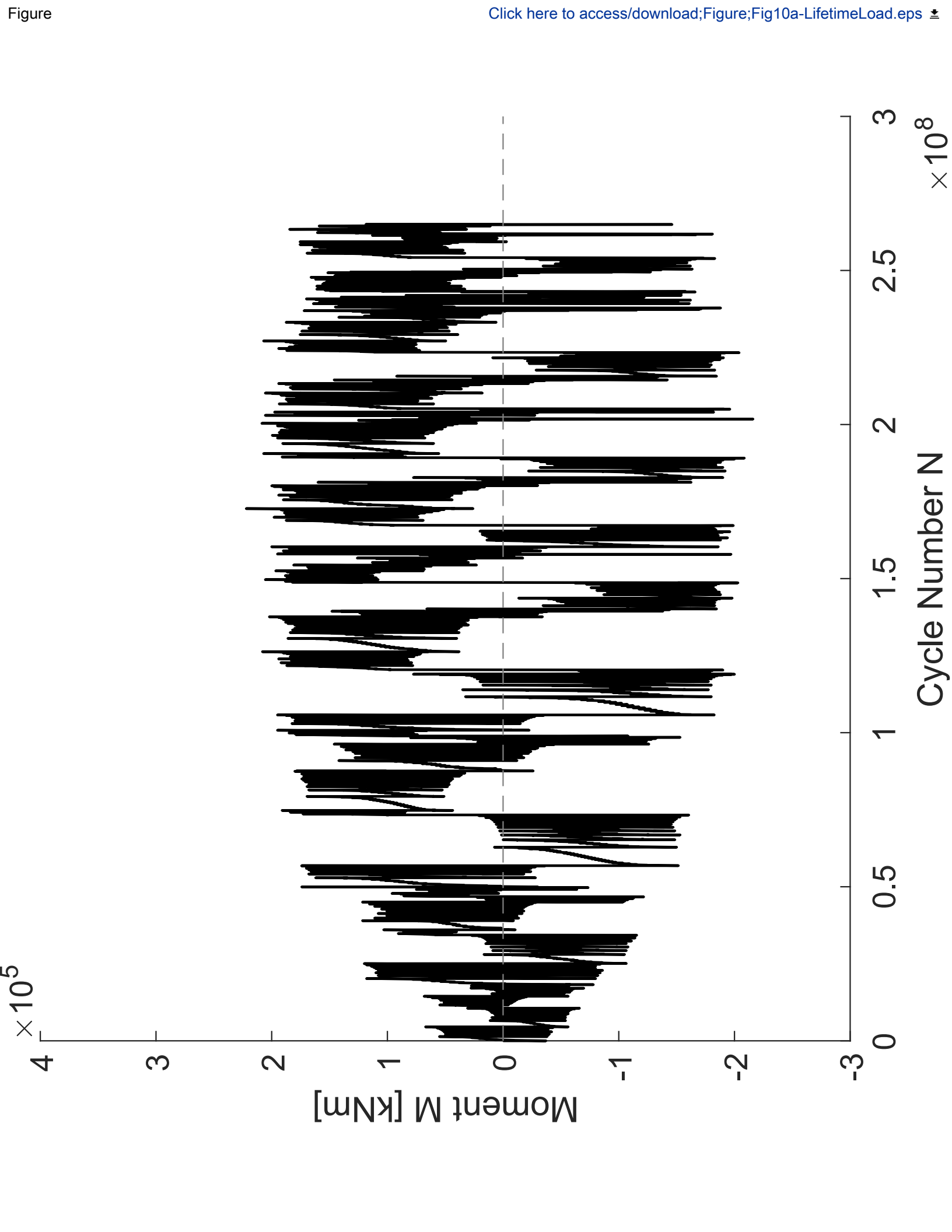

Figure

Click here to access/download;Figure;Fig10b-LifetimeLoad.eps

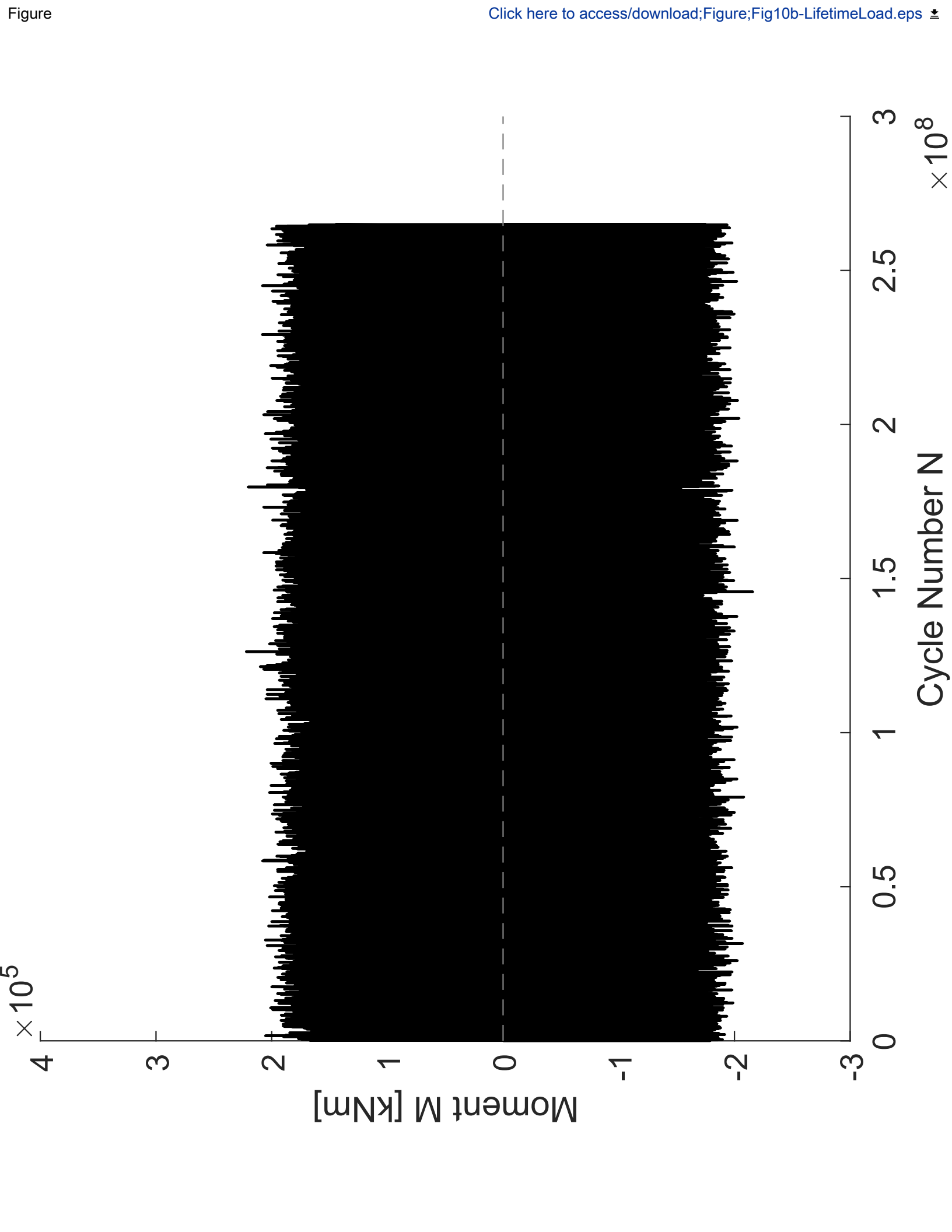

Figure

Click here to access/download;Figure;Fig10c-Lifetime.eps

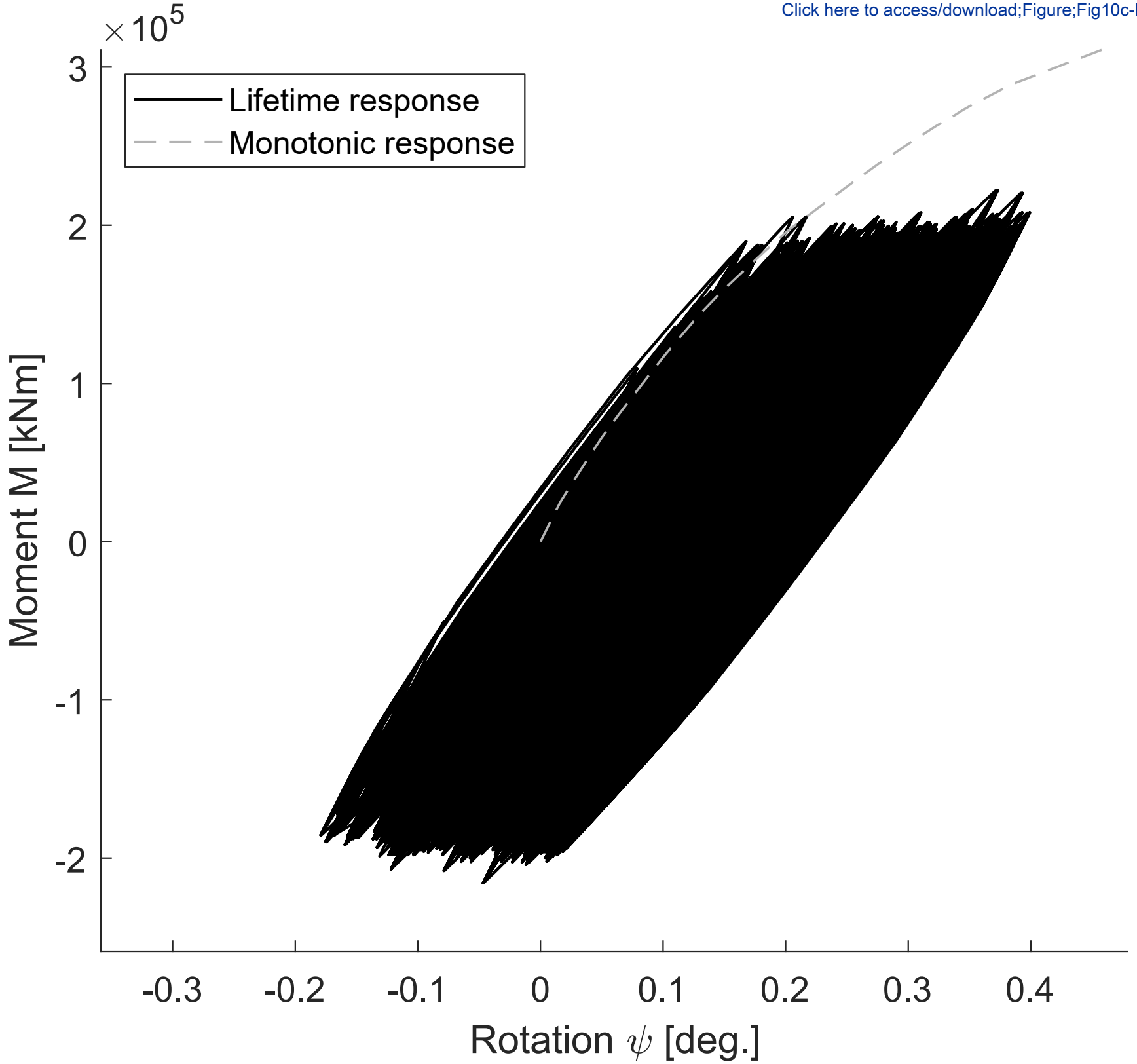

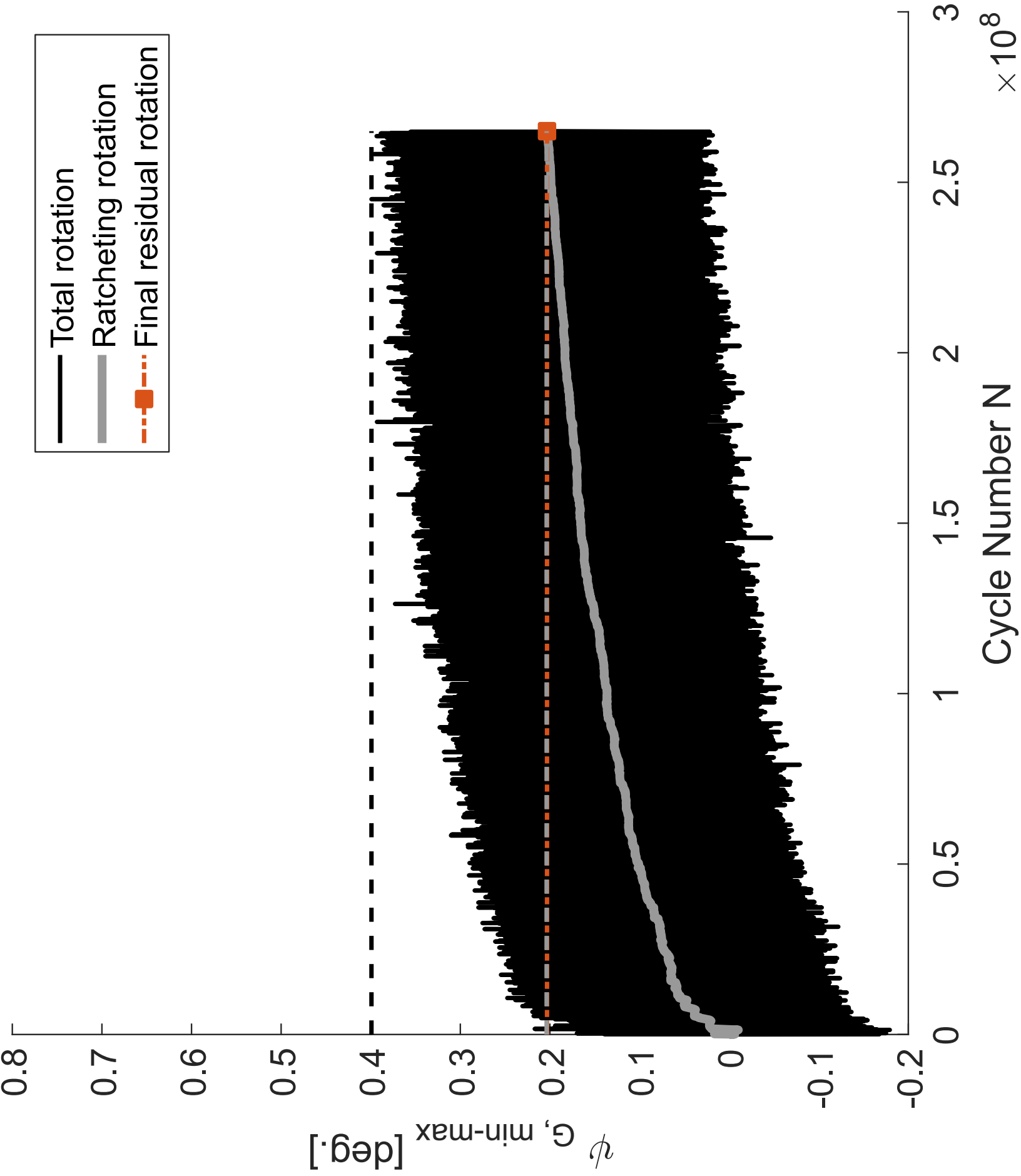

Figure

Click here to access/download;Figure;Fig11-History.eps

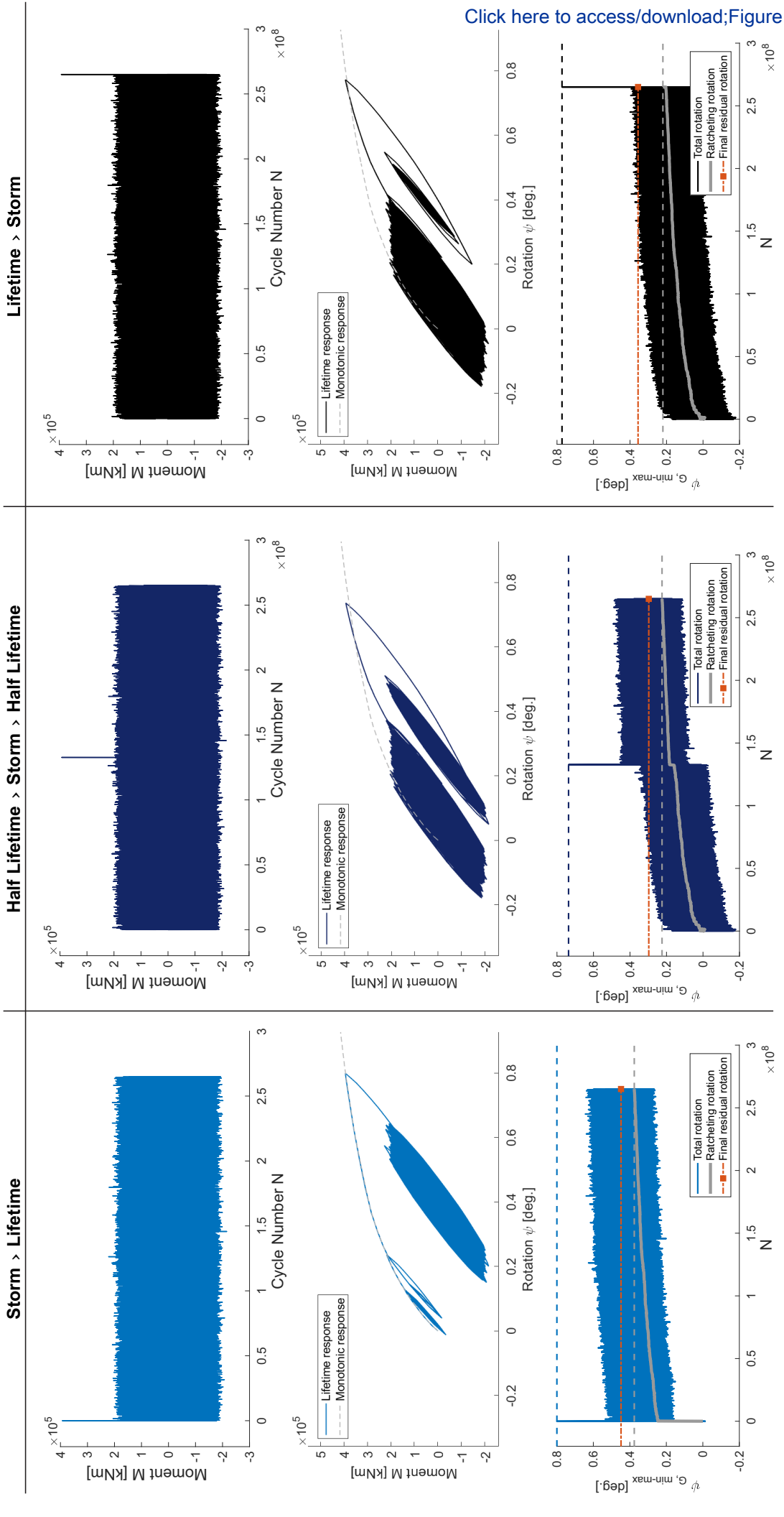

Figure

Click here to access/download;Figure;Fig12a-CuttingPrinciple.eps

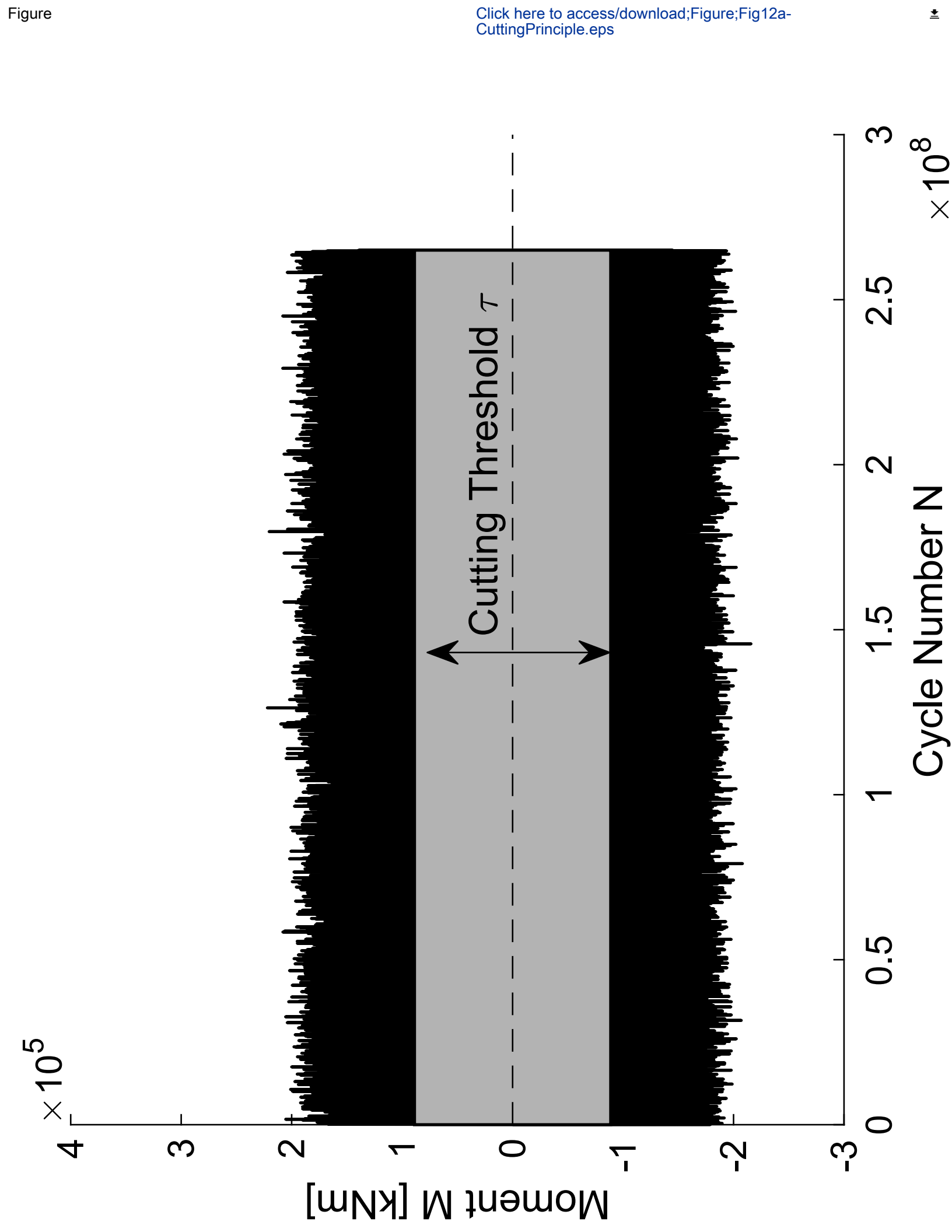

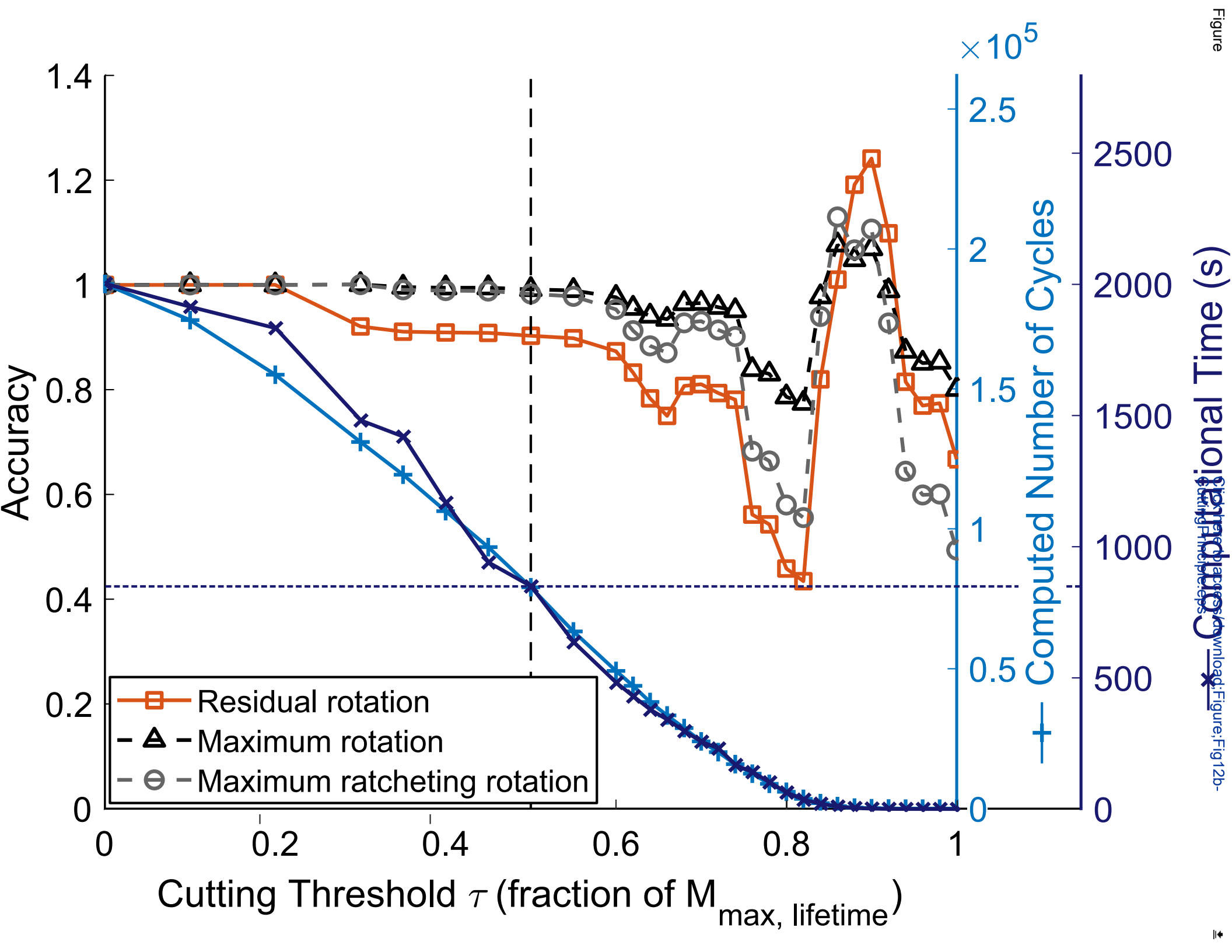
Accuracy
Cutting Threshold τ (fraction of $M_{max,\ lifetime}$)
Computed Number of Cycles
Computational Time (s)
$\times 10^5$
Residual rotation
Maximum rotation
Maximum ratcheting rotation
0
0.2
0.4
0.6
0.8
1
1.2
1.4
0.5
1.5
2
2.5
500
1000
1500
2000
2500

Figure

Click here to access/download;Figure;Fig12c-CuttingPrinciple.eps

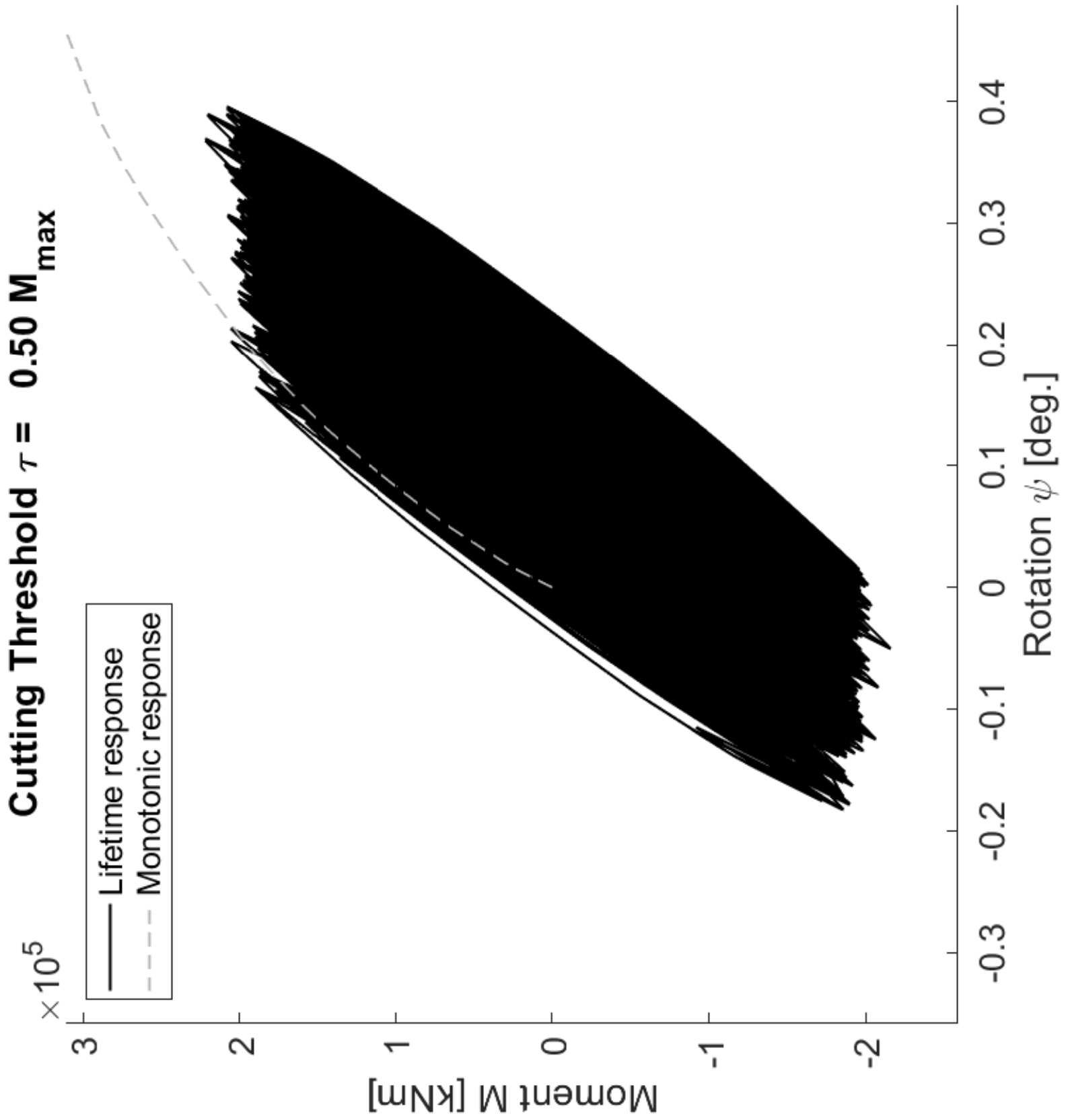

Figure

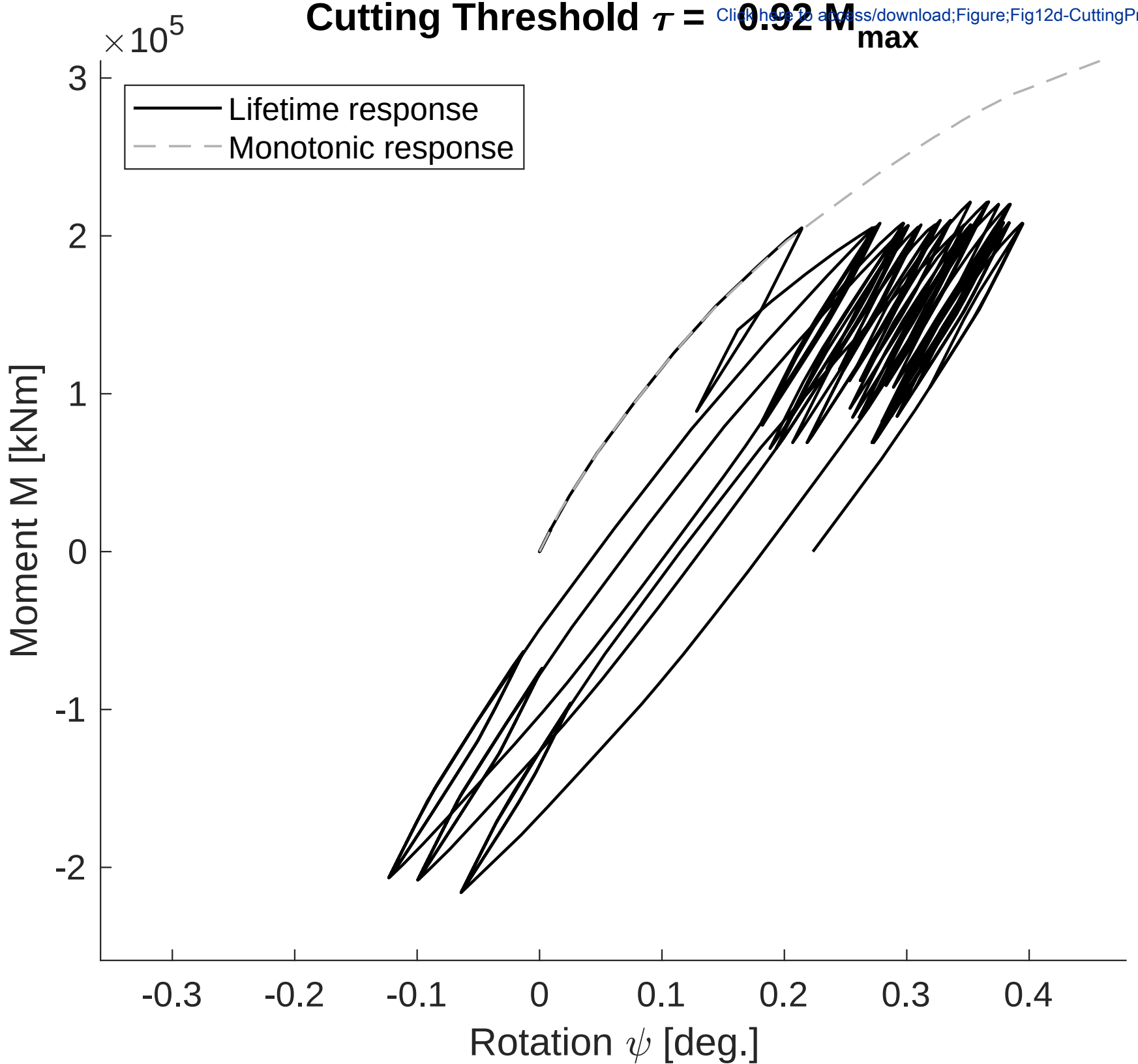

Figure

Figure

Click here to access/download;Figure;Fig14-Eevol.tif

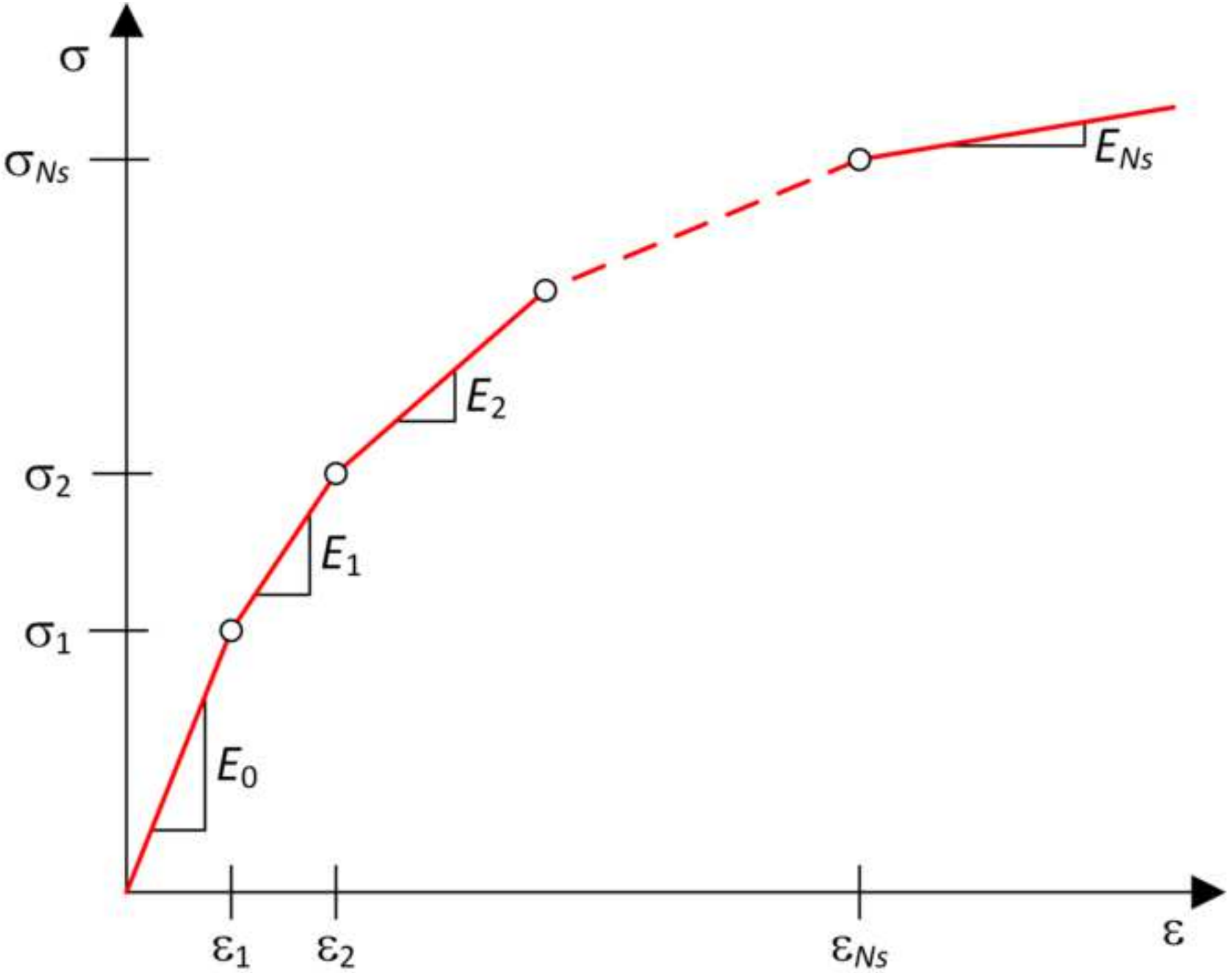

Figure

Click here to access/download;Figure;Fig15a-AccRot-CM5-6.tif

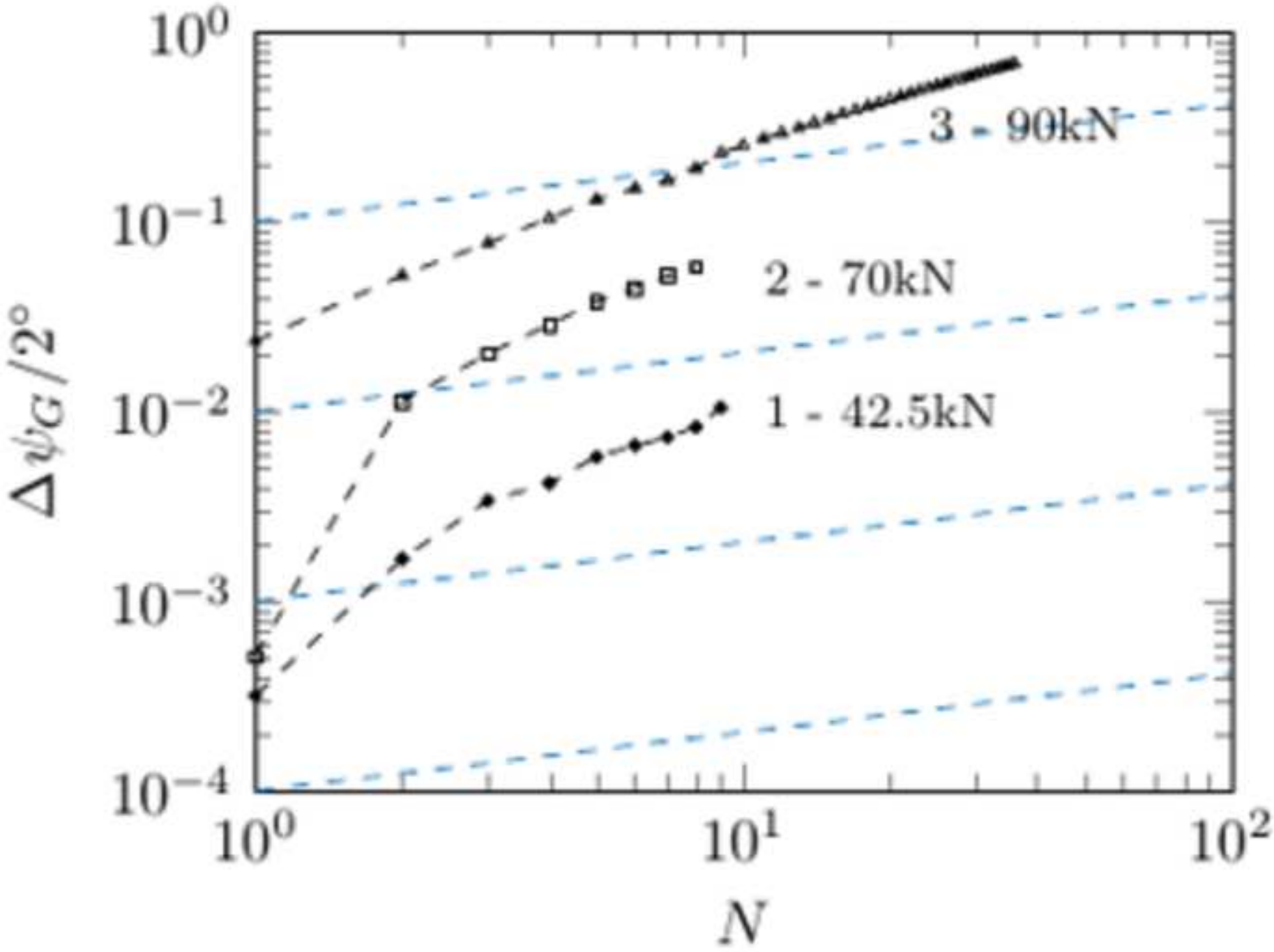

Figure

Click here to access/download;Figure;Fig15b-AccRot-CM5-6.png.tif

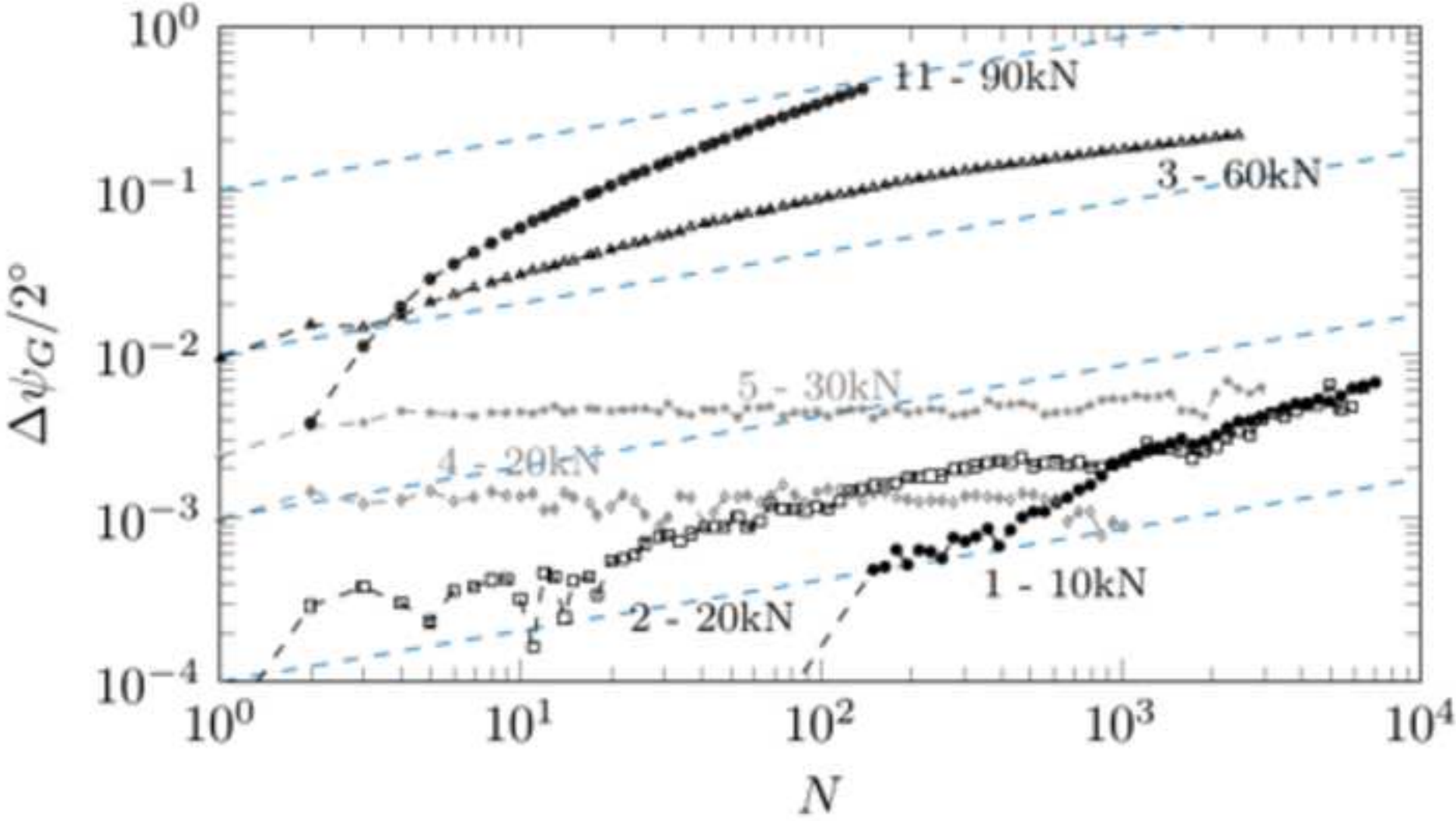

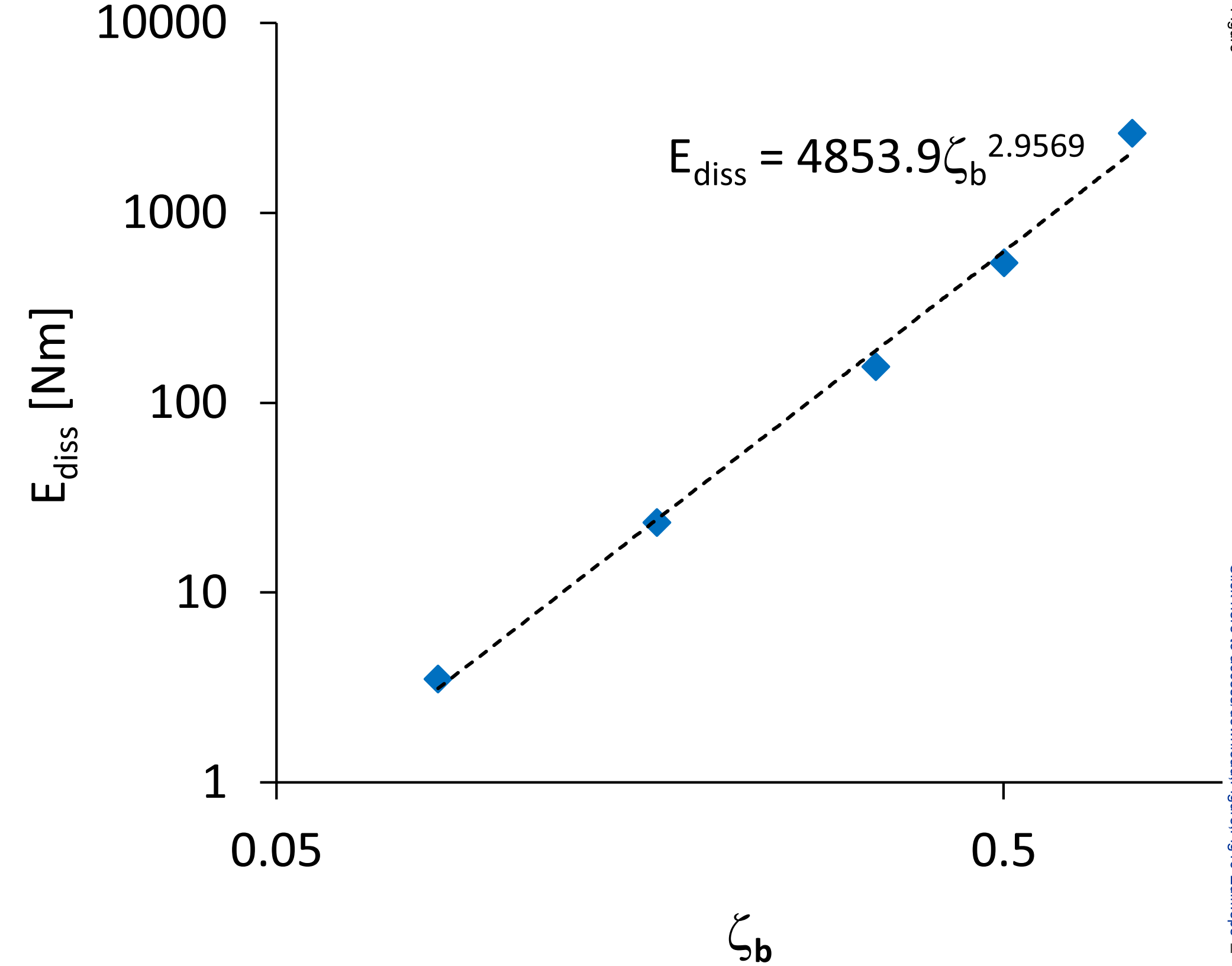

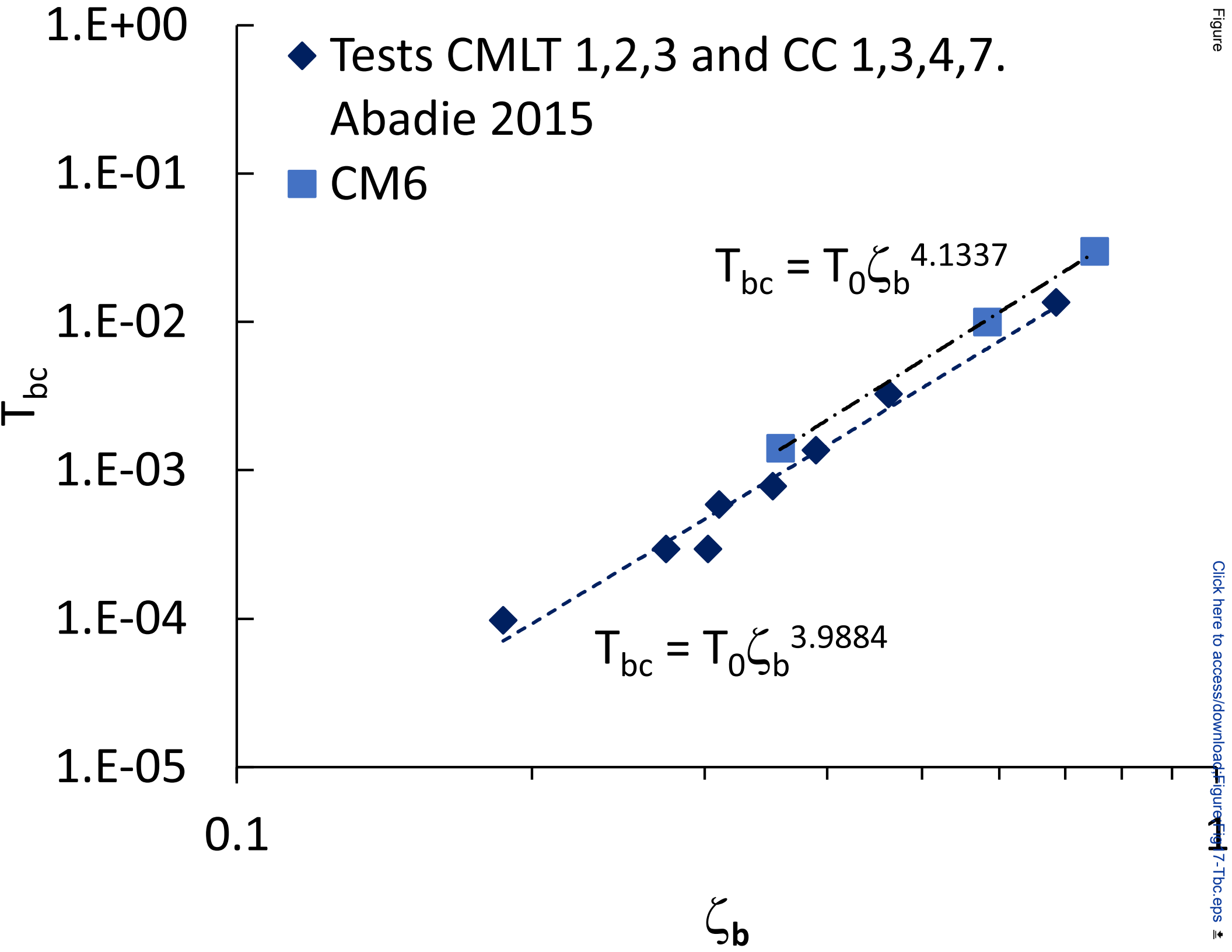

"Modelling Lifetime Performance of Monopile Foundations for Offshore Wind Applications"
by **Abadie, C.N.** et al.

Response to Reviewers:

Major point:

The most significant comment that required addressing was the issue of timings of computations. This is of course a difficult area to address because the hardware and software available to different users varies widely, as well as the algorithms employed. Our view is that relative timings are relevant but absolute measures of computation time are not helpful, and we have adjusted the text to reflect this, and we hope that we have indicated where significant savings are achievable. We have given significantly more information about the algorithms used.

Minor points:

1. References have been updated and corrected, and specifically the Byrne et al (2020) references checked.
2. Rewording around the (old) line 132 has been made.
3. A brief reference to Kementzetzidis et al (2022) has been added, as this is indeed relevant.
4. Some minor improvements have been made to the text flow, allowing Appendix C to be removed entirely.
5. The redundant Table 8 has been removed and Table 9 renumbered.